

The Mass Budget of Arctic Glaciers

Extended abstracts

**Workshop and GLACIODYN planning meeting,
29 January - 3 February 2006
Obergurgl (Austria)**

IASC Working group on Arctic Glaciology



**Institute for Marine and Atmospheric Research Utrecht
Utrecht University, The Netherlands**

The Mass Budget of Arctic Glaciers

Extended abstracts

**Workshop and GLACIODYN Planning Meeting,
29 January - 3 February 2006, Obergurgl (Austria)**

IASC Working Group on Arctic Glaciology

Organized by J. Oerlemans and C.H. Tijn-Reijmer



**Institute for Marine and Atmospheric Research Utrecht
Utrecht University, The Netherlands**

CONTENTS

Preface	7
<i>Johannes Oerlemans</i>	
Program	9
List of participants	12
Abstracts	15
Rapid thinning of Langfjordjøkelen in northern Norway	16
<i>Liss M. Andreassen, Bjarne Kjøllmoen, Al Rasmussen and Øyvind Nordli</i>	
A first order model of calving glacier dynamics.....	20
<i>Doug Benn, Nick Hulton and Ruth Mottram</i>	
Geometry, mass balance and climate change response of Langjökull ice cap, Iceland.....	22
<i>Helgi Björnsson, Sverrir Guðmundsson, Tómas Jóhannesson, Finnur Pálsson, Guðfinna Aðelgeirsdóttir and Hannes H. Haraldsson</i>	
Focus on the Arctic calving glaciers: Promotion of the IPY GLACIODYN project and glaciological knowledge within tourists - our taxpayers	26
<i>Elisabeth Bukowska-Jania, J. Jania, P. Glowacki, L. Kolondra and M. Grabiec</i>	
Dynamical downscaling of ERA-40 precipitation for modeling snow accumulation on ice caps in Iceland	30
<i>Philippe Crochet, Tómas Jóhannesson, Oddur Sigurðsson, Helgi Björnsson and Finnur Pálsson</i>	
The Effect of the Firn layer on glacial runoff of Hofsjökull ice cap, Iceland	32
<i>Mattias de Woul, Regine Hock, Matthias Braun, Thorsteinn Thorsteinsson, Tómas Jóhannesson and Stefanía Halldórsdóttir</i>	
Regional climate modeling of the Greenland ice sheet.....	34
<i>Janneke Ettema, Michiel van den Broeke, Erik van Meijgaard, Jonathan Bamber, Rupert Gladstone and Jennifer Griggs</i>	
Changes in geometry and hydrothermal structure of Fridtjovbreen, a polythermal glacier in Spitsbergen, following its surge in the 1990s model	39
<i>Andrey Glazovsky, I.I. Lavrentiev, Yu.Ya. Macheret, F.J. Navarro and E.V. Vasilenko</i>	
Calving glaciers of Novaya Zembyla and Franz Joseph Land	43
<i>Andrey Glazovsky, Yury Macheret and Evgeny Vasilenko</i>	

Assessment of the surface mass balance of 18 Svalbard glaciers from the MODIS/Terra albedo product.....	45
<i>Wouter Greuell, Jack Kohler, Friedrich Obleitner, Piotr Glowacki, Kjetil Melvold, Erik Bernsen and Johannes Oerlemans</i>	
More on elevation changes on Austfonna Ice Cap	49
<i>Jon Ove Hagen, Trond Eiken, Even Loe, Jack Kohler, Ketil Melvold, Thomas V. Schuler and Andrea Taurisano</i>	
Engabreen - Mass balance results and the Svartisen subglacial laboratory.....	52
<i>Miriam Jackson and Hallgeir Elvehøy</i>	
Changes in the topography of selected glaciers in southern Spitsbergen in the light of the GPS survey in 2005.....	54
<i>Jacek Jania, Mariusz Grabiec, Grzegorz Gajek, Leszek Kolondra, Piotr Glowacki and Dariusz Puczko</i>	
Long-term high arctic mass balance: comparison of balances and volume changes on Midre Lovénbreen, Svalbard.....	60
<i>Jack Kohler, Chris Nuth, Ola Brandt, Tavi Murray, Tim James and Nick Barrand</i>	
Energy and mass balance at Etonbreen, Austfonna.....	63
<i>Even Loe, Trond Eiken, Jon Ove Hagen, Kjetil Melvold, Thomas Schuler and Andrea Taurisano</i>	
Mass balance and velocity studies on McCall Glacier	65
<i>Matt Nolan</i>	
Short scale variations in mass balance and density of the Greenland snowpack and firn	67
<i>Victoria Parry, Peter Nienow, Douglas Mair, Jemma Wadham, Bryn Hubbard and Julian Scott</i>	
Columbia Glacier at Mid-Retreat.....	70
<i>Tad Pfeffer</i>	
Considerations on short-term and seasonal fluctuations of Hansbreen - a Svalbard tidewater glacier	73
<i>Dariusz Puczko, Jacek A. Jania, Piotr Glowacki and Krzysztof Migala</i>	
Modelling future glacier mass balance and volume changes of Storglaciären, Sweden, using ERA40-reanalysis and climate models data	78
<i>Valentina Radić and Regine Hock</i>	
The multi-layer snow model SOMARS in a distributed energy and mass balance model.....	81
<i>Carleen Reijmer and Regine Hock</i>	
A surface mass balance model for Austfonna, Svalbard.....	86
<i>Thomas V. Schuler, Trond Eiken, Jon Ove Hagen, Even Loe, Kjetil Melvold, Andrea Taurisano</i>	

Exegesis of interferometric and altimetric observations in South Spitsbergen.....	88
<i>Aleksey I. Sharov</i>	
Parameterizing scalar transfer over a rough ice surface.....	94
<i>Paul Smeets and Michiel van den Broeke</i>	
Assessing unspirated temperature measurements using a thermocouple and a physically based model	99
<i>Paul Smeets</i>	
Dynamics of large tidewater glaciers in East Greenland: recent results from satellite remote sensing and fieldwork	102
<i>Leigh Stearns and Gordon Hamilton</i>	
New results from geodetic mass budget studies at Swiss Camp (Greenland) and extension of research area to lower altitudes..	105
<i>Manfred Stober</i>	
A Statistical Approach to Estimating the Contribution of Glaciers to Future Sea-level Rise	110
<i>Andy Wright, Ros Death, Tony Payne and Gemma Wadham</i>	
GLACIODYN	111
GLACIODYN planning meeting	112
Contributions.....	115

PREFACE

The Working Group on Arctic Glaciology of the International Arctic Science Committee (IASC-WAG) held its 2006 - workshop on the mass budget of Arctic glaciers in Obergurgl, Austria. The meeting was hosted by the teaching and conference centre of the University of Innsbruck, and once more this location turned out to be an outstanding one. The pleasant atmosphere in the centre, the excellent conference facilities and the splendid surroundings all contributed to a very successful meeting.

About 40 scientific contributions were presented (10 posters and 30 oral presentations) on a range of subjects, but with a focus on the mass budget of Arctic glaciers. Extended abstracts of many of these presentations can be found in this book.

This year the IASC-WAG workshop was combined with the first planning meeting of GLACIODYN, an IPY-endorsed project in which the dynamic response of arctic glaciers to climate warming will be studied with a variety of techniques. GLACIODYN is now starting and it is expected to continue for several years following the official IPY (2007-08). Scientists from 17 nations plan to contribute to GLACIODYN.

The main aim of the first planning meeting was to become acquainted with plans of individual institutes/research groups and to see how logistics facilities, technical expertise and modelling expertise can be shared among the participants.

Some more information on GLACIODYN and on the meeting can be found in this book.

No doubt there will be another workshop next year (probably in March 2007). Interested persons may visit the website of the IASC-WAG, where more information will be posted later this year.

[website: www.phys.uu.nl/%7Ewwwimau/research/ice_climate/iasc_wag/]

I am indebted to Professor Michael Kuhn und Angelika Neuner (University of Innsbruck) for their help in the organization of this meeting.

I like to thank the Institute for Marine and Atmospheric Research of Utrecht University (IMAU) for the generous support that made it possible to print this report.

I am particularly grateful to Carleen Tijm-Reijmer for chasing the participants to submit their texts and for doing all the editorial work.

Johannes Oerlemans

Chairman, IASC Working Group on Arctic Glaciology

PROGRAM

Monday 30

- 13:00 – 13:20 *Johannes Oerlemans*: Welcome
- 13:20 – 13:40 *Jonathan Bamber*: Modelling the past and future mass balance of the Greenland ice sheet within a climate model
- 13:40 – 14:00 *Janneke Ettema*: Regional climate modelling of the Greenland ice sheet
- 14:00 – 14:20 *Manfred Stober*: New results from geodetic mass budget studies at Swiss Camp (Greenland) and extension of research area to lower altitudes.
- 14:20 – 14:40 *Roderik van de Wal and IMAU members*: Mass balance measurement along the K-transect Greenland

14:40 – 15:10 Coffee break

- 15:10 – 15:30 *Paul Smeets and M. van den Broeke*: Scalar roughness length observations at the Greenland ice sheet over a wide range of ice surface roughness
- 15:30 – 15:50 *Carleen Reijmer and R. Hock*: A multi layer snow model (SOMARS) in a distributed energy balance model
- 15:50 – 16:10 *Regine Hock and V. Radic*: Modelling future glacier mass balance and volume changes using ERA40-reanalysis and climate models data
- 16:10 – 16:30 *Friedrich Obleitner*: Critical issues in modelling Arctic snow

19:00 – Dinner

Tuesday 31

- 09:00 – 09:15 *Gordon Hamilton*: Dynamics of large tidewater glaciers in East Greenland: recent results from satellite remote sensing and fieldwork Part1
- 09:15 – 09:30 *Leigh Stearns*: Dynamics of large tidewater glaciers in East Greenland: recent results from satellite remote sensing and fieldwork Part 2
- 09:30 – 09:50 *Andrey Glazovsky and Yu. Ya. Macheret*: Calving glaciers of Franz Josef Land and Novaya Zemlya
- 09:50 – 10:10 *Dariusz Puczko, J. Jania, P. Glowacki, K. Migala*: Considerations on diurnal and seasonal fluctuations of velocity of Hansbreen a Svalbard tidewater glacier

10:10 – 10:40 Coffee break

- 10:40 – 11:00 *Carl Egede Bøggild*: Thinning of the south Greenland ice sheet margin
- 11:00 – 11:20 *Doug Benn, N. Hulton, R. Mottram*: Mass loss by calving: a new theoretical framework
- 11:20 – 11:40 *Johannes Oerlemans*: Simple modelling of tidewater glaciers with sediment dynamics
- 11:40 – 12:00 *Jack Kohler*: Long-term high arctic mass balance: comparison of balances and volume changes on Midre Lovénbreen, Svalbard

12:00 – 13:30 LUNCH

- 13:30 – 13:50 *Mattias de Woul, R. Hock, M. Braun, T. Thorsteinsson, T. Jóhannesson, S. Halldórsdóttir*: The effect of the firn layer on glacial runoff of Hofsjökull ice cap, Iceland
- 13:50 – 14:10 *Wouter Greuell*: Assessment of the surface mass balance of 18 Svalbard glaciers from the MODIS/Terra albedo product
- 14:10 – 14:30 *Anthony Arendt*: Errors in Regional Extrapolation of Glacier Volume Changes Using Data from the Western Chugach Mountains, Alaska, USA
- 14:30 – 14:50 *Aleksey I. Sharov*: Exegesis of interferometric observations in South Svalbard
- 14:50 – 15:20 Poster Introduction

15:20 – 16:00 Coffee break and Poster session

16:00 – 17:30 **National representatives meeting**

18:00 – Dinner

19:00 – 21:30 Ski event !!

Wednesday 1 February

- 09:00 – 09:20 *Francisco Navarro, A.F. Glazovsky, I.I. Lavrentiev, Yu. Ya. Macheret, F.J. Navarro, E.V. Vasilenko*: Changes in geometry and hydrothermal structure of Fridtjovbreen, a polythermal glacier in Spitsbergen, following its surge in the 1990s
- 09:20 – 09:40 *Jacek Jania, M. Grabiec, G. Gajek, L. Kolondra, P. Glowacki, D. Puczko*: Changes in topography of selected glaciers in South Spitsbergen in the light of the GPS survey in 2005
- 09:40 – 10:00 *Thomas Schuler*: A surface mass balance model for Austfonna, Svalbard
- 10:00 – 10:20 *Jon Ove Hagen, T. Eiken, E. Loe, J. Kohler, K. Melvold, T.V. Schuler and A. Taurisano*: More on elevation changes on Austfonna Ice Cap, Svalbard
- 10:20 – 10:40 *Even Loe*: Energy and mass balance at Etonbreen, Austfonna

10:40 – 11:10 Coffee break

- 11:10 – 11:30 *Matt Nolan*: Mass balance and ice velocity studies on McCall Glacier
- 11:30 – 11:50 *Tad Pfeffer*: Columbia Glacier, Alaska at mid-retreat: Current status, and thoughts on hydrology and dynamics of irreversibility
- 11:50 – 12:10 *Miriam Jackson*: Engabreen - mass balance results and work in the subglacial lab
- 12:10 – 12:30 *Liss Andreassen*: Rapid thinning of Langfjordjøkelen in northern Norway

12:20 – LUNCH and afternoon off

19:00 – Dinner

Thursday 2 February

- 9:00 – 12:00 IPY-GLACIODYN meeting, project presentations
- 16:00 – 18:30 IPY-GLACIODYN meeting, project presentations

19:00 – Dinner

Friday 3 February

- 9:00 – 11:00 IPY-GLACIODYN meeting, education & outreach, discussion

POSTERS

- [*Elzbieta Bukowska-Jania, J. Jania, P. Glowacki, L. Kolondra, M. Grabiec:*](#) Focus on the Arctic calving glaciers. Promotion of the IPY GLACIODYN project and glaciological knowledge within tourists - our taxpayers.
- [*Helgi Björnsson, S. Gudmundsson, T. Johannesson, F. Pálsson and H.H. Haraldsson:*](#) Geometry, mass balance and climate change response of Langjökull ice cap, Iceland.
- [*P. Chrochet, Tomas Jóhannesson, O. Sigurðsson, H. Björnsson and F. Pálsson:*](#) Dynamical downscaling of ERA40 precipitation for modelling snow accumulation on ice caps in Iceland.
- [*E. Dowdeswell and Julian Dowdeswell:*](#) Glacier fluctuations on Bylot Island, Arctic Canada
- [*P. Glowacki, Marius Grabiec, J. Jania and P. Dolnicki:*](#) The importance of changing snow cover for dynamics of environmental processes in the High Arctic Archipelago.
- [*Jennifer Griggs and J. Bamber:*](#) A comparison of surface observations, climatologies and satellite datasets of cloud amounts over the Greenland Ice Sheet.
- [*A. Guterch, P. Glowacki, Jacek Jania and M. Grabiec:*](#) Arctic science in the public interest – A perspective from Poland.
- [*Vicky Parry, P. Nienow, D. Mair, J. Wadham, B. Hubbard and J. Scoff:*](#) Short scale variations in mass and density of the Greenland snowpack and firn.
- [*Paul Smeets:*](#) Assessing unventilated temperature measurements using a thermocouple and a physically based model.
- [*A. Wright, R. Death, A.J. Payne and Jemma Wadham:*](#) A Statistical Approach to Estimating the Contribution of Glaciers to Future Sea-level Rise.

LIST OF PARTICIPANTS

1. Andreas Peter Ahlstrøm (apa@geus.dk)
Geological Survey of Denmark and Greenland, Copenhagen, Denmark
2. Liss Andreassen (lma@nve.no)
Norwegian Water Resources and Energy Directorate, Oslo, Norway
3. Anthony Arendt (Anthony.Arendt@gi.alaska.edu)
University of Alaska, Fairbanks, Alaska
4. Jonathan Bamber (j.bamber@bristol.ac.uk)
University of Bristol, UK
5. Doug Benn (doug.benn@unis.no)
The University Centre in Svalbard
6. Helgi Björnsson (hb@raunvis.hi.is)
University of Iceland, Reykjavik, Iceland
7. Carl Egede Bøggild (Carl.Egede.Boggild@unis.no)
The University Centre in Svalbard
8. Elzbieta Bukowska-Jania
University of Silesia, Sosnowiec, Poland
9. Luke Copland (luke.copland@uottawa.ca)
University of Ottawa, Canada
10. Nicolas Cullen (nicolas.cullen@uibk.ac.at)
University of Innsbruck, Austria
11. Mattias de Woul (mattias.dewoul@natgeo.su.se)
Stockholm University, Sweden
12. Julian Dowdeswell (jd16@cam.ac.uk)
Scott Polar Research Institute, Cambridge, UK
13. Janneke Ettema (j.ettema@phys.uu.nl)
IMAU, Utrecht University, Netherlands
14. Grzegorz Gajek
University M. Curie-Sklodowska, Lublin, Poland
15. Rupert Gladstone (R.Gladstone@bristol.ac.uk)
University of Bristol, UK
16. Andrey Glazovsky (icemass@yandex.ru)
Russian Academy of Sciences, Moscow, Russia
17. Piotr Glowacki
Institute of Geophysics, PAS, Warszawa, Poland
18. Mariusz Grabiec
University of Silesia, Sosnowiec, Poland
19. Wouter Greuell (w.greuell@phys.uu.nl)
IMAU, Utrecht University, Netherlands
20. Jennifer Griggs (j.griggs@bristol.ac.uk)
University of Bristol, UK
21. Jon Ove Hagen (j.o.m.hagen@geo.uio.no)
University of Oslo, Norway
22. Gordon Hamilton (gordon.hamilton@maine.edu)
University of Maine, Orono, USA
23. Regine Hock (regine.hock@natgeo.su.se)
Stockholm University, Sweden

24. Per Holmlund (pelle@natgeo.su.se)
Stockholm University, Sweden
25. Miriam Jackson (mja@nve.no)
Norwegian Water Resources and Energy Directorate, Oslo, Norway
26. Jacek Jania (jjania@uranos.cto.us.edu.pl)
University of Silesia, Sosnowiec, Poland
27. Tómas Jóhannesson (tj@vedur.is)
Icelandic Meteorological Office, Reykjavik, Iceland
28. Georg Kaser (georg.kaser@uibk.ac.at)
University of Innsbruck, Austria
29. Jack Kohler (jack.kohler@npolar.no)
Norwegian Polar Institute, Tromsø, Norway
30. Leszek Kolondra
University of Silesia, Sosnowiec, Poland
31. Michael Kuhn (Michael.kuhn@uibk.ac.at)
University of Innsbruck, Austria
32. Even Loe (even.loe@geo.uio.no)
University of Oslo, Norway
33. Yury Macheret (macheret@gol.ru)
Russian Academy of Sciences, Moscow, Russia
34. Ruth Mottram (rhm6@st-andrews.ac.uk)
University of St Andrews, UK
35. Francisco Navarro (fnv@mat.upm.es)
Madrid Polytechnical University, Spain
36. Matt Nolan (fnman@uaf.edu)
University of Alaska, Fairbanks, Alaska
37. Friedrich Obleitner (Friedrich.Obleitner@uibk.ac.at)
University of Innsbruck, Austria
38. Hans Oerlemans (J.Oerlemans@phys.uu.nl)
IMAU, Utrecht University, Netherlands
39. Vicky Parry (V.L.Parry@sms.ed.ac.uk)
University of Edinburgh, UK
40. Tad Pfeffer (pfeffer@tintin.colorado.edu)
University of Colorado, Boulder, USA
41. Dariusz Puczko
Institute of Geophysics, PAS, Warszawa, Poland
42. Cecilie Rolstad (cecilie.rolstad@umb.no)
The Norwegian University of Life Sciences (UMB), Norway
43. Thomas Schuler (t.v.schuler@geo.uio.no)
University of Oslo, Norway
44. Aleksey I. Sharov (aleksey.sharov@joanneum.at)
Joanneum Research, Graz, Austria
45. Paul Smeets (c.j.p.p.smeets@phys.uu.nl)
IMAU, Utrecht University, Netherlands
46. Leigh Stearns (leigh.stearns@maine.edu)
University of Maine, Orono, USA
47. Manfred Stober (manfred.stober@hft-stuttgart.de)
Stuttgart University of Applied Sciences, Germany
48. Carleen Tijm-reijmer (c.h.tijm-reijmer@phys.uu.nl)

- IMAU, Utrecht University, Netherlands
49. Roderik van de Wal (R.S.W.vandeWal@phys.uu.nl)
IMAU, Utrecht University, Netherlands
 50. Michiel van den Broeke (m.r.vandenbroeke@phys.uu.nl)
IMAU, Utrecht University, Netherlands
 51. Jemma Wadham (j.l.wadham@bristol.ac.uk)
School of Geographical Sciences, Bristol, UK
 52. Okitsugu Watanabe (okitugu@f4.dion.ne.jp)
National Institute of Polar Research, Tokyo, Japan



ABSTRACTS

RAPID THINNING OF LANGFJORDJØKELEN IN NORTHERN NORWAY

LISS M. ANDREASSEN^{1,2}, BJARNE KJØLLMOEN¹, AL RASMUSSEN³ AND ØYVIND NORDLI⁴

¹ Norwegian Water Resources and Energy Directorate, Oslo, Norway

² Department of Geosciences, University of Oslo, Norway

³ University of Washington, Seattle, USA.

⁴The Norwegian Meteorological Institute, Oslo, Norway.

Introduction

Glaciers cover about 1% of the land area in Norway. The Norwegian glaciers span over large distances and cover different climatic regimes from wet to dry conditions and from south to north. The Norwegian glacier measurement record is extensive and reveals both local and regional variations in glacier behaviour. In order to gain knowledge of glaciers in the northernmost parts of Norway, NVE began investigations in 1989 on an east-facing outlet of the maritime plateau glacier Langfjordjøkelen (70°10'N, 21°45'E) (Fig.1). Langfjordjøkelen has an area of about 8.4 km² (1994), and of this 3.7 km² drains eastward. The investigations are performed on this east-facing part, ranging from 280 to 1050 m a.s.l.



Figure 1. Location map of Norway. Glaciers are shaded in blue. The position of Langfjordjøkelen is indicated.

Mass balance regime

Langfjordjøkelen has been the subject of mass balance measurements since 1989 with the exception of 1994 and 1995. The mass balance measurements reveal a

large annual mass turnover in the same order as at the maritime glaciers located much farther south in Norway. The mean summer balance (-3.0 m w.e.) exceeds the winter balance (2.2 m w.e.) resulting in an annual deficit of -0.78 m w.e./a. for the period 1989-2005. The mass deficit of Langfjordjøkelen is in contrast to the maritime glaciers in southern Norway, which experienced mass surplus in the same period. Most of the mass loss of Langfjordjøkelen has occurred over the last nine years (1997-2005). In the period 1989-1995 the glacier has a slightly negative mass balance, while all the other observed glaciers in mainland Norway including the continental ones had a transient mass surplus (Andreassen et al, 2005).

Glacier fluctuations

Historical records, photos and maps show that Langfjordjøkelen has retreated about 1.4 km since 1900, the mean annual retreat being about 13 m. Length change measurements began in 1998 and show a mean annual retreat of more than 30 m. The recent increased thinning and retreat of Langfjordjøkelen is stronger than observed for any other glacier in mainland Norway.

Reconstruction of mass balance

Mass balance correlates poorly between Langfjordjøkelen and glaciers in Svalbard. In mainland Norway the glacier correlates best with the maritime glaciers, however, the correlation is too low to use for reconstruction of the mass balance back in time. Instead, a model using upper-air meteorological variables (wind, humidity and temperature) in the U. S. National Centers for Environmental Prediction and U. S. National Center for Atmospheric Research (NCEP-NCAR) Reanalysis database was used to extend the mass balance back in time. Further description of the model can be found in Rasmussen and Conway (2005). The model was calibrated between 1989 and 1999 and used to reconstruct the balance back to 1948 (Fig. 2). Model error is comparable to uncertainty in mass balance measurements. The reconstructed series from 1948 until 1989 reveal an average balance of -0.6 m w.e./a.

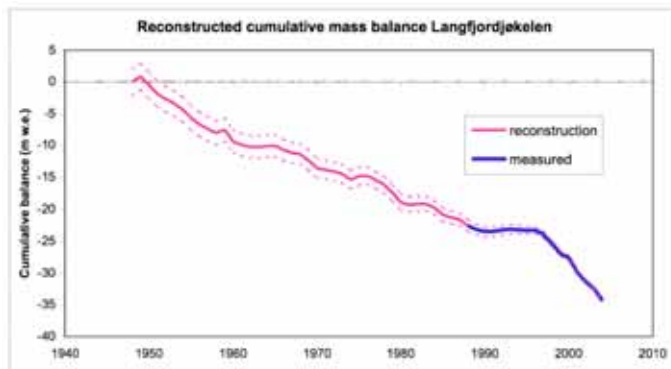


Figure 2. Reconstructed (1948-1988, 1994-1995) and measured (1989-1993, 1996-2005) cumulative mass balance of Langfjordjøkelen. The dotted curves are the one-sigma error band.

Volume change calculated from comparison of maps in 1966 and 1994 suggest thinning and retreat of the glacier in this period, but overestimates the mass deficit

compared with the results from the upper air model in the same period. As shown in Figure 3 the area decreased and the surface generally lowered over 1966-94. The eastern outlet had a recession of about 700 m and the total area decreased from 9.8 km² to 8.4 km². Average thinning over the entire glacier was 13 m w.e. and for the east-ward draining part area 19 m w.e. Thinning has occurred over 96 % of the entire glacier surface. The greatest mass loss is, as expected, on the glacier tongue, where the thinning is more than 100 metres. Some areas in the middle and north of the glacier indicate no elevation change (± 2 m) of the glacier surface. There are even some minor areas indicating increasing surface elevation, but this is within the uncertainty of the method comparing the maps.

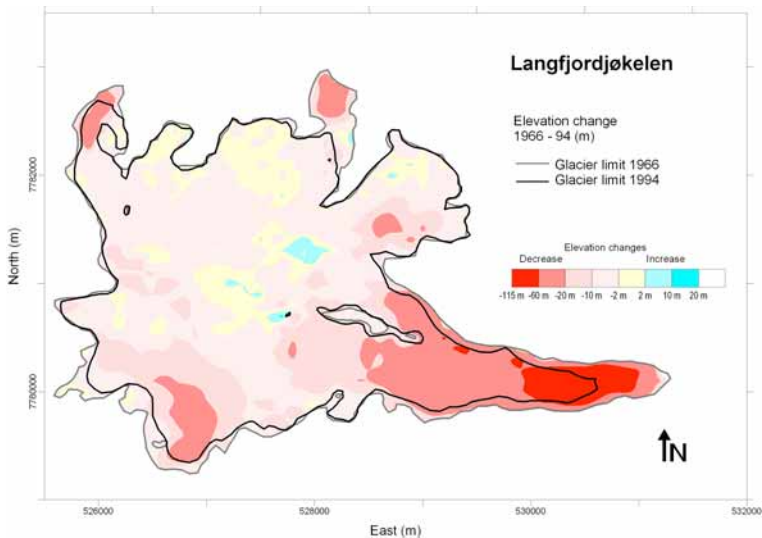


Figure 3. Volume change of Langfjordjøkelen 1966-1994.

Past and future climate

Temperature regions for Norway have been defined using a combination of principal component analysis and clustering analysis (Hanssen-Bauer and Nordli, 1998). As there are no long-term temperature measurements near Langfjordjøkelen the mean values for the whole region (Hanssen-Bauer, 2005) might be the best choice for temperature trend analyses for the glacier. The mean regional linear trend during summer (JJA) for the region is +0.09 per decade, amounting to about 1.2°C for the 130-year period 1875-2004. However, most of the temperature increase took part early in the 20th century in connection with a warming event during the 1910s and 1920s (The Early 20th Century Warming). Around 1950 the temperature started to decrease, but has been increasing again the last 30 years.

During the period 1966-2005 temperature variations at the glacier can be studied in more detail as measurements were established at Nordstraum, only 34 km to the south of the glacier. For the 40-year period the temperature has increased about 1°C (Fig. 4). Most of the increase has been concentrated in the period 1997-2005, where summer temperatures in all years have been above the 1971-2000 normal.

An empirical-statistical downscaling analysis for monthly mean temperature is presented by Benestad (2005) for a multi-model ensemble of the most recent climate scenarios (Special Report Emission Scenario A1b) produced for the upcoming IPCC Assessment Report 4 (AR4). In his dataset for Tromsø (120 km WSW of Langfjordjøkelen) the mean temperature trend is based on the whole ensemble amounts to 0.2°C/decade. Thus, summer temperature is expected to have increased by 1°C in 2050 and by 2°C in 2100 compared to present day climate. Thus, Langfjordjøkelen will continue to decrease and retreat and might disappear completely during the next 100 years.

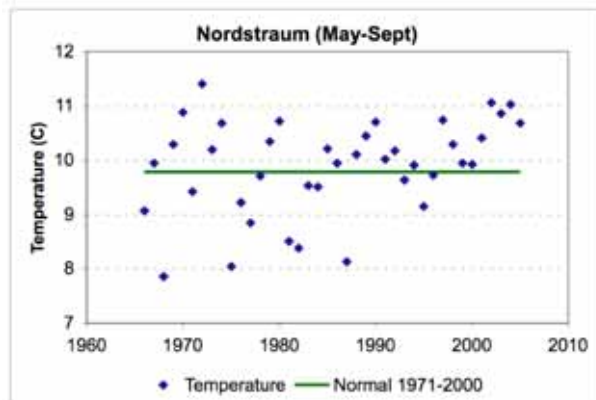


Figure 4. Summer temperatures (May-September) observed at Nordstraum, 34 km to the south of Langfjordjøkelen. The summer temperature has been above the mean (1971-2000) for the nine last years (1997-2005).

References

- Andreassen, L. M., Hallgeir Elverøy, Bjarne Kjølmoen, Rune V. Engeset, and Nils Haakensen. 2005. Glacier mass balance and length variation in Norway. *Annals of Glaciology*, 42 (in press).
- Benestad, R.E. 2005: Climate change scenarios for northern Europe from multi-model IPCC AR4 climate simulations. *GRL*, Vol. 32, L17704, doi:10.1029/2005GL023401
- Hanssen-Bauer, I, Ø. Nordli. 1998: Annual and seasonal temperature variations in Norway 1876 – 1997. *DNMI-report*, 25/98, 29 pp.
- Hanssen-Bauer, I. 2005. Regional temperature and precipitation series for Norway: Analyses of time-series updated to 2004. *met. no report*, No. 15/2005 Climate, 34 pp.
- Rasmussen, L. A., and H. Conway. 2005. Influence of upper-air conditions on glaciers in Scandinavia. *Annals of Glaciology*, 42 (in press).

A FIRST ORDER MODEL OF CALVING GLACIER DYNAMICS

DOUG BENN¹, NICK HULTON² AND RUTH MOTTRAM²

¹ The University Centre in Svalbard, Norway

² University of St Andrews, UK

Iceberg calving accounts for a high proportion of mass lost from high latitude ice sheets and glaciers. Recently-observed acceleration and retreat of calving glaciers worldwide indicates that the contribution of calving glaciers to sea-level rise is higher than previously thought, and that prediction of future water fluxes to the oceans must take glacier dynamics into account. The development of predictive models, however, is hampered by incomplete understanding of calving processes and associated glacier dynamics. Here we describe a new first-order model of calving glacier dynamics, which builds on previous work by van der Veen and Vieli, but incorporates additional key physical processes determining glacier terminus position and iceberg flux.

We assume that the position of the glacier terminus is defined by the point at which surface crevasses penetrate to the waterline. Below the waterline, creep closure is opposed by water pressure, so crevasses are able to penetrate the full thickness of the glacier, triggering calving. Crevasse depth is defined using the model of Nye (1955), which assumes that the equilibrium depth of a crevasse is where longitudinal strain rates are exactly balanced by creep closure due to ice overburden pressure. Glacier terminus position is therefore determined by longitudinal strain rates, or the downglacier velocity gradient ($\partial U / \partial x$). Where velocity gradients are high, crevasses may be able to penetrate to the waterline before the glacier reaches flotation, producing a grounded calving front. On the other hand, where there are only small longitudinal velocity gradients near the grounding line, an ice shelf may form.

The crucial issue is the way in which glacier velocity changes as ice thins towards the flotation thickness. This in turn depends upon the dominant source of resistance to glacier flow. Force balance analyses of both floating and grounded ice margins indicate that longitudinal stress gradients are of minor importance compared with lateral and basal drag. Where all or most of the driving stress is supported by lateral drag at flow-unit margins (as is the case for ice shelves and ice streams such as the Whillans), the centre-line velocity is independent of basal effective pressure, and is mainly controlled by flow-unit width. High longitudinal strain rates, therefore, will not occur across the grounding line if flow-unit width remains constant. Calving margins will tend to be located at flow-unit widenings, such as fjord mouths and the limits of embayments where lateral resistance decreases rapidly, ice accelerates, and high strain rates cause crevasses to deepen.

Ice sheet models commonly assume that all resistance to the driving stress is provided by drag at the bed, and that sliding velocity is directly proportional to the driving stress and inversely proportional to effective pressure at the bed

(Weertman-type sliding functions). In this case, ice velocity increases exponentially as ice thins towards the flotation thickness and effective pressure tends towards zero. Sliding functions of this sort predict infinite velocities when effective pressure vanishes, but this problem will not occur when the Nye crevasse-depth model is used to define the terminus position, because calving is predicted before flotation occurs. The coupled behaviour of Weertman sliding and the Nye calving criterion also provides insights into the causes of rapid glacier retreat between 'pinning points'.

In nature, resistance to flow is provided by both lateral and basal drag, in varying proportions. Using present approaches, incorporating both basal and lateral drag involves a considerable increase in model complexity, which is impractical for many applications. The development of simple sliding functions with both basal and lateral drag terms is an important goal for the future.

Geometry, mass balance and climate change response of Langjökull ice cap, Iceland

Helgi Björnsson¹, Sverrir Guðmundsson¹, Tómas Jóhannesson², Finnur Pálsson¹, Guðfína Aðalgeirsdóttir³, Hannes H. Haraldsson⁴

¹ Institute of Earth Sciences, University of Iceland, Sturlugata 7, 101 Reykjavík, Iceland

² Icelandic Meteorological Office, Bústaðavegur 9, 150 Reykjavík, Iceland

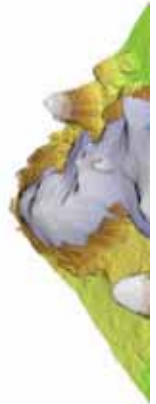
³ Department of Geography, University of Wales, Swansea, Singleton Park, Swansea SA2 8PP, Wales

⁴ National Power Company, Háaleitisbraut 68, 103, Reykjavík, Iceland

ABSTRACT The geometry of the surface and bed of Langjökull, Iceland, was constructed from GPS and radio-echo surveys in 1997. The mass balance of the ice cap was measured from 1996-1997 to 2004-2005 and linked to climatic variables recorded in automatic weather stations on the glacier every summer since yr. 2001, and to the records of the Hveravellir meteorological station east of the ice cap. A degree-day mass balance model was calibrated against stake observations of winter and summer balance on the glacier for 1997 to 2004. We used the mass balance model, coupled to a 3-D ice flow model, to simulate the evolution of Langjökull, over the next two centuries in response to a prescribed climate change scenario for Iceland (the Nordic CWE project). The volume of ice is predicted to decrease by half in 150 yrs and the glacier will have disappeared within 200 yrs. Runoff will increase until the close of the 21st century but decrease thereafter.

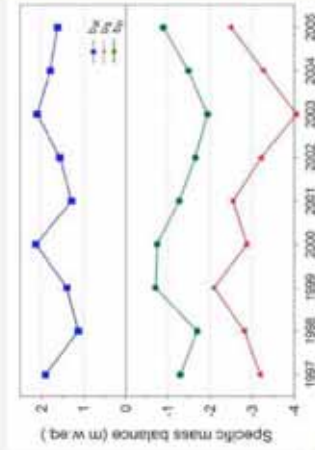
I. LOCATION AND GEOMETRY

Langjökull is the second largest ice cap in Iceland, 925 km² in area and 195 km³ in volume, with a maximum ice thickness of 580 m. Surface elevation ranges from 400 up to 1450 m and bed elevation from 390 to 1290 m a.s.l.



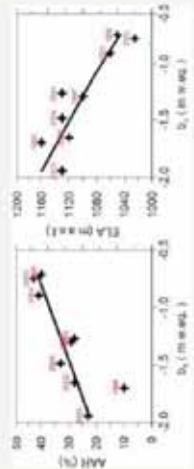
II. MASS BALANCE

Mass balance observations were carried out at 22 balance stakes (red dots, right) from 1996-1997 to 2005 (Björnsson et al. 2002).

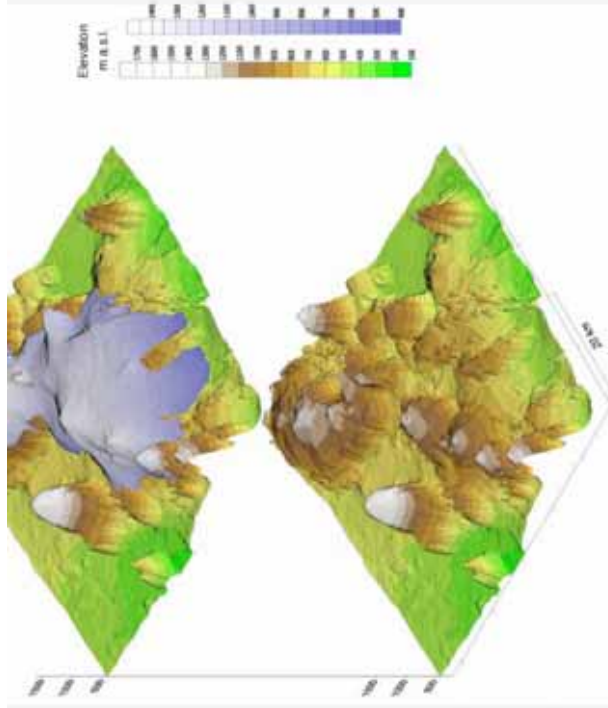


The mass balance was negative during the 9 yr period and the ice cap lost 6% of its total mass, equivalent to 11.7 m_{ice}, distributed equally over its surface.

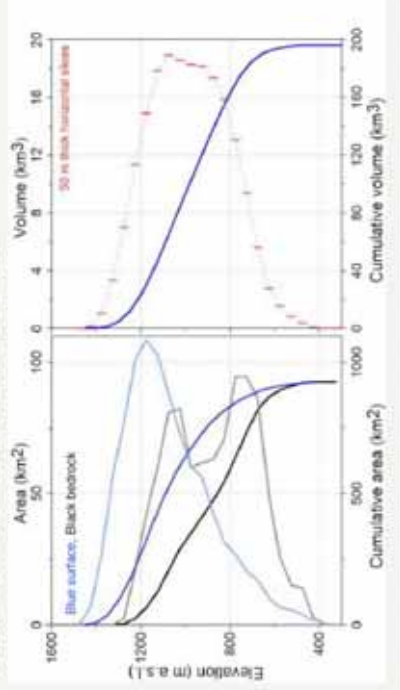
A typical specific runoff was about 3 m_{ice} a⁻¹ (left).



Equilibrium line altitude (ELA) and accumulation area ratio (AAR) in relation to annual mass balance (b_y) during 1997-2005.



Geometry: DEMs of the glacier surface and bed were constructed from GPS and radio-echo surveys in 1997. Area and volume distribution is shown below.

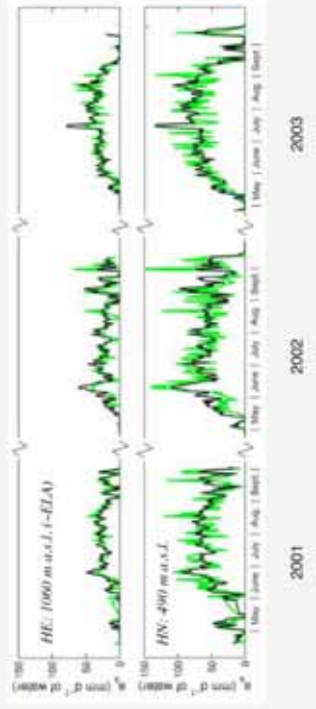
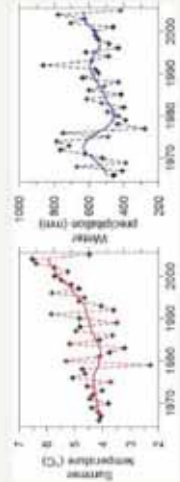


III. METEOROLOGICAL OBSERVATIONS, ENERGY BALANCE AND DEGREE-DAY MELTING MODELS



Automatic weather stations (AWS, red triangles) have been run during summer at two locations, HN and HE (providing energy balance) on the glacier and on two locations, SOD and NSK south of the glacier since 2001. HVE is a meteorological station (run by the Icelandic Meteorological Office, east of the ice cap where temperature and precipitation have been recorded since 1962).

HVE summer temperatures increased after 1980 but there is no apparent trend in winter precipitation. Measured HVE precipitation shows low correlation with the mean glacier winter balance.



Comparison of daily values of melting at the two AWS sites, computed by energy balance models (green) and degree-day temperature index models (black), calibrated to the 2001 temperature data at SOD. The correlation is 0.87 (HE) and 0.86 (HN).

IV. MASS BALANCE MODELING

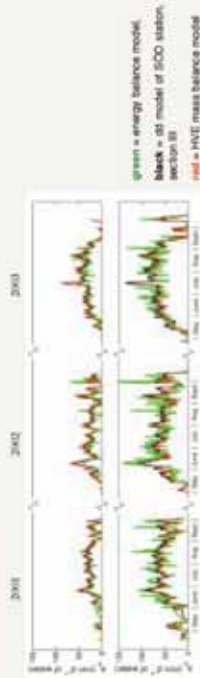
A degree-day mass balance model (Jóhannesson et al., 1995; Jóhannesson, 1997) uses daily temperature and precipitation data from Hveravellir (HVE, 641 m a.s.l.). Glacier surface temperature and precipitation fields were spatially-distributed and the mass balance model calibrated against 22 stake observations of winter and summer balances 1997 to 2004.

Model parameters:

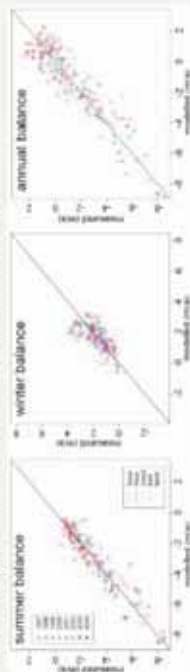
Constant vertical elevation lapse rate of $0.6\text{ }^{\circ}\text{C}$ per 100 m
 Constant snowfall temperature threshold of $1\text{ }^{\circ}\text{C}$

Degree-day factors: for ice $0.0071\text{ m}_{\text{ice}}\text{ }^{\circ}\text{C}^{-1}\text{ d}^{-1}$; for snow $0.0049\text{ m}_{\text{snow}}\text{ }^{\circ}\text{C}^{-1}\text{ d}^{-1}$

The parameters were in good agreement with those obtained for the degree-day model described in section III.

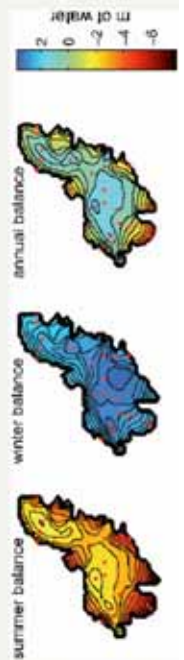


Measured and modeled mass balance on Langjökull 1996-2005



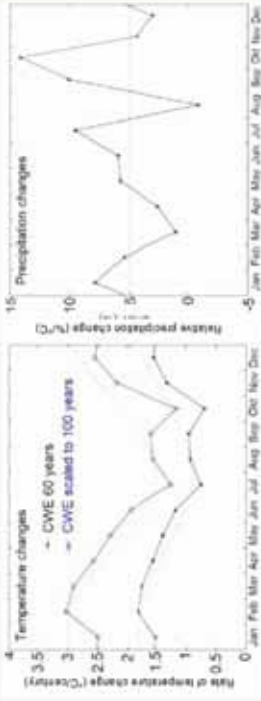
The mass balance model explains:

- 86% of the variance in the summer balance
- 35% of the variance in the winter balance
- 92% of the variance in the annual balance



VI. RESPONSE TO A PRESCRIBED CLIMATE CHANGE SCENARIO FOR ICELAND

The mass balance and ice flow models were coupled to simulate the response of the glacier to climate change. A climate change scenario, near Iceland 1990-2050, was defined in the Nordic CWE research program (Rummukainen et al. 2003).



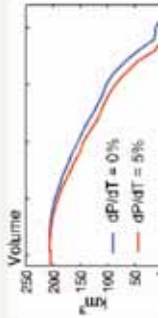
The dashed curves were used in the glacier model simulations

Temperature changes with time:

- Sinusoidal variation through the year
- Continuous linear warming rate of $+0.3\text{ }^{\circ}\text{C}$ per decade in mid-winter and $0.15\text{ }^{\circ}\text{C}$ per decade in mid-summer, starting from 1990.

Precipitation changes with temperature (dP/dT):

- 5% per $1\text{ }^{\circ}\text{C}$ of warming, independent of season
- The period 1961-2000 was chosen as initial reference climate and the simulation started in 1990.



Model prediction:

The volume of the ice cap is reduced by half within 150 years from now and the glacier disappears within 200 years. The retreat is relatively slow during the next 50 years but after just over 100 years the ice cap will be split into two separate

FOCUS ON THE ARCTIC CALVING GLACIERS: PROMOTION OF THE IPY GLACIODYN PROJECT AND GLACIOLOGICAL KNOWLEDGE WITHIN TOURISTS - OUR TAXPAYERS

E. BUKOWSKA-JANIA¹, J. JANIA², P. GLOWACKI³, L. KOLONDRAS² AND M. GRABIEC²

¹ Unit of Geo-Ecotourism, Faculty of Earth Sciences, University of Silesia, Poland,

² Department of Geomorphology, Faculty of Earth Sciences, University of Silesia, Poland

³ Institute of Geophysics, Polish Academy of Sciences

Introduction

The importance of ice masses in the context of global climate changes and sea-level rises is far from well understood by the majority of those responsible for the allocation of research funds - the politicians and taxpayers. This is despite the fact that many glaciers, especially calving forms, are highly attractive to thousands of tourists who take millions of photographs of them (Fig. 1). Further, we believe that, in many cases, a majority of local tourist agencies, tourist operators and individual guides are largely ignorant in respect of basic concepts of glacier behaviour (Fig. 2) and even geographic location. There are, thankfully, a few exceptions to this general rule (e.g. Iceland).



Figure 1. Tourists close to the ice-cliff of Hansbreen (Spitsbergen, Svalbard) one of the GLACIODYN target glacier (Photo by Leszek Kolondra).

One of the priorities of the 4th International Polar Year dissemination of scientific results is education at different levels within general society. The aim of this paper is to suggest a way of promoting knowledge about glaciers, especially tidewater ones, in the context of global warming and sea level change among the general public. We propose to do this by improving the "teaching of the tourist". We propose to use the tourists who visit the Arctic glaciers as our "ambassadors", i.e.

Severnaya Zemlya; Glacier No. 1, Hall Island, Franz Josef Land; Devon Ice Cap, Canada; McCall Glacier, Alaska). In any case, they are not easy to visit, even by scientists. Logistic problems, costs of travel, political situation and environment protection restrictions are, in fact, different for all of the target glaciers.



Figure 3. Location of target glaciers of the GLACIODYN project (red dots). Most popular tourist areas indicated by arrows.

Proposed means of promotion

For better transfer of knowledge on studies of glaciers to the “average” tourist, the direct involvement of scientists who are partners in the IPY project is desirable. We propose the establishment of a sub-project within the GLACIODYN publicly oriented. Publication of a folder only seems to us to be inadequate.

We propose that a small group from within the partnership collate and provide basic information on target glaciers and the most spectacular (from a public relations point of view) experiments or monitoring results on these.

By assembling such data, three levels of information and advice might be prepared and disseminated.

1. Advice to local tourist authorities on a wider and deeper inclusion of glaciological science in general tourist information (regional tourist information booklets, information boards located in the field etc.). Exposition of the importance of the GLACIODYN project for particular glaciers (or area).
2. Suggestions to tourist operators on how to make a particular glacier a more attractive "tourist product", apropos its role in the IPY program and with the demonstration of examples of specific experiments and their results.
3. Providing tourist operators, their guides and tourists themselves with properly edited booklets on these glaciers, the glacial processes in the areas of interest and the leading aims of the GLACIODYN project, stressing, not only in English, what results ought to be forthcoming from these efforts. As a backup to this, an attractive web page has to be run and updated at regular intervals. At this level, some financial contributions from tourist agencies are to be invited.

The proposed booklet should contain:

- general information on glaciers and glacial processes with clear diagrams;
- explanation of why glaciers are important for the global environment changes, especially tidewater forms;
- a short description of the GLACIODYN project and an annotated list of the target glaciers;
- an extended description of glaciers easily accessible to tourists;
- examples of the most spectacular glaciers and important experiments/monitoring programs, with preliminary results if available;
- a short glossary of glaciological terms;
- references to popular and scientific books and web pages.

Conclusions

As Arctic tourists usually share impressions of their holidays with families, friends and club members, they are, in a sense, prospective ambassadors of glaciological knowledge and the GLACIODYN project details should be extended to the relevant tourist agencies, thereby improving the attractiveness of their business offer.

The small sub-project of the GLACIODYN, as proposed here, would have as its aims:

- to help tourist operators improve the scientific content of the tour programs by the publication of a comprehensive booklet on calving glaciers; also by the provision of "approved" scientists (such as research students) in the execution of some tours (i.e. a pool of scientists/specialists should be available for particular regions);
- to monitor number of visitors of target glaciers or their proximity;
- to study programs of excursions and level of guidance (where possible);
- to monitor results of this sub-project and interactive web page, asking tourists on comments and impressions;
- to prepare reports on results of the sub-project activity.

Publication of a booklet for tourists and the establishment of a web page (in different languages) seems to be essential.

The suggested activity should be regarded as complimentary to alternative methods by which the scientific results of the IASC Working Group on Arctic Glaciology are traditionally made available to the general public.

DYNAMICAL DOWNSCALING OF ERA-40 PRECIPITATION FOR MODELLING SNOW ACCUMULATION ON ICE CAPS IN ICELAND

PHILIPPE CROCHET¹, TÓMAS JÓHANNESSON¹, ODDUR SIGURÐSSON², HELGI BJÖRNSSON³ AND FINNUR PÁLSSON³

¹Icelandic Meteorological Office, Bústaðavegur 9, IS-150 Reykjavík, Iceland

²National Energy Authority, Hydrological Service Division, Reykjavík, Iceland

³Institute of Earth Sciences, University of Iceland, IS-107 Reykjavík, Iceland

Extended abstract

Spatial distribution of precipitation in Iceland is estimated by dynamical downscaling of ERA-40 precipitation, using the theory of orographic precipitation proposed by Smith and Barstad (2004). The airflow pattern over complex terrain is simulated using linear mountain-wave theory and the resulting precipitation field is found using a linear cloud physics representation. The input parameters of the model are large-scale surface temperature, wind speed, wind direction and background precipitation (all given by ERA-40 reanalysis data), static stability and cloud-water conversion and hydrometeor fallout times (estimated by calibration against glaciological data). This procedure makes it possible to simulate the distribution of snow accumulation on glaciers and ice caps in much more detail than has usually been done in glacier mass balance studies, and opens up new possibilities to model mass balance on glaciers and ice caps in complex topography.

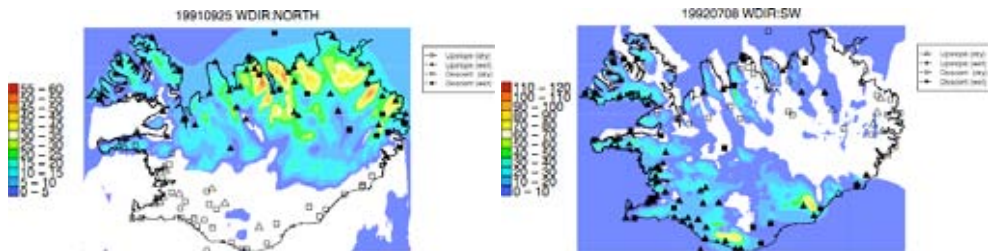


Figure 1. Simulated daily precipitation on 25 September 1991 when the main wind direction on and near Iceland was from the north (left) and on 8 July 1992 when the wind direction was from the southwest (right). Locations of weather stations are shown with symbols. Filled (open) symbols denote station where precipitation was observed (not observed). Triangles (squares) denote stations on the windward (lee) side of mountains.

As an example Figure 1 shows simulated precipitation for two days in 1991 and 1992, one with northerly winds and the other with wind from the southwest. Intensification of the precipitation on the windward side of mountains near the coast and a precipitation shadow on the lee side of the mountains is clearly visible.

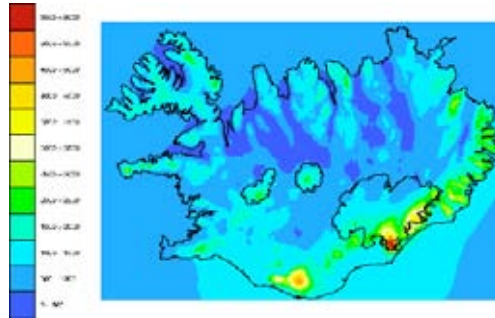


Figure 2. Simulated accumulated precipitation during the winter 1997/1998.

Figure 2 shows the pattern of the accumulated precipitation for the winter 1997/1998. The figure shows various small-scale features related to orographic generation of precipitation, which are in general agreement with what is known about the distribution of precipitation in Iceland from glacier mass balance measurements and from observations at meteorological stations.

Acknowledgements

This study was carried out as a part of the projects *Climate and Energy* (CE), funded by the Nordic Energy Research of the Nordic Council of Ministers, and *Veðurfar og orka* (VO), sponsored by the National Power Company of Iceland and the National Energy Fund of Iceland. We thank R. B. Smith and I. Barstad for providing the source code of the linear orographic precipitation model.

References

Smith, R. B. and I. Barstad. 2004. A linear theory of orographic precipitation. *J. Atmos. Sci.*, **61**, 1377–1391.

THE EFFECT OF THE FIRN LAYER ON GLACIAL RUNOFF OF HOF SJÖKULL ICE CAP, ICELAND

MATTIAS DE WOUL¹, REGINE HOCK¹, MATTHIAS BRAUN², THORSTEINN THORSTEINSSON³, TÓMAS JÓHANNESSON⁴ AND STEFANÍA HALLDÓRSDÓTTIR³

¹ Department of Physical Geography and Quaternary Geology, Stockholm University, Sweden

² Center for Remote Sensing of Land Surfaces, University of Bonn, Germany

³ Orkustofnun (National Energy Authority), Reykjavik, Iceland

⁴ Icelandic Meteorological Office, Reykjavik, Iceland

A mass balance-runoff model is applied to Hofsjökull, an 880 km² ice cap in Iceland, in order to assess the importance of the firn layer on glacial runoff. The model is forced by daily temperature and precipitation data from a nearby meteorological station. Water is routed through the glacier using a linear reservoir model assuming different storage constants for firn, snow and ice. The model is calibrated and validated using mass balance data and satellite derived snow facies maps. Simulated mass balances as well as snow line retreats are generally in good agreement with observations. Modelled cumulative mass balance for the entire ice cap over the period 1987/1988 to 2003/2004 is -7.3 m with uninterrupted negative mass balances since 1993/1994. Perturbing the model with a uniform temperature

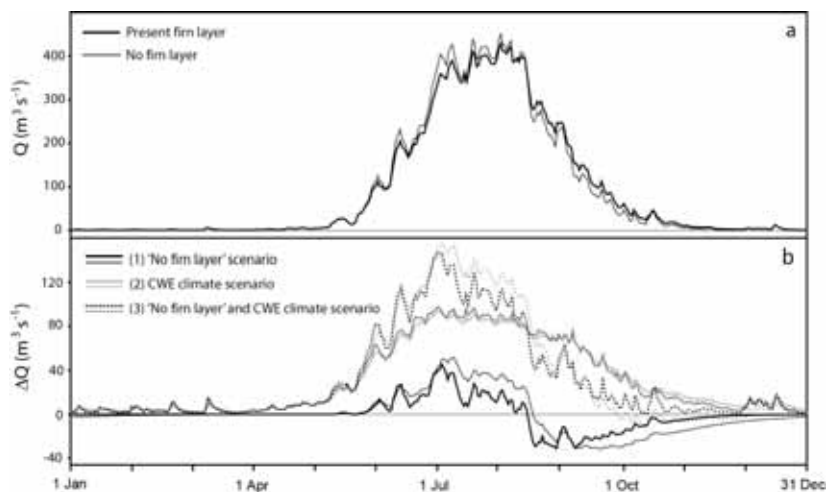


Figure 1. (a) Modelled daily discharge, Q ($\text{m}^3 \text{s}^{-1}$), from Hofsjökull ice cap averaged over the period 1988 to 2004 for two model runs assuming present firn layer extent and a scenario where the firn layer is removed; both runs using present climate conditions. (b) Differences in daily discharge, ΔQ ($\text{m}^3 \text{s}^{-1}$), between two model runs averaged over the period 1988 to 2004: (1) model results assuming removal of firn layer minus results assuming present firn layer, both runs using present climate conditions, (2) model results assuming CWE climate scenario (Rummukainen et al., 2003; Kuusisto, 2004) minus results assuming present day climate, both runs with present firn layer, (3) as (2) but both model runs without firn layer. Thicker and thinner lines refer to two different model runs using two different sets of storage coefficients in the linear reservoir discharge model.

(+1 K) and precipitation (+10%) increase yields static mass balance sensitivities of -0.95 m a^{-1} and $+0.23 \text{ m a}^{-1}$, respectively. Removing the firn layer under otherwise likewise conditions results in almost unchanged total runoff volumes but yields a redistribution of discharge within the year (Fig. 1). Early summer discharge (June to mid August) is amplified by roughly 5-10% while late summer/autumn discharge (mid August to November) is reduced by 15-20% as a result of accelerated water flow through the glacial hydrological system. In comparison, applying a climate model based temperature and precipitation scenario for Iceland until 2050 results in higher runoff throughout the year, increasing total runoff by roughly one third. Our results emphasize the role of the firn layer in delaying water flow through glaciers, and the influence on discharge seasonality when firn areas shrink in response to climate change induced glacier wastage.

References

- Kuusisto E. 2004. *Climate, Water and Energy. A summary of a Joint Nordic Project 2002-2003*. CWE Rep. No. 4, 28 pp.
- Rummukainen M, Räisänen J, Bjørge D, Christensen JH, Christensen OB, Iversen T, Jylhä K, Ólafsson H, Tuomenvirta H. 2003. Regional climate scenarios for use in Nordic water resources studies. *Nordic Hydrology* **34**(5): 399-412.

REGIONAL CLIMATE MODELLING OF THE GREENLAND ICE SHEET

JANNEKE ETTEMA¹, MICHEL VAN DEN BROEKE¹, ERIK VAN MEIJGAARD²,
JONATHAN BAMBER³, RUPERT GLADSTONE³ AND JENNIFER GRIGGS³

¹ Utrecht University, Institute for Marine and Atmospheric Research (IMAU)

² Royal Netherlands Meteorological Institute (KNMI)

³ Bristol University, School of Geographical Sciences

Introduction

The results presented here are part of the RAPID-project “Mass balance and freshwater contribution of the Greenland ice sheet: a combined modelling and observational approach” that aims to study rapid climate changes in the North Atlantic and its effects on the surface mass balance and freshwater contributions of Greenland ice sheet using an atmospheric limited area model. We use the Regional Atmospheric Climate Model version 2.1 (RACMO2.1) of the Royal Netherlands Meteorological Institute (KNMI). This model has been successfully applied in Antarctic climate studies (Van de Berg *et al.*, 2004, Reijmer *et al.*, 2005). The strong seasonal melting in the well-defined ablation zone of the Greenland ice sheet is important for its mass balance. Simulations with two different snow schemes in the single column model version of RACMO2.1 over a location in the ablation zone shows that processes like retention and refreezing of melt water are important for realistically representing snow under melting conditions.

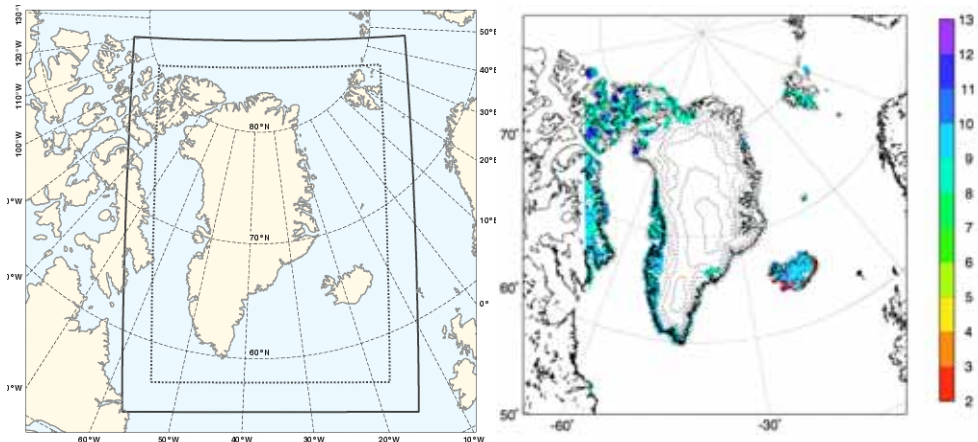


Figure 1. Left: RACMO2.1 model grid for Greenland. Right: low vegetation map RACMO2.1. Numbers refer to low vegetation type (2: short grass, 7: tall grass, 8: desert, 9: tundra, 11: semi desert, 13: bogs and marshes). Contour lines indicate surface height on 500 m intervals from US Navy dataset.

Model Setup

The atmospheric dynamics in RACMO2.1 originates from the High Resolution Limited Area Model (HIRLAM, version 5.0.6). The description of the physical processes is adopted from the European Centre for Medium-Range Weather

Forecasts (ECMWF, cycle 23r4). The horizontal resolution of RACMO2.1 over Greenland will be ~18 km (figure 1). The model has 40 atmospheric hybrid-layers in the vertical, of which the lowest is ~10 m above the surface. The hybrid-layers follow the topography close to the surface and pressure levels at higher altitudes. ECMWF Re-Analysis (ERA-40) fields force the model at lateral boundaries, while the interior of the domain is allowed to evolve freely. Sea surface temperature and sea ice fraction are prescribed from ERA-40.

For an accurate topographic representation of the Greenland ice sheet, height data of the digital elevation model of Bamber *et al.* (2001) will be used. The global U.S. Navy data is used as standard height dataset in RACMO2.1, but it gives non-smooth height contours as shown in Figure 1. Other adjustments are needed to the vegetation map underlying RACMO, which exposes too little tundra along the east coast (Figure 1).

Here, two snow schemes are tested for their ability to simulate melting snow. The original description of snow in RACMO2.1 describes the Greenland ice sheet as a single layer of snow with a climatological depth of 10 m w.e. Because a single layer of 10 m w.e. has a too large thermal inertia, the depth of the thermal calculations is limited to 1 m of snow. There is no melt or refreezing in this snow scheme. The second snow scheme tested is the englacial module of a surface mass balance model (Bougamont *et al.*, 2005) including subsurface processes in snow such as water percolation, retention and refreezing. These processes are modelled for 25 m w.e. of firn/snow/ice, composed of a maximum of 100 layers. Initially the thickness of each individual layer increases linearly with depth with an upper layer thickness of 0.09 m. Layer thickness varies due to melting, freezing or accumulation. An infinitely thin skin layer is used to calculate the surface energy fluxes and the surface temperature as input to both schemes. For testing and comparing both snow schemes they were imbedded in the single column version of RACMO2.1, which is essentially an isolated column of air over a snow surface located in the ablation zone.

Results

A number of experiments was performed with the single column model to test both schemes, the original snow scheme as reference (ref) and the new multilayer snow approach (smb). The experiments presented here are driven by prescribed initial atmospheric profiles of temperature, humidity and wind speed taken from ERA-40. Due to the initially cold atmosphere there is no melt at the surface. The single snow layer in the original scheme is initialized as 10 m w.e. snow with the same properties as the upper 5 m snow in the new scheme that is lying on top of 20 m of colder ice. The single column model is allowed to evolve freely over the full period of 6.5 days starting at 12 UTC. In two subsequent melting experiments (ref-melt and smb-melt) the temperature profile is increased such that the lower atmosphere is warmer than the melting point. No precipitation is simulated in the experiments.

Figure 2 shows surface albedo and snow temperature and density of the single layer for the original snow scheme and of the first snow layer in case the new scheme is used. The single layer of snow is rather insensitive to the increase of atmospheric temperature (ref and ref-melt). Its snow temperature, density and

surface albedo are very similar under these very different atmospheric conditions due its large volumetric heat capacity. Splitting the snow pack into multiple layers, like done in the new snow scheme, does not largely affect the snow properties of the top layer under non-melting conditions (Figure 2, smb). Differences in surface albedo and snow density between the schemes are due to different parameterizations used. Under warmer atmospheric conditions the upper snow layer quickly reaches the melting point and starts to melt. At day 4 the upper snow layer is fused with the underlying layer causing a jump in snow density and surface albedo.

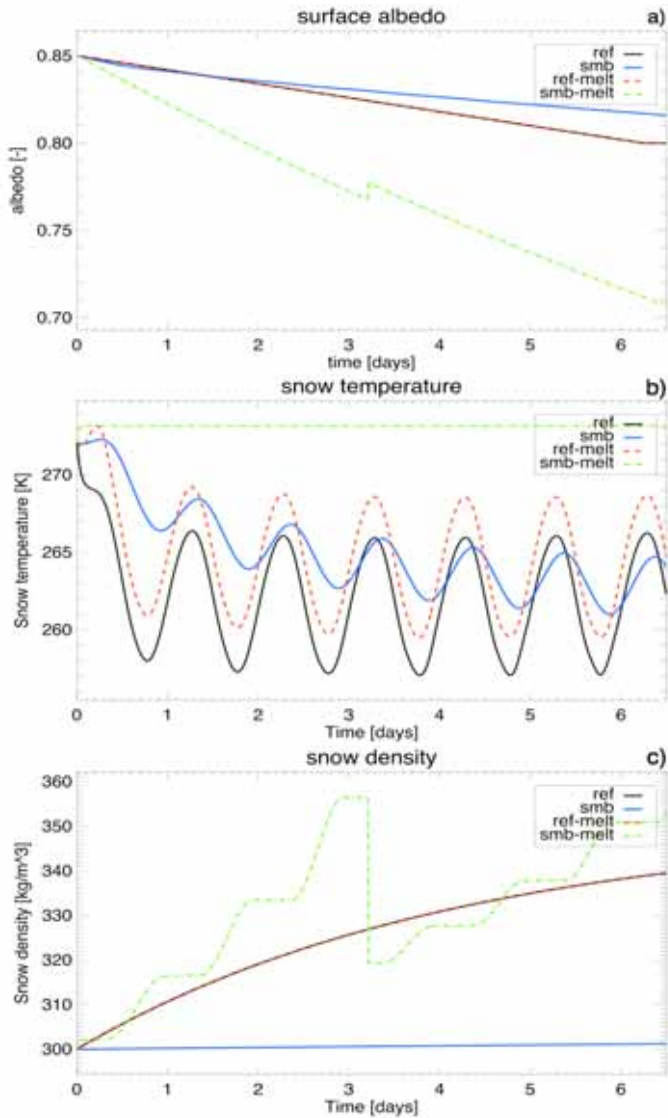


Figure 2. Time series of surface albedo (a), snow temperature (b) and density (c) of the top layer simulated with the original (ref) and new (smb) snow scheme imbedded in single column model version of RACMO2.1 under non-melting and potential melting (melt) atmospheric conditions.

Snow temperature, density and water content of the upper 5 m of fresh snow under melting conditions are presented in Figure 3. The warm atmosphere persistence in time allows underlying snow layers to warm up and an isothermal layer is formed. Melt water is present and percolates further downward if the maximum retention capacity is exceeded. Due to high temperatures at the surface no refreezing of melt water in the snow pack is occurring.

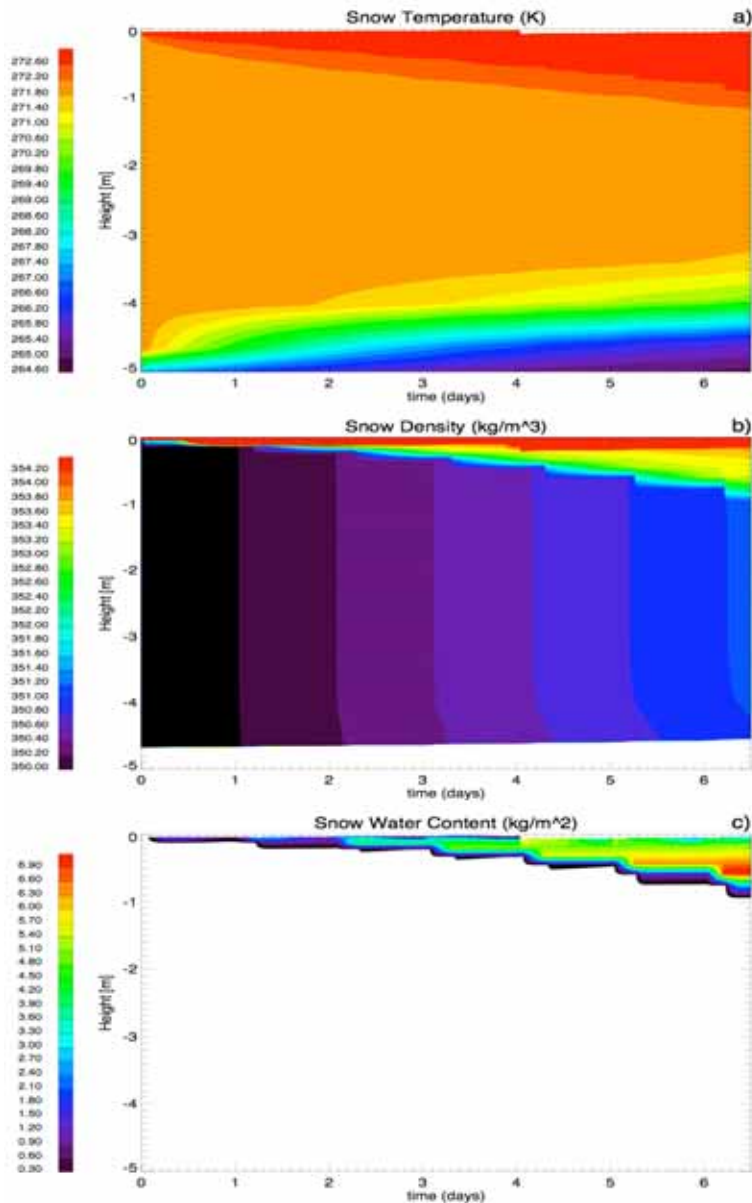


Figure 3. Evolution in time of the multilayer snow pack properties in smb-melt for temperature (a), density (b) and water content (c) under melting conditions.

Conclusions and outlook

To accurately estimate the surface mass balance of the Greenland ice sheet it is important to simulate the widespread seasonal melt in time and space. Two different snow schemes are tested under melting and non-melting atmospheric conditions with a single column model version of RACMO2.1. For non-melting conditions both schemes perform very similar. Under melting conditions the new snow scheme is able to melt a thin layer of snow, where as the warming of the single snow layer in the original scheme is much slower due to its thickness. In this study we have seen that a single layer approach of the Greenland ice sheet is not capable to deal with melt. Instead the new snow scheme of Bougamont *et al.* (2005) will be used in RACMO2.1.

References

- Bamber J., S. Ekholm, W.B. Krabill (2001), A new, high-resolution digital elevation model for Greenland fully validated with airborne laser altitude data, *J. Geophys. Res.*, 106, 33773-33780
- Bougamont, M., J.L. Bamber, W. Greuell (2005), A surface mass balance model for the Greenland Ice Sheet, *J. Geophys. Res.*, 110, F04018, doi:10.1029/2005JF000348
- Reijmer, C.H., E. van Meijgaard, M.R. van den Broeke (2005), Evaluation of temperature and wind over Antarctica in a Regional Atmospheric Climate Model using one year of automatic weather station data and upper air observations, *J. Geophys. Res.* 110, D04103, doi:10.1029/2004JD005234
- Van de Berg, W.J., M.R. van den Broeke, C.H. Reijmer, E. van Meijgaard (2005), Characteristics of the Antarctic surface mass balance (1958-2002) using a Regional Atmospheric Climate Model, *Ann. Glac.* 41, in press

CHANGES IN GEOMETRY AND HYDROTHERMAL STRUCTURE OF FRIDTJOVBREEN, A POLYTHERMAL GLACIER IN SPITSBERGEN, FOLLOWING ITS SURGE IN THE 1990s MODEL

A.F. GLAZOVSKY¹, I.I. LAVRENTIEV², YU.YA. MACHERET¹, F.J. NAVARRO³
AND E.V. VASILENKO⁴

¹ Institute of Geography, Russian Academy of Sciences, Moscow, Russia

² Moscow State University, Moscow, Russia

³ Polytechnic University of Madrid, Spain

⁴ Institute "Akademprigor", National Academy of Sciences of Uzbekistan, Tashkent, Uzbekistan

Fridtjovbreen, a tidewater glacier in Spitsbergen, is one among the many glaciers in Svalbard identified as polythermal from data of airborne radio-echo soundings (RES) performed by Soviet, British and Norwegian expeditions in 1974-1984 at frequencies of 440, 620 and 60 MHz (Dowdeswell et al., 1984; Bamber, 1989; Macheret and Zhuravlev, 1975; Macheret et al., 1992; Jiscot et al., 2000). Such glaciers are characterized by an upper cold ice layer overlying a temperate ice layer; strong radar internal reflections from the boundary between both layers is the most striking indicator of their polythermal character. Fridtjovbreen is one among only five glaciers in Svalbard for which two surges have been observed; at Fridtjovbreen they occurred in the 1860s and ~133 years later, in the 1990s, probably between 1992 and 1997 (Murray et al., 2003).

In this paper we consider the changes in ice thickness and hydrothermal structure of the glacier, as determined by comparing repeated ground-based radio-echo-sounding (RES), geodetic, GPS and radio wave velocity (RWV) measurements performed before and after its surge in the 1990s; in particular, during the period from 1977 to 2005 (Figure 1). RES measurements were made in 1977, using 620 MHz radar, along a transverse profile at the ice divide (Macheret et al., 1980) and along a longitudinal profile from the ice divide to the glacier terminus; in 1988, they were done, using 8 MHz radar together with geodetic positioning, along a set of transverse and longitudinal profiles covering the whole glacier (Glazovsky et al., 1991); in 2005, using 18 MHz radar together with GPS positioning, along two profiles previously measured in 1977 and 1988 plus along a transverse profile at a distance of 2 km from the glacier calving front. Repeated RWV measurements were made at the ice divide in 1977 (Macheret and Glazovsky, 2000) and 2005 (sites 1a and 1b in Figure 1, respectively); and at a distance of 3 km from it in 1979 and 1988 (site 2a) (Macheret and Glazovsky, 2000) and 2005 (site 2b).

Comparison of the repeated RES data shows that remarkable changes in ice thickness (ranging from -180 to +60 m) occur along the whole glacier. These changes consist of thinning at higher elevations and thickening at lower elevations, consistent with the surge occurrence and with the pattern of elevation changes derived from airborne lidar data by Bamber et al. (2005). Remarkable changes are also observed in the hydrothermal structure of the glacier and in the water content

of its temperate ice layer, as shown by repeated RWV measurements. In particular, at the ice divide (sites 1a and 1b) the average RWV changed from 161.4 m/ μ s in July 1977 to 165.0 m/ μ s in August 2005; at the location 3 km apart from the ice divide (sites 2a and 2b) the average RWV was 169.6 \pm 2.1 m/ μ s in April 1988 and 173.8 m/ μ s in August 2005; at the ice divide the average water content in the temperate ice layer was 2.4% in July 1977 and 0.8% in the whole ice column in August 2005. Note, however, that the sites for 1977-79-88 measurements are not exactly coincident with those of 2005 measurements. Other related RWV and ice thickness data are summarized in Table 1.

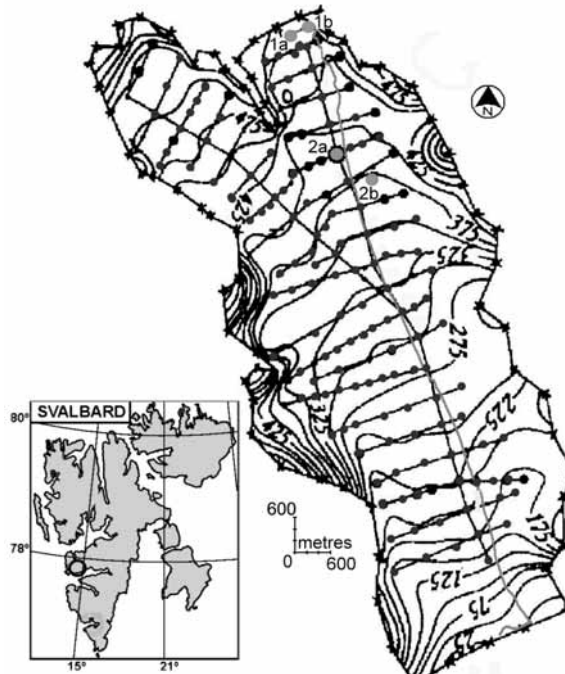


Figure 1. Map of Fridtjovbreen. Contour lines every 25 m. Black straight segments are RES profiles done in 1977-1988 with 8 MHz radar and partly with 620 MHz radar (along the upper transverse profile at the ice divide and along the central longitudinal profile), while grey line corresponds to 2005 18 MHz RES profile. Gray dots are points of RWV measurements. The small circle in the inset shows the location of the glacier within Svalbard.

Evident from the data are: 1) an increase in RWV and, correspondingly, a decrease in water content, which could be understood as an indicator of colder ice; 2) a noisy pattern of internal reflections/diffractions, probably as a consequence of the chaotic pattern of fractures and closed-up crevasses observed on the glacier surface; and 3) the absence of a distinguishable reflection from the cold-temperate ice boundary (perhaps due to 2). Caution should be taken, however, with regard to the first observation, because of the slightly different location of 1977-79-88 and 2005 RWV measurements, as well as the different period within the year when the

measurements were done, so that the spatial and seasonal variations in glacier conditions could account for at least a part of the observed differences in RWV.

Further radar profiling, using a higher frequency radar, and CMP measurements (as close as possible to 1977-79-88 CMP locations) are planned for Spring 2007. These are expected to provide additional data which, combined with the above-mentioned and other available geodetic, lidar and radiointerferometry data on glacier surface elevation for the periods 1936-1988, 1936-1997 and 1996-2002 (Glazovsky et al., 1991; Zinger et al., 1997; Bamber et al., 2005) and data on ice velocity for the period 1991-1997 (Murray et al., 2003), will allow us to estimate the connection between the hydrothermal structure of the glacier and its geometry and dynamics for the periods before the surge (1936-1990s) and after surging (1990s-2005).

Table 1. Hydrothermal structure of Fridtjovbreen, at the ice divide (sites 1a and 1b) and 2 km apart from it (sites 2a and 2b), before and after its surge in the 1990s, retrieved from RWV measurements. H is the total ice thickness, h_d is the thickness of the cold ice layer, h_s is the thickness of the whole temperate ice layer, h_{s1} is the thickness of the upper part of the temperate ice layer, V is the average RWV in the whole ice column, V_s is the average RWV in the whole temperate ice layer, V_{s1} is the average RWV in the upper part of the temperate ice layer, W is the average water content in the whole ice column, W_s is the average water content in the whole temperate ice layer, W_{s1} is the average water content in the upper part of the temperate ice layer.

Parameter	Site 1a July 1977	Site 1b August 2005	Site 2a July 1979	Site 2a April 1988	Site 2b August 2005
H , m	213 ± 5	158	220 ± 10	247 ± 10	137
h_d , m	72 ± 5		120 ± 10	125 ± 10	
h_s , m	141 ± 5		100 ± 10	122 ± 10	
h_{s1} , m			28		
V , m/μs	161.4	165.0	-	169.6 ± 2.1	173.8
V_s , m/μs	156.4 ± 0.5		-	167.3 ± 4.3	
V_{s1} , m/μs			147.7		
W , %		0.8			0
W_s , %	2.4		-	0.17 $\frac{+0.88}{-0.17}$	
W_{s1} , %			4.5		

References

- Bamber J.L. Ice/bed interface and englacial properties of Svalbard ice masses from airborne radio-echo sounding. *Journal of Glaciology*, vol. 35, No 119, 1989, p. 30-37
- Bamber J.L., Krabill W., Paper V., Dowdeswell J.A., Oerlemans J. Elevation changes measured on Svalbard glaciers and ice caps from airborne lidar data. *Annals of Glaciology*, vol. 42, 2005 (in press).
- Dowdeswell J.A., Drewry D.J., Liestøl O., Orheim O. Airborne radio-echo sounding of sub-polar glaciers in Spitsbergen. *Norsk Polarinstitutt Skrifter* 182, 1984, 42 pp.
- Glazovsky A.F., Macheret Yu. Ya., Moskalevsky M.Yu., Jania J. Tidewater glaciers in Spitsbergen. *Glacier-Ocean-Atmosphere Interactions. Proceedings of St. Petersburg Symposium*, September 1990. IASH Publ. No 208, 1991, p. 229-239.
- Jiscoot H., Murray T., Boyle P. Controls on the distribution of surge-type glaciers in Svalbard. *Journal of Glaciology*, vol. 42, No 154, 2000, p. 412-421.

- Macheret Yu.Ya., Glazovsky A.F. Estimation of absolute water content in Spitsbergen glaciers from radar sounding data. *Polar Research*, vol. 19, No 2, 2000, p. 204-216.
- Macheret Yu. Ya., Zhuravlev A.B., Gromyko A.N. Radiolokatsionnye issledovaniya na Shpitsbergene v 1977 godu [Radar sounding studies in Spitsbergen in 1977]. *Materialy glyatsiologicheskikh issledovaniy*, vol. 38, 1980, p. 279-286.
- Macheret Yu.Ya., Glazovsky A.F., Ignatieva I.Yu., Krass M.S., Konstantinova T.N., Larina T.B., Moskalevsky M. Yu. Stroyeniye, gidrotermicheskoye sostoyaniye i rezhim subpolyarnykh lednikov. [Structure, hydrothermal state and regime of subpolar glaciers]. In: V.M. Kotlyakov (ed.). *Rezhim i evolyutsiya polyarnykh lednikovykh pokrovov* [Regime and evolution of polar ice sheets]. St-Petersburg, 1992, p. 48-115.
- Macheret Yu., Ya., Zhuravlev A.B. Tolshchina, ob'yem i srtoeniye lednikov [Ice thickness, volume and structure of glaciers]. In: V.M. Kotlyakov (ed.). *Glyatsilogiya Shpitsbergena* [Glaciology of Spitsbergen]. Moscow, Publishing House "Nauka", 1975, p. 7-35.
- Murray T., Luckman A., Strozzi T., Nuttall. A.-M. The initiation of glacier surging at Fridtjovbreen, Svalbard. *Annals of Glaciology*, vol. 36, 2003, p. 110-116.
- Zinger E.M., Zakharov V., G., Zhidkov V.A. Nablyudeniya za podvikhoy lednika Fridtiov na Shpitsbergene v 1997 godu [Observations on surge at Fridtjovbreen in 1997]. *Materialy glyatsiologicheskikh issledovaniy*, vol. 83, 1997, p. 231-233.

CALVING GLACIERS OF NOVAYA ZEMBLA AND FRANZ JOSEPH LAND

ANDREY GLAZOVSKY, YURY MACHERET AND EVGENY VASILENKO

Institute of Geography, Russian Academy of Sciences, Moscow, Russia

Tidewater glaciers constitute a large portion of glacierized area of the Russian Arctic. Total number of these glaciers is 852 on Franz Josef Land, 48 on Severnaya Zemlya, and 39 on Novaya Zemlya. The total length of their ice fronts is 2510 km, 443 km, and 230 km, respectively.

These glaciers are the iceberg producers for the waters of the Arctic shelf seas. It is important that the iceberg production is estimated, seen on the background of general glacier recession in the archipelagos. In the last 50 years the glacierized area has decreased by 725 km² (1.3%) as minimum estimate: this includes 375.4 km² (2.7%) on Franz Josef Land, 284.2 km² (1.2%) on Novaya Zemlya, and 65.4 km² (0.4%) on Severnaya Zemlya. This recession amplifies the ice front instability and might favour the occurrence of large icebergs.



Figure 1. The area where airborne radio echo sounding on Franz Josef Land were carried out, April 2005

Icebergs are a potential threat to the development of the Arctic shelf resources. For example on Shtokman gas-condensate field in the Barents Sea, the mass of the largest iceberg was expected to be up to $0.6 \cdot 10^6$ t. However, the AARI expedition in May 2003 spotted a fleet of 96 icebergs in this area, and the largest one was $3 \cdot 10^6$ t.

In spring 2005 we performed field studies including radio echo sounding of glaciers in southern Franz Josef Land (Fig.1) and in north-western Novaya Zemlya (Fig. 2),

as well as on the icebergs in the Barents Sea waters. The measured iceberg thickness varied in the range of 30 to 100 m.

The maximum sizes of potential icebergs have been assessed for the glaciers of southern Franz Josef Land by the data of ice thickness and ice surface elevation and based on flotation criteria estimations. The iceberg sizes might reach up to 3 km long and up to 200 m thick.

The glaciers most favourable for large iceberg production have been identified in north-western Novaya Zemlya using relationships of ice thickness change with current ice surface elevation derived from radar data.

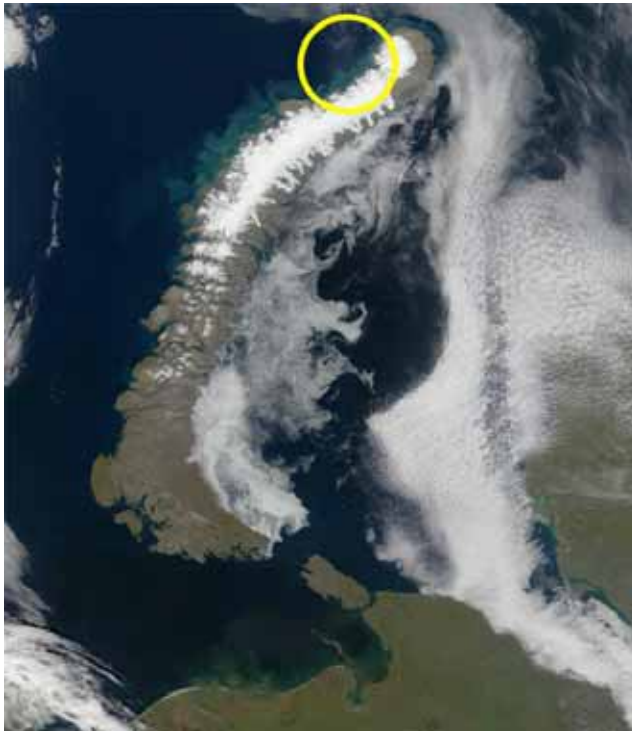


Figure 1. The area where airborne radio echo sounding on Novaya Zemlya were carried out, April 2005

Reliable forecast of iceberg origin requires (besides the ice thickness measurements on ice fronts) the following measurements: ice surface elevation on glacier tongues and front heights, ice front change rates, ice surface velocity, bathymetry of adjacent water parts.

Acknowledgements

The study was supported by Russian Foundation of Basic Research (Grant no 05-05-64732) and by Presidium of RAS (Programme P-34). Field studies were in the frame of project of "Sevmorneftegaz" Corporation and number of oil-and-gas companies.

ASSESSMENT OF THE SURFACE MASS BALANCE OF 18 SVALBARD GLACIERS FROM THE MODIS/TERRA ALBEDO PRODUCT

Wouter Greuell¹, Jack Kohler², Friedrich Obleitner³, Piotr Glowacki⁴, Kjetil Melvold⁵, Erik Bernsen¹ and Johannes Oerlemans¹

¹ Institute for Marine and Atmospheric Research Utrecht (IMAU), Utrecht University

² Norwegian Polar Institute, Tromsø

³ Institute for Meteorology and Geophysics, Innsbruck University

⁴ Institute of Geophysics, Polish Academy of Sciences, Warszawa

⁵ Norwegian Water Resources and Energy Directorate (NVE), Oslo

Goal

Direct surface mass balance measurements of glaciers are generally limited in space and duration. As far as Svalbard is concerned, all the existing series of direct measurements cover glaciers located in the western and central part of the main island of Spitsbergen. Measurements do not exist for the remainder of the archipelago. The aim of our study is to estimate the annual surface mass balance of a large number of glaciers that are more representative of all the glaciers of the archipelago than the glaciers covered by the direct measurements. For this purpose we use the method of Greuell and Oerlemans (2006). In this method the “satellite-derived mass balance” is estimated from temporal variations in the satellite-derived surface albedo, using a simple equation based on surface energy balance considerations. The satellite-derived albedos were taken from the “MODIS/Terra albedo product”. The method needs no other input variables.

Method

The following equation is used for the calculation of the satellite-derived mass balance (B_{sat}) from the satellite-derived albedo averaged over the glacier surface (α_{sat}):

$$B_{\text{sat}} = \frac{\int_{j_1}^{j_2} \max\{I_0 \tau_{\text{atm}} (1 - \overline{\alpha_{\text{sat}}}) + Q_0, 0\} dt}{L_f}$$

In this equation I_0 is the incoming radiation at the top of the atmosphere, τ_{atm} the transmission of the atmosphere, Q_0 the sum of the net long-wave radiative flux and the turbulent fluxes and L_f the latent heat of fusion. The Julian days j_1 and j_2 confine the part of the summer with substantial melt. The parameters τ_{atm} , Q_0 , j_1 and j_2 were obtained from independent measurements made with weather stations on the glacier of Kongsvegen. The main reasons for the success of the method (De Ruyter de Wildt et al., 2002, Calluy et al., 2006, and Greuell and Oerlemans, 2006) are the dominance of the contribution of net-short wave radiation to the surface energy balance of glaciers in summer and the positive feedback between albedo and melt rate. Therefore, B_{sat} represents the summer balance. However, in theory accumulation also affects B_{sat} since less accumulation leads, in summer time, to an earlier exposition of bare ice with relatively low albedos. So, it is unclear whether

B_{sat} should be considered as an estimate of the annual balance or as an estimate of the summer balance only. Earlier studies demonstrated that B_{sat} may provide a valuable estimate of the mass balance anomaly, but not of the absolute value of the mass balance.

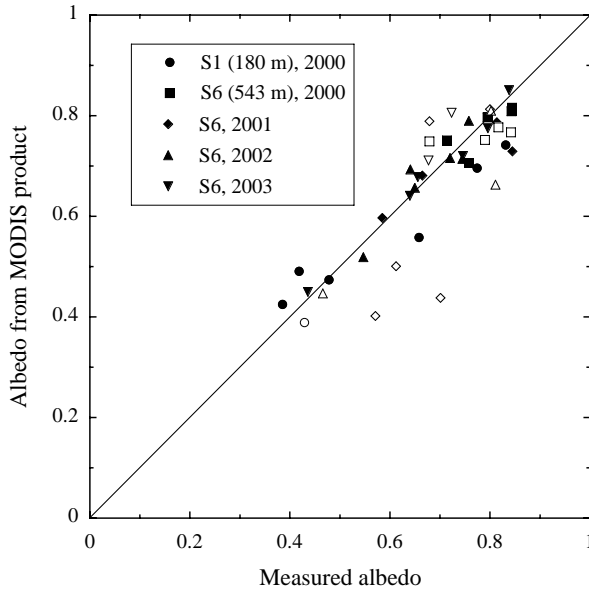


Figure 1. Comparison of surface albedos distracted from the MODIS/Terra albedo product with in-situ measurements from two sites on Kongsvegen (2000-2003). Empty symbols correspond to lower quality data.

MODIS/Terra albedo product

As input for our calculations we used the MODIS/Terra albedo product. This product provides 16-day mean surface albedos for the entire land surface of the Earth, with the exception of the area polewards of 80° , at a resolution of 1 km. Since a part of Svalbard is situated north of 80°N , the product covers $\sim 90\%$ of the glaciers of the archipelago. The satellite (Terra) carrying the MODIS sensors was launched in December 1999. This limits the available data set to six summer seasons (2000-2005). We validated the MODIS albedos by comparing them with in-situ measurements collected by means of two weather stations placed on Kongsvegen (Figure 1). Each point in the scatter plot represents a period of 16 days. If we exclude lower-quality data (open symbols), the root mean square difference between satellite-derived and in-situ measured albedo is 0.04. This test lends considerable confidence in the satellite product.

Results

We selected 18 glaciers that are more or less evenly distributed over the archipelago (Figure 2). We determined the performance of the method by comparing B_{sat} with direct measurements of the mass balance, which are available only for Kongsvegen and Hansbreen (Figure 3). Correlation coefficients for annual balances are 0.94 and 0.87, respectively, and for summer balances 0.93 and 0.82,

respectively. For both Kongsvegen and Hansbreen the standard deviation in B_{sat} is lower than the standard deviation in the measured mass balance. The underestimate is severe for Hansbreen (90 mm w.e. in the calculations; 360 mm w.e. in the measured annual balance and 250 mm w.e. in the measured summer balance) and smaller for Kongsvegen (250 mm w.e. in the calculations and 370 mm w.e. in both the measured annual and the measured summer balance). Figure 2 shows the anomalies in B_{sat} with respect to the mean for the six-year period for the summer of 2000. According to our calculations, this was, on average for all eighteen glaciers, the year with the highest summer balance during the studied period. The spatial consistency of B_{sat} lends confidence in the method. Similar figures for other years show similar spatial consistency.

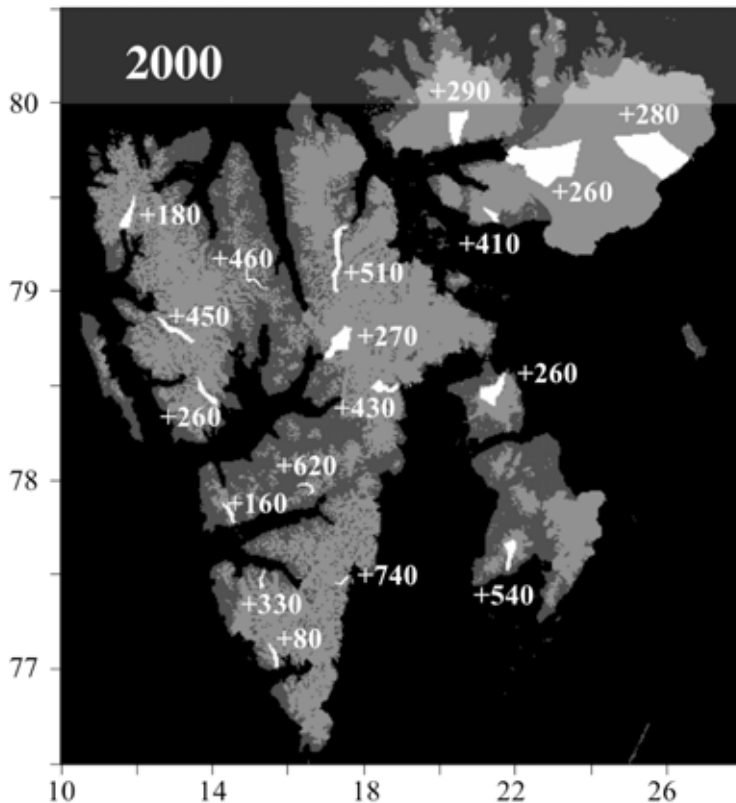


Figure 2. Anomalies in B_{sat} (mm w.e.) for the year 2000 for the 18 selected glaciers.

Conclusions

From the good agreement between the satellite-derived albedos and the in-situ measurements (root mean square error = 0.04), we conclude that the MODIS/Terra albedo product is a useful tool for our purpose, namely the estimation of the mass balance of glaciers from satellite data. We made such estimates for 18 glaciers in Svalbard. The spatial coherence of the result, as well as the correlation coefficient between calculated and measured mass balance for two glaciers lends confidence

in our results. On the other hand, the interannual variability in the satellite-derived mass balance is too low. This might in the future be corrected by equations to be established with mass balance models. Such models might also be used to clarify whether B_{sat} represents the annual or the summer balance. This has not become clear from the current study, partly due to the shortness of the time series (six years). A longer version of this abstract has recently (March 2006) been submitted to the Journal of Geophysical Research - Atmospheres.

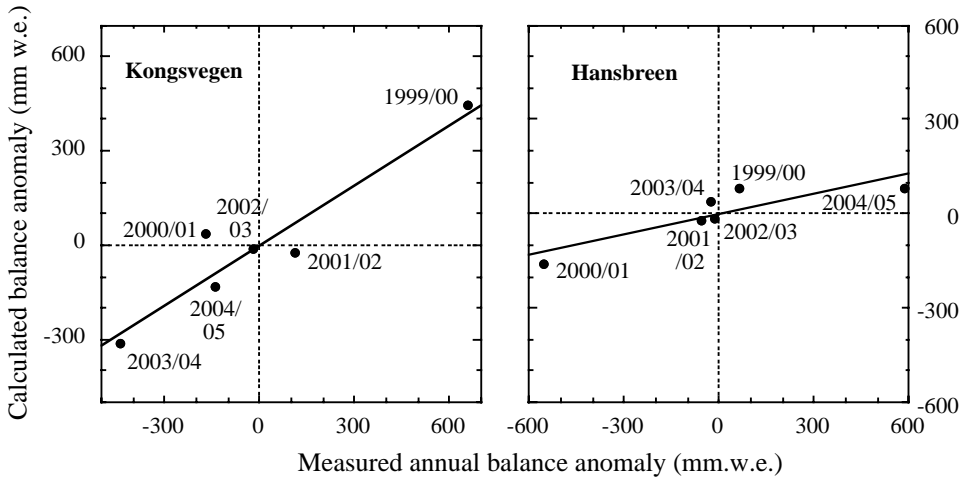


Figure 3. Comparison of the anomalies in B_{sat} with direct measurements of the annual balance. Scales on the vertical and horizontal axes and in both panels are the same. The lines indicate least-square fits.

References

- Calluy, G.H.K., H. Björnsson, J.W. Greuell and J. Oerlemans, 2006: Estimating the mass balance of Vatnajökull from NOAA-AVHRR imagery. Accepted by *Ann. Glaciol.*, **42**.
- De Ruyter de Wildt, M.S., J. Oerlemans and H. Björnsson. 2002. A method for monitoring glacier mass balance using satellite albedo measurements, application to Vatnajökull (Iceland). *J. Glaciol.*, **48**(161), 267-278.
- Greuell, W. and J. Oerlemans, 2006: Assessment of the surface mass balance along the K-transect (Greenland ice sheet) from satellite-derived albedos. Accepted by *Ann. Glaciol.*, **42**.

MORE ON ELEVATION CHANGES ON AUSTFONNA ICE CAP

JON OVE HAGEN¹, TROND EIKEN¹, EVEN LOE¹, JACK KOHLER², KETIL MELVOLD¹, THOMAS V. SCHULER¹ AND ANDREA TAURISANO²

¹ Department of Geosciences, Faculty of Mathematics and Natural Sciences, University of Oslo, Norway

² Norwegian Polar Institute, Tromsø, Norway

On Austfonna ice cap repeated airborne laser profiles carried out by NASA in 1996 and 2002 [1] indicated a clear thickening of the upper central part of the ice cap with as much as up to 3.5 m over the six year period; a change of about 0.6 m a^{-1} , and a peripheral thinning. This indicated a positive mass balance of the ice cap. The net balance derived from shallow cores from the period 1986-1999 indicated, however, a balance close to zero of the ice cap [2]. A shallow ice core drilled in 2004 at the same location as the 1999 core gave the same net accumulation of 1986-2004 of $0,47 \pm 0,03 \text{ m water eq.}$, or the same as the long term trend of the period 1963-1999.

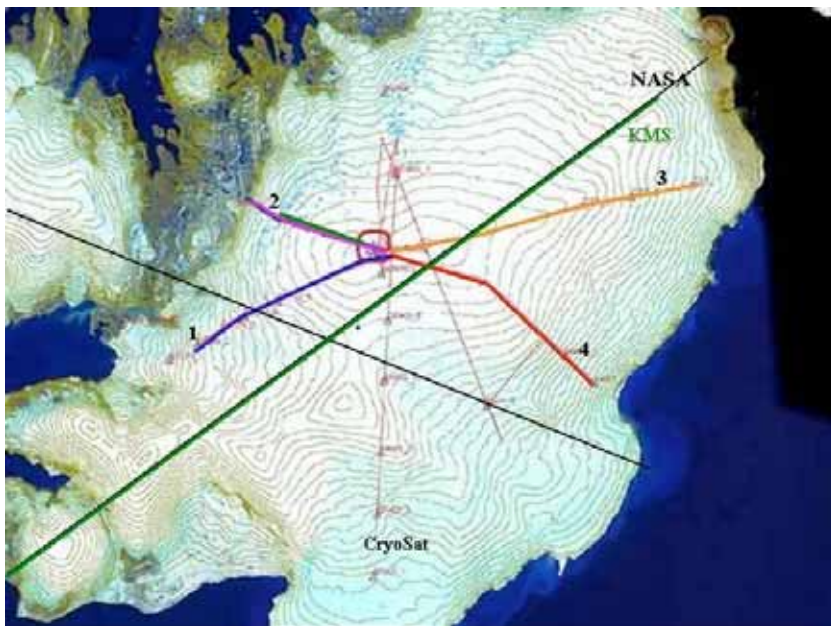


Figure 1. Location of repeated elevation profiles on Austfonna. The ice cap is about 100 km across.

We have now conducted additional ground-based repeated GPS profiles in 1999, 2004 and 2005 (Fig. 1.) The GPS profiles indicate less pronounced thickening and less thinning, see Fig. 2. The GPS-profiles also show that different parts of the ice cap can develop differently. In two profiles taken from the summit, one to the

South-West (Etonbreen), fig. 2., and one to the North-West (Fig. 3.) showed a different trend with thickening towards the lower part in North-West and thinning in South-West, see also Fig. 4. The ground based differential GPS are not overlapping the NASA profiles, but in parts the profiles are crossing.

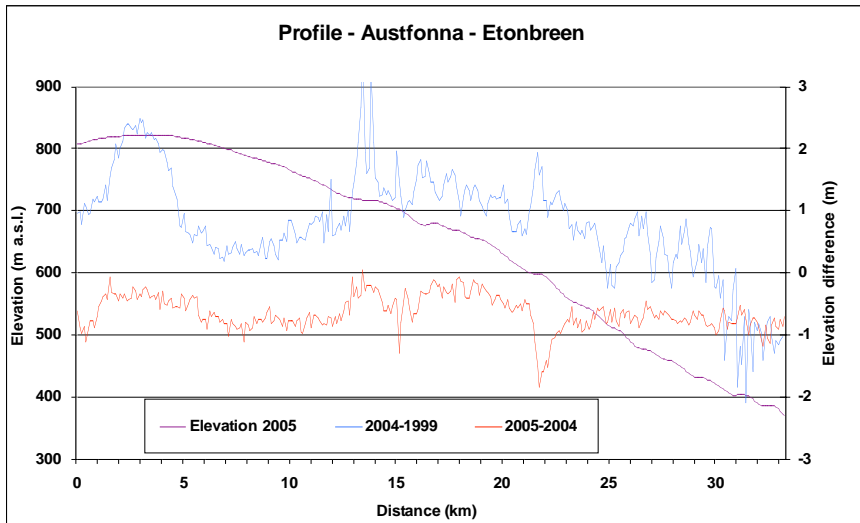


Figure 2. Comparison of surface elevation along profile line 1 in fig. 1 for 3 different years. The elevation changes from 1999 to 2004 (blue line) and 2004 to 2005 (red line) are displayed on the right y-axis.

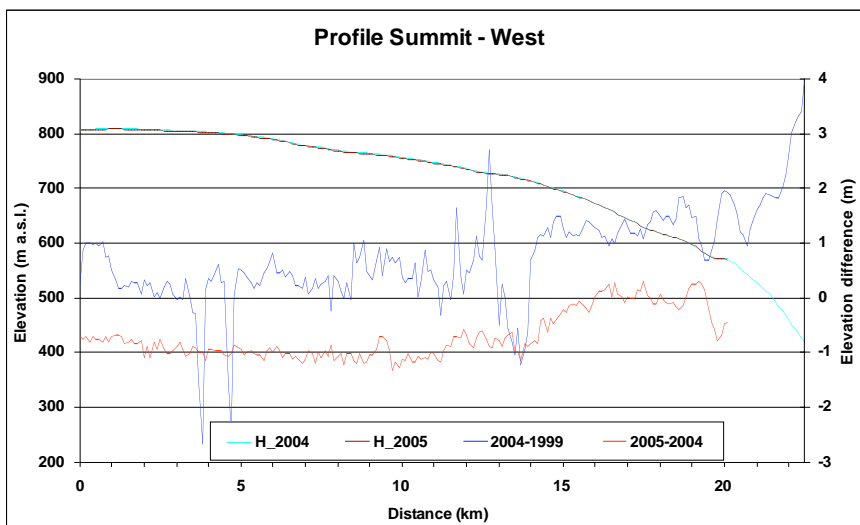


Figure 3. Comparison of surface elevation along profile line 2 in fig. 1 for 3 different years. The elevation changes from 1999 to 2004 (blue line) and 2004 to 2005 (red line) are displayed on the right y-axis.

Surface elevation along profile lines was surveyed using differential GPS. The GPS data indicate that in 2004/05 the surface elevation decreased over much of the ice

cap, even in the central part. This finding is in contrast to that of previous years (e.g. 1999/2004 which indicate a slight thickening in the central part. This difference may reflect the variability of surface elevation at shorter time scales due to differences in snow accumulation and mass balance. The results from 2004/05 may thus also reflect the overall negative mass balance derived from diagnostic modelling.

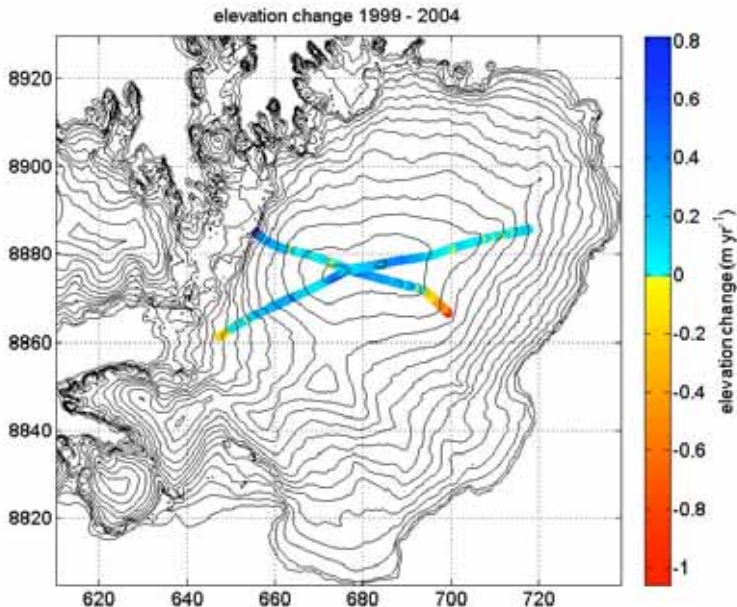


Figure 4. Elevation changes between 1999 and 2004 along the ground-based GPS-profiles 1-4 seen in figure 1.

It is, however, clear from all the different data sets that we need extensive data to be able to make reliable assessments of mass balance, covering different types and sizes of glaciers in which the dynamic effect must be considered [3].

In 2006 it is planned to carry out more both of ground-based GPS profiles, airborne laser profiles and also to drill additional shallow cores to verify the mean mass balance

References

- [1] Bamber, J.L., W. Krabill, V. Raper and J.A. Dowdeswell (2004). Anomalous recent growth of part of a large Arctic ice cap: Austfonna, Svalbard. *Geophys. Res. Lett.* 31(12): doi:10.1029/2004GL019667.
- [2] Hagen, J.O., K. Melvold, F. Pinglot and J. A. Dowdeswell. 2003a. On the net mass balance of the glaciers and ice caps in Svalbard, Norwegian Arctic. *Arct. Antarct. Alp. Res.*, **35**(2), 264-270.
- [3] Hagen, J. O., T. Eiken, J. Kohler, K. Melvold, in print: Geometry changes on Svalbard glaciers – mass balance or dynamic response? *Annals of Glaciology* 42

ENGABREEN - MASS BALANCE RESULTS AND THE SVARTISEN SUBGLACIAL LABORATORY

MIRIAM JACKSON AND HALLGEIR ELVEHØY

Norwegian Water Resources and Energy Directorate, Oslo, Norway

Engabreen in northern Norway is an outlet glacier of the Svartisen icecap and is one of the glaciers in NVE's mass balance programme. Mass balance measurements have been performed annually on Engabreen since 1970 in connection with a hydropower station in the area that uses water from the glacier. The water is collected as run-off from the glacier as well as being collected directly through subglacial intakes.

Mass balance results for 1970 to 2004 show that most years showed a positive balance, especially up to 2000. The total cumulative balance for this period was 22 m w. e. The positive mass balance was also reflected in the front position of the glacier, which advanced over 100 m between 1970 and 2000, but then retreated over 110 m between 2000 and 2004.

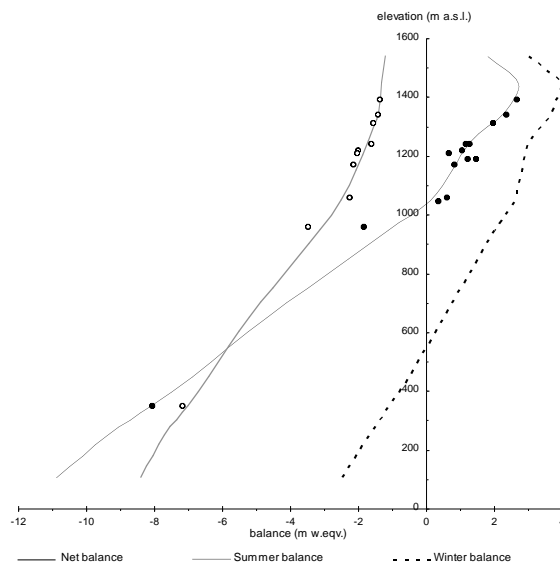


Figure 1. Mean values of specific winter, summer and net balance as a function of altitude on Engabreen. The elevations of the measurement stakes used are also shown.

Measurement stakes are set out on the glacier to assist in measuring the summer and winter balances. Snow depth soundings are also performed at over one hundred sites on the glacier, between 950 m a.s.l. and 1460 m a.s.l., and two density profiles are measured. Winter balance for 2004 was 2.9 ± 0.2 m w.e., which

is 100 % of the mean value for 1970-2003 and 130 % of the mean value for 1999-2003. The summer balance was -2.1 ± 0.2 m w.e., which is 91 % of the average for 1970-2003 and 84 % of the average for 1999-2003. The net balance for 2004 was $+0.8 \pm 0.3$ m w.e. This is a very positive result compared with the mean value for 1970-2003 of $+0.63$ m w.e., and -0.25 m w.e. for 1999-2003.

Engabreen is unique in that there exists a subglacial laboratory underneath the glacier. Several load cells are installed at the glacier bed and measure the total hydrostatic pressure normal to the load cell. The pressure is measured at 15 minute intervals and shows variations in pressure at the bed due to variations in surface meltwater or changes in the subglacial discharge. It is also possible to pump water up to the glacier bed and artificially change the subglacial conditions in order to see how the system responds. This gives us valuable information on the differences in the subglacial hydrology between the winter and the summer. The wealth of data existing for Engabreen from over three decades of mass balance measurements as well as the additional observations and opportunity for experiment in the subglacial laboratory make Engabreen a unique site for glaciological studies.

CHANGES IN THE TOPOGRAPHY OF SELECTED GLACIERS IN SOUTHERN SPITSBERGEN IN THE LIGHT OF THE GPS SURVEY IN 2005

JACEK A. JANIA¹, MARIUSZ GRABIEC¹, GRZEGORZ GAJEK², LESZEK KOLONDRA¹, PIOTR GLOWACKI³ AND DARIUSZ PUCZKO³

¹ Department of Geomorphology, Faculty of Earth Sciences, University of Silesia, Poland

² Institute of Earth Sciences, Maria Curie Skłodowska University, Lublin, Poland

³ Institute of Geophysics, Polish Academy of Sciences, Warszawa, Poland

Glacier topography changes reflect trends in mass balance and dynamic processes (surge type phenomena and calving intensity of tidewater glaciers). Both factors are sensitive to climatic impact. General decrease of extend and elevation of South Spitsbergen Glaciers during the 20th century has been recorded and described for the majority of them (e.g. Koryakin, 1975; Jania, 1988; Lefauconnier, Hagen, 1991; Palli *et al.*, 2003). Repeated survey of elevation was done for a selected set of glaciers during the last decades and compared with data from topographic maps of the Norwegian Polar Institute showing the state in 1936.

The aim of the project is to detect type and scale of changes in glacier geometry during the last period and to find factors driving them. This work presents preliminary results.

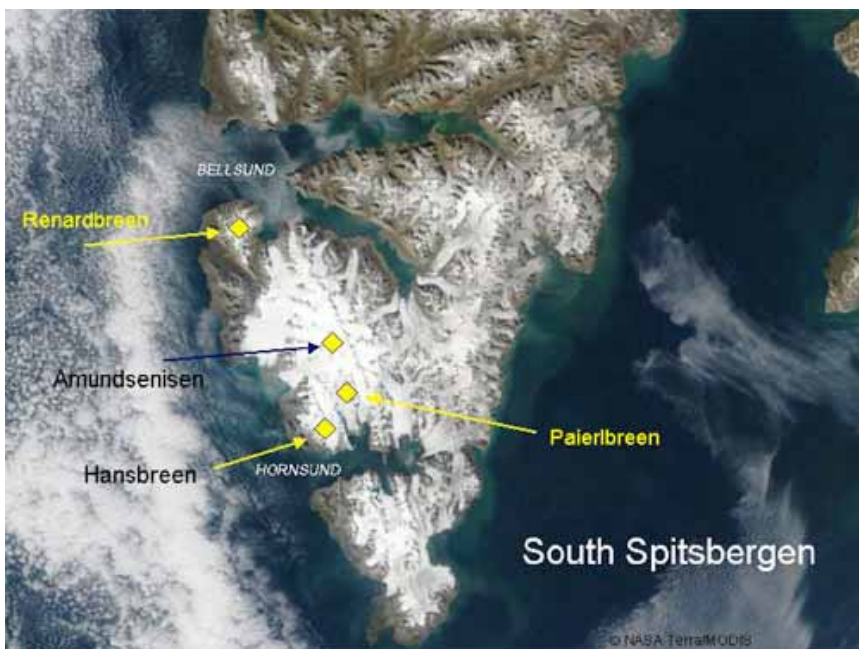


Figure 1. South Spitsbergen on the satellite image Terra/MODIS (© NASA – Visible Earth). Studied glaciers are indicated.

Topography changes of Hansbreen, the Amundsenisen accumulation field and its outlet glaciers (Fig. 1) were monitored using different techniques. Data from a survey done in April 2005 were compared with previous data. Results from it together with data from the land based glacier Renardbreen (Fig. 1) are presented here.

Hansbreen is a medium size (c. 56 km²) tidewater glacier terminating in Hornsund Fiord close to the Polish Polar Station. Amundsenisen (cf. Fig. 4) is the thickest accumulation ice field in Svalbard (> 700 m) located in the central part of South Spitsbregren. Nornebreen-Paierlbreen outlet glacier system is flowing in SSE direction, while Hogstebreen is flowing in western direction and feeding vestre Torellbreen. Renardbreen (c. 30 km²) is a valley type glacier oriented in WNW direction. Their terminus retreated from the sea (Recherchefjorden) to land after 1960.

The following data sources and methods were used. Differential kinematic GPS surveys were done in April 2005 along profiles of airborne laser altimetry (ALA) of the NASA from May 1996 and May 2002 (cf. Bamber *et al.*, 2005). Precise GPS (L₁/L₂) Ashtech Z-Surveyor receivers were used in 2000 and 2005. Antenna of the rover receiver was mounted on a mast on a snowmobile. Vectors between reference GPS station and the rover receiver did not exceed 10 km. The accuracy of the kinematic survey has been estimated as better than ±0.3 m horizontally and ±0.5 m in elevation. For comparison with other data one can consider differences in snow cover thickness on glaciers in particular years. Data from topographic maps in scale 1:25 000 prepared from aerial photos taken in July 1960 and in August 1990 (Jania *et al.*, 1992; Kolondra, Jania, 1998) were also used, similarly as topographic maps of Norwegian Polar Institute mentioned above.

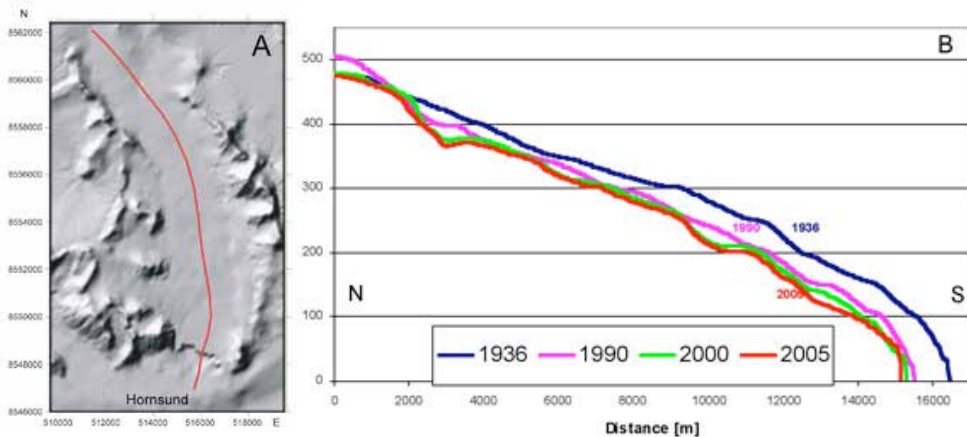


Figure 2. Geometry changes of Hansbreen: a) location map of the longitudinal profile; red line (N and E coordinates in meters); b) changes of the glacier surface elevation along the profile.

Thinning of Hansbreen along its centreline has been noted since 1936, including last 5 years (Fig. 2). It is worth noting that thinning occurs along the whole length of

glacier, including the accumulation zone. Thinning rate averaged over the entire length of the glacier increased between particular survey dates: -0.45 m/yr in period 1936-1990; -0.96 m/yr in period 1990-2000; -1.40 m/yr in period 2000-2005. Results could be interpreted as an effect of more intense melting and dynamic response of the glacier to climate warming. Comparison of the mass balance with the glacier flow velocity and topography changes for the period 1990-2000 has been done (Fig. 3). The estimated ice discharge across the transverse profile “T” (located below the ELA) is significantly higher than the mean annual net accumulation rate above it and did not compensated the net mass losses in the ablation zone (including calving). Discharge of ice across the “T” profile was estimated from data on the glacier superficial velocity in the summers of 1998 and 1999 (measured by electronic distance meter and differential GPS) and InSAR data from spring 1996 (cf. Vieli *et al.*, 2004) together with the cross section area obtained from the RES to the bedrock (Moore *et al.*, 1999). The shape factor and calculated deformational velocity were taken into the estimation. Obtained results match with the data on elevation changes in the ablation area (below the “T” profile) in the period in question. No surge type phenomena of Hansbreen has been observed during this period.

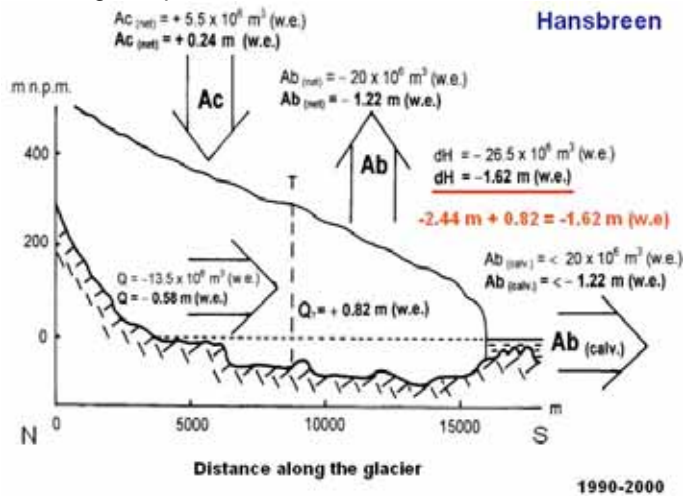


Figure 3. Mean annual mass turnover of Hansbreen in the period of 1990-2000: Ac – net accumulation above the “T” transverse cross section; Q – ice discharge across the “T” profile (sign “minus” indicates outflow of ice and “plus” inflow); Ab – net ablation below the “T” cross profile; Ab_(calv.) – estimated mass loss due to calving; dH – mean annual elevation changes of the area below “T” profile (calculated from comparison of DTM from 1990 and 2000 survey) underlined in red. All data expressed both as the total volume in m³ of water and the equivalent layer in m w.e.. In red: calculation of decrease of ice thickness below the “T” cross profile from the mass balance data only: Ab + Ab_(calv.) + Q_T = dH. Result fits with thinning rate obtained from comparison of DTMs.

Elevation of the Amundsenisen glacier system (Fig. 4) shows none or small changes in the central part of the accumulation area, while decrease of thickness was significant in upper parts of two outlets Hogstebreen and Nornebreen in periods 1990-1996 and 1996-2002 respectively. It is interpreted as an effect of the

surge type dynamic displacements of ice masses. The surge of the Nornebreen-Paierlbreen glacier system has been observed after 1993 and continued during almost the next decade. Massive calving of the glacier has been noted in this period. Mass loss in the lower part of ablation area of Paierlbreen (below 260 m a.s.l.) have had reflection in its thinning rate in periods between surveys (1960-1990: -1.39 m/yr; 1990-1996: -2.06 m/yr; 1996-2002: -3.14 m). Mass transfer from Hogstebreen seems to be of surge origin and probably had been propagated down to the Vestre Torellbreen. The event wasn't been observed directly in the field due to more remote location from the Polish Polar Station, Hornsund. It will be analyzed using remote sensing methods.

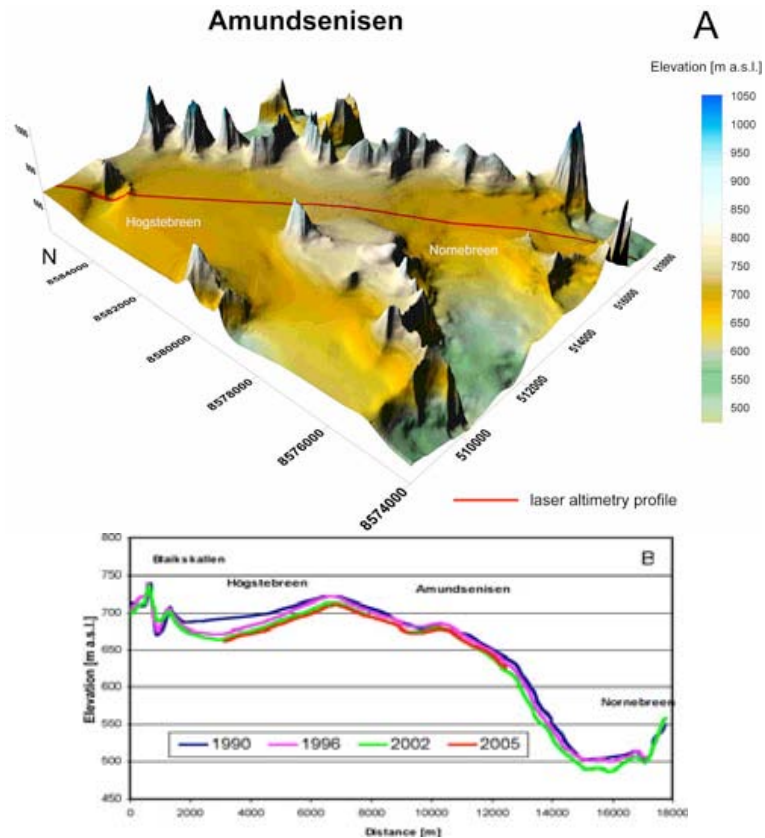


Figure 4. Geometry changes of Amundsenisen. a) location of the profile; b) results of survey from particular years.

Elevation changes of Renardbreen along the longitudinal profile shows significant thinning of the ablation area and thickening of in the accumulation zone in the period of 1936-2005 (Fig. 5). Such result is similar to other slowly flowing glaciers as Aavatsmarkbreen, Comfortlessbreen and Kongsvegen in NW Spitsbergen (Jania *et al.*, 2002; Hagen *et al.*, 2005) where thinning of lower parts of glaciers is reaching 60-90 m and thickening of accumulation areas are in order of 40-80 m for the period in question.

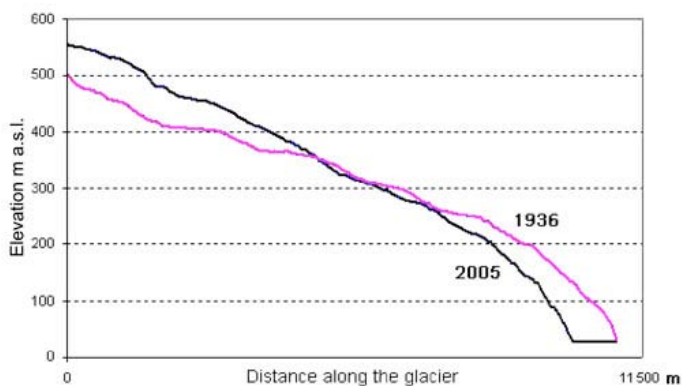


Figure 5. Renardbreen - differences in elevation along the southern longitudinal profile (1936-2005).

The following conclusions appear in the actual stage of studies.

- Thinning rates of glaciers are increasing during recent period.
- Topography changes of glaciers in South Spitsbergen reflect more distinctly their dynamic response to climate warming than negative mass balance.
- Three types of glacier geometry changes could be distinguished in respect to their dynamics: (1) fast thinning of tidewater glaciers as a consequence of surge and massive calving events (periods); (2) significant decrease of ice thickness of the whole glacier when ice flow is faster than balance discharge of ice across the ELA (the Hansbreen case); (3) decrease of elevation in lower parts and increase in upper parts of glaciers when they are slowly flowing i.e. land based or terminated in shallow sea (the Renardbreen case).
- Central part of Amundsenisen seems to be a specific case. Elevation changes in there weren't distinct. It suggests that intense discharge of ice towards two surging outlets doesn't affect the area. Bedrock topography could be considered as the responsible factor. Further studies of mass balance and glacier flow of Amundsenisen with its outlets is needed to solve the problem.

Acknowledgements

Authors wish to thank colleagues from particular wintering crews of the Polish Polar Station for support in the field survey campaign. Special thanks are directed to Dr. Adam Balut (AGH – Technical University in Krakow) for consultancy during processing of the GPS survey results. Aerial photos were kindly provided by the Norwegian Polar Institute for photogrammetric mapping. The project is supported by the Polish Ministry of Education and Science under terms of the research grant No. PBZ-KBN-108/P04/2004 and partly by the University of Silesia (grant No. BS/KG-2/2006).

References

- Bamber J. L., Krabill, W., Raper, V., Dowdeswell, J.A., 2005 (in print): Interpretation of elevation changes on Svalbard glaciers and ice caps from airborne lidar data. *Annals of Glaciology*, 42.
- Hagen J.O., Eiken, T., Kohler, J., Melvold, K, 2005 (in print): Geometry changes on Svalbard glaciers – mass balance or dynamic response? *Annals of Glaciology*, 42.

- Jania, J., 1988: Dynamiczne procesy glacialne na południowym Spitsbergenie [Dynamic glacial processes in South Spitsbergen – English summary]. Prace Naukowe Uniwersytetu Śląskiego, No. 955, Katowice, 258 pp.
- Jania, J., Kolondra, L., Schroeder, J. (Eds.), 1992: Hans Glacier 1:25 000, Topographic Map. Department of Geomorphology, University of Silesia, Sosnowiec, 1 sheet.
- Jania, J., Stober, M., Perski, Z., 2002: Changes of geometry and dynamics of NW Spitsbergen glaciers based on the ground GPS survey and remote sensing. Proceedings from the Sixth Ny-Aalesund International Scientific Seminar "The Changing Physical Environment", Tromsø, Norsk Polarinstitut, Internraport Nr. 10, 137-140.
- Kolondra, L., Jania, J., 1998: Changes of Longitudinal Profiles of Large Glaciers in Southern Spitsbergen Based on the Airborne Laser Altimetry. [in] : P.Głowacki & J.Bednarek (Eds.), Polish Polar Studies, Proceedings of the 25th International Polar Symposium, Warszawa, Institute of Geophysics of Polish Academy of Sciences, Warszawa, p. 273-277.
- Koryakin, V.S., 1975: Kloebanya lednikov [Fluctuations of glaciers – in Russian]. In: Oledeneniye Spitsbergena (Svalbarda). Nauka, Moskva, 165-186.
- Lefauconnier, B., Hagen, J.O., 1991: Surging and calving glaciers in eastern Svalbard. Norsk Polarinstitut Meddelelser No. 116, 130 pp.
- Moore J.C., Päli A., Ludwig F., Blatter H., Jania J., Gądek B., Głowacki P., Mochnecki D., Isaksson E., 1999. High-resolution hydrothermal structure of Hansbreen, Spitsbergen mapped by ground-penetrating radar. *Journal of Glaciology*, 45 (151), 589 – 590.
- Pälli, A., Moore, J.C., Jania, J., Głowacki, P., 2003: Glacier changes in southern Spitsbergen, Svalbard, 1901-2000. *Annals of Glaciology*, 37, 219-225
- Vieli, A.; Jania, J.; Blatter, H.; Funk, M., 2004: Short-term velocity variations on Hansbreen, a tidewater glacier in Spitsbergen. *Journal of Glaciology*, 50 (170), 389-398.

LONG-TERM HIGH ARCTIC MASS BALANCE: COMPARISON OF BALANCES AND VOLUME CHANGES ON MIDRE LOVÉNBREEN, SVALBARD

JACK KOHLER¹, CHRIS NUTH¹, OLA BRANDT¹, TAVI MURRAY², TIM JAMES² AND NICK BARRAND²

¹ Norwegian Polar Institute, Polar Environmental Centre, N-9296 Tromsø

² Dept. Geography, U. of Wales. Swansea, SA2 8PP UK

Introduction

The Norwegian Polar Institute (NPI) measures mass balance on three glaciers near Ny-Ålesund, Svalbard, including Midre Lovénbreen (MLB). The record from MLB is the second longest High Arctic record (1968-present). Available data for MLB includes winter, summer, and net balances B_i , where i = winter, summer, and net. The data show consistently negative mass balance since the beginning of the record (Figure 1). That the glacier overall is not in balance is evident from its continual retreat, which started early in the 1900s. Average ice loss at the tongue is about 0.5 m a^{-1} . In general, winter precipitation is less variable than summer melt, but there are no statistically significant trends in any of the balances during the measuring period. The last 5 years, however, represent the longest succession of negative net balances on record.

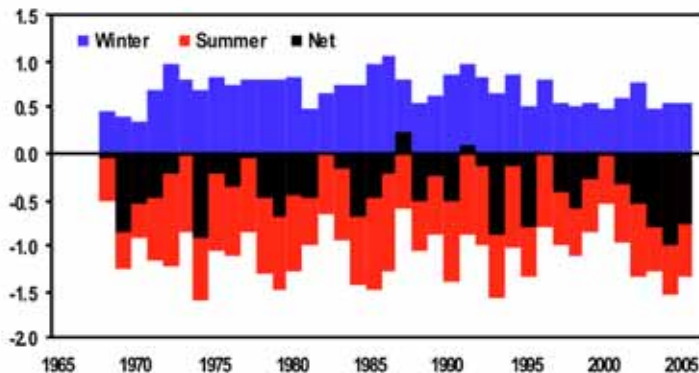


Figure 1. Winter, summer, and net balances for Midre Lovénbreen (MLB).

The balances B_i are all available digitally. Also interesting from a climatic perspective are the specific balances, which at many glaciers, including MLB, can be described as a function of elevation. We attempt to fit a relation to specific balance measurements, with elevation as the main explaining variable. Balance as a function of elevation has, of course, been estimated throughout the years by NPI, since it is required to calculate B_i , but the data have never been reported in table form, and prior to 1999, these data have not been preserved. We have recently re-derived a time-series of the balances as a function of elevation $b_i(z)$, using original

stake data from archived field notebooks and maps, and graphs of balance as a function of elevation taken from old reports. We use the $b_i(z)$ together with the new hypsometry to recalculate the aerielly-averaged mass balance B_i .

We seek a suitable objective method for fitting an elevational relation to the observed specific balances. However, there is no simple analytical relation for $b_i(z)$, one that involves a handful of readily obtainable parameters, so we use a robust linear fit to the data. This has the advantage that it is conceptually straightforward to apply, and furthermore relations involving a larger number of parameters generally do not yield results that are statistically preferable to a straight line, at least when comparing recalculated and older values of B_i . And since the fitting necessarily involves extrapolation, in many years paucity of data or bad data at critical elevations can cause a higher-order fitting relation to go seriously awry.

In general, we find good agreement between the recalculated and original balances (Figure 2), particularly B_n lies mostly within the error limits.

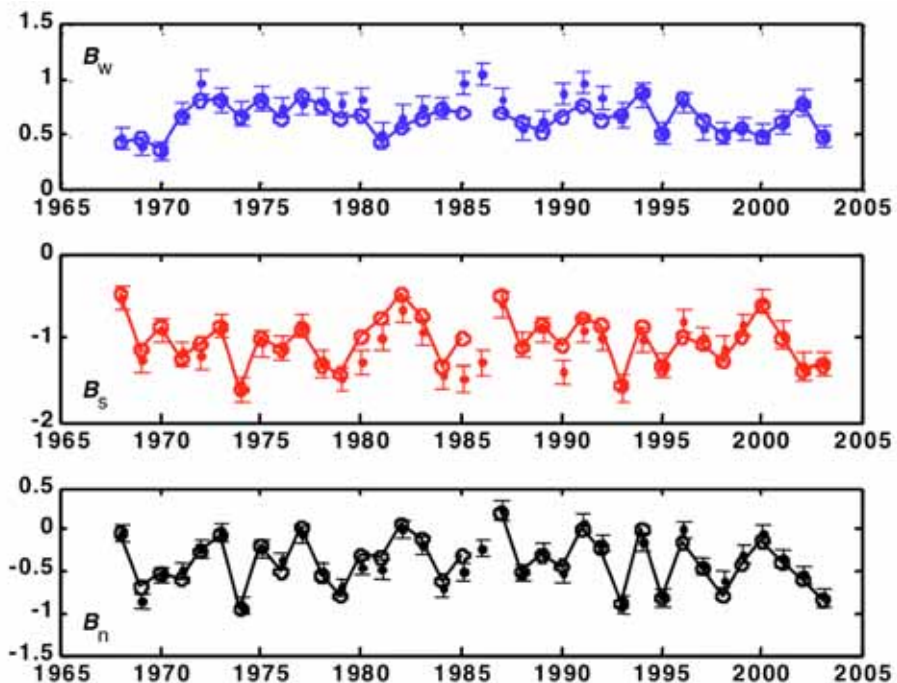


Figure 2. Reconstructed winter, summer, and net balances for MLB, using a robust linear fit to old field data to generate $b_i(z)$ and a new time-varying hypsometry. Originally reported data are shown with error bars of constant ± 10 cm w.eq.

We have also digitized older maps of MLB which are then differenced to calculate the geodetic balance, that is the long-term volume changes, as well as calculate a new temporally-variable hypsometry necessary in the mass balance calculations. We use digitized topographic maps (1969, 1977), a digital elevation model (DEM)

from 1995, and a DEM from a recent NERC lidar campaign (2003). The 1969 and 1977 10 m contour interval maps (unpublished) were made on a photogrammetric stereo plotter, using vertical aerial photographs (at a scale of 1:50,000) taken by the Norwegian Polar Institute on July 28, 1969 and August 7, 1977. The 1995 DEM was constructed in a digital photogrammetric work station from Norwegian Polar Institute aerial photographs (1:15000) taken on August 18 1995, and has a 5 m pixel resolution. The Lidar-derived DEM was retrieved in late July 2003 at a spatial resolution that varies from 0.7 m to 1.5 m. (Arnold et. al., 2006). The DEM was formed at a 20 m resolution using an average of all points within a 20 m window.

Individual contours for the older maps were hand-digitized. While only paper copies of the maps were available, these were all unfolded and clean. The data from the older maps were transformed to the same datum and projection as the DEMs (WGS84: UTM zone 33N). Changes in elevation relative to the 1995 reference surface was then calculated by linearly interpolating the easting and northing positions of the digitized contour points into the 1995 DEM. Changes over 1995 to 2003 were calculated by simply subtracting the two DEMs, each sampled on the lowest resolution grid (20 m).

Differences were then interpolated across the glacier surface, and similar to the $b_i(z)$, a robust linear fit of the surface elevation change was derived as a function of elevation, and used with the hypsometry to calculate the volume change between map/DEM epochs.

The net glaciological balances are then summed and compared to the map/DEM differences (Figure 3), with all data adjusted so that 1969 (the first map year) represents zero balance. The agreement between the geodetic and glaciological mass balance is quite good, within the error limits; these are obtained from comparing differences of non-glaciated terrain between maps/DEMs.

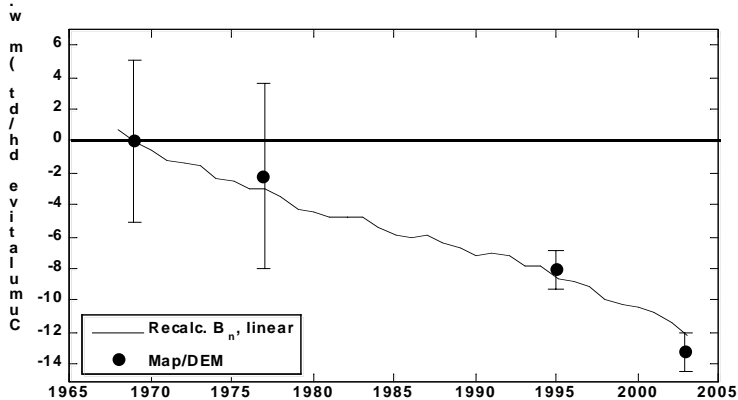


Figure 3. Comparison of summed reconstructed net balances for MLB, compared to geodetic balance derived from old maps (1969,1977) and newer more accurate DEMs (1995,2003). Error bars on geodetic data are obtained from comparing differences of non-glaciated terrain between maps/DEMs.

ENERGY AND MASS BALANCE AT ETONBREEN, AUSTFONNA

EVEN LOE¹, TROND EIKEN¹, JON OVE HAGEN¹, KJETIL MELVOLD², THOMAS SCHULER¹ AND ANDREA TAURISANO³

¹Department of Geosciences, University of Oslo

²Norwegian Water Resources and Energy Directorate, Oslo

³Norwegian Polar Institute, Tromsø

This work aims to explore the relationship between summer balance and winter temperature. The physical link between these two parameters is that winter temperature governs ice temperature, which, in turn, has influence on the melt because cold ice is a heat sink. In other words cold ice will absorb energy, which would have produced melt if the ice was temperate. Since the current climate change is likely to bring about warmer Arctic winters (ACIA, 2004), the contribution to the mass balance from the cold content is likely to be reduced, as pointed out by Woodward et al. (1997).

By using data from an automatic weather station (AWS) and ice temperature measurements on Etonbreen (Western part of Austfonna), the contribution to the mass balance from the winter cold during the melt season of 2004, has been estimated for one point about 350 m.a.s.l., well below the equilibrium line.

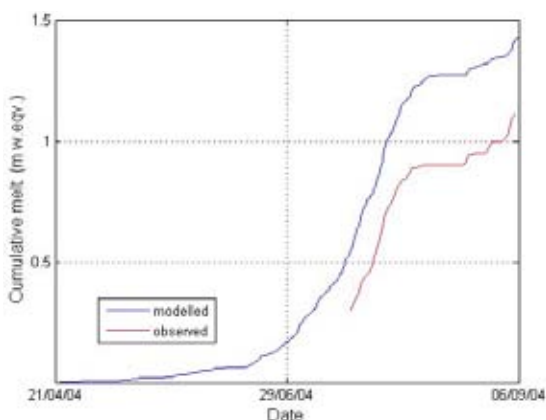


Figure 1. Modelled and observed melt from the start of the measurement period to the end of the melt season of 2004. The observed melt curve which is derived from ultra sonic ranger measurements starts on the day when the snow disappears, because it can not be resolved before this as the evolution of snow density is unknown.

The AWS data has been used in an energy balance. The radiation components of the energy budget are taken directly from measurements, and the turbulent fluxes are modelled using bulk aerodynamic formulas (Oerlemans, 2000). The value of the turbulent exchange coefficient is tuned so that the model reproduces measured melt during a short period after the snow has melted, when the heat flux into the ice is small. The resulting value is 0.0032. When this value is used also in the rest

of the model period, the model is thought to calculate potential melt, i.e. the melt as it would have been if the initial cold content was zero. Measured melt is derived from the ultra sonic ranger. Total melt from the model should, when compared to total measured melt, give an idea about the magnitude of the reduction in melt due to cold ice. Modelled melt totals to 1.428 m w.e. and measured to 1.111 m w.e (Figure 1). The difference between these (0.317 m w.e.) should correspond to the change in cold content in the ice at this location during the model period. This change has been calculated from the ice temperature measurements shown in Figure 2. If the calculated change is expressed in terms of melt, i.e. divided by the latent heat of fusion, it amounts to 312 m w.e. The discrepancy is small, just 5 mm, which suggests that the surface energy fluxes have been modelled successfully.

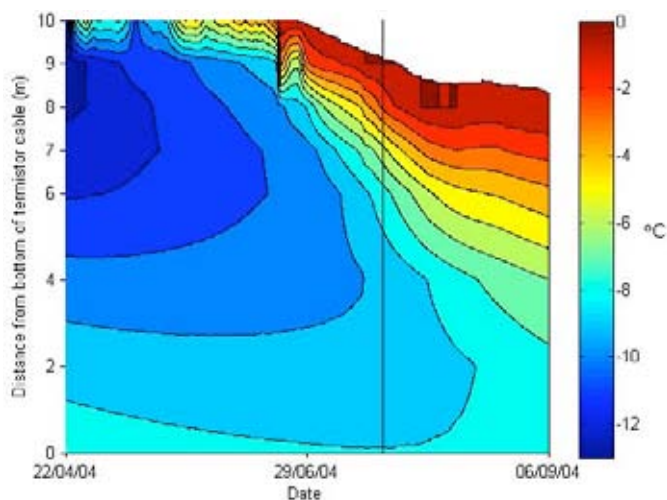


Figure 2. Time-depth contour plot showing the temperature evolution in the ice and the lowering of the glacier surface due to melt at the location of the AWS. Measurements were made at the depths indicated by the tick marks on the y-axis. Values for each day are interpolated linearly between the measured values. The bottom thermistor is used as datum (depth = zero) to avoid confusion arising from the lowering of the surface. The vertical line indicates the day on which the snow disappears.

This shows that the winter cold contributes to the net balance at this location by ~0.3 m w.e., roughly equal to the winter balance and to about 30 % of the summer balance at this location. The magnitude of the contribution from the cold content on the mass balance is therefore substantial and is likely to decrease as MAAT, and especially winter temperature increases.

References

- ACIA, 2004. Impacts of a Warming Arctic: Arctic Climate Impact Assessment. Cambridge University Press 2004.
- Oerlemans, J., 2000. Analysis of a 3 year meteorological record from the ablation zone of Morteratschgletscher, Switzerland: energy and mass balance. *Journal of Glaciology*, vol. 46, nr. 155, 571-9.
- Woodward, J., Sharp, M. and Arendt, A., 1997. The influence of superimposed-ice formation on the sensitivity of glacier mass balance to climate change. *Annals of Glaciology*, vol. 24, 186-90.

MASS BALANCE AND VELOCITY STUDIES ON McCALL GLACIER

MATT NOLAN

University of Alaska Fairbanks

We used a network of approximately 60 stakes on McCall Glacier to examine mass balance and velocity between 2003-2005. McCall Glacier is a small (6.5 km²) land-terminating glacier in the north-eastern Brooks Range in Alaska, about 100 km from the Arctic Ocean. In this abstract, I present some preliminary findings on the linkages between mass balance and ice dynamics.

All of our stakes, except for two, showed significant seasonal differences in speed. The stakes were measured twice per year in 2003, 2004, and 2005 – once at the end of winter in May and once at the end of summer in August. Nearly all of these stakes showed a summer increase in speed, though the stake at the highest elevation showed a summer decrease. The percentage change at all the poles ranged from 5% to 100% seasonally. Small differences were also observed in winter speeds between years on most poles. Figure 1 gives an example of this seasonal variation at a pole located in mid-ablation area, where the fastest speeds are observed. Maximum summer speeds are about 4 cm/day, with the summer increase about 1 cm/day through much of the ablation area. Our general interpretation of these seasonal variations is that the ice at the bed of the glacier must be at or near freezing, rather than frozen solidly to the bed. One of the poles that showed no seasonal change in speed was located near the terminus, which is largely wasting away in place due to insufficient ice flux above. The other pole that showed no seasonal change was located at the confluence of two tributaries, just below the equilibrium line, where we suspect that the basal ice may be frozen to the bed.



Figure 1. Speed of a pole in the mid-ablation area. Red dots indicate measurements, blue lines are the average speed in between measurements. The error bars are about the size of the red dots.

We investigated the nature of this summer-speed increase by installing a continuously-recording D-GPS network on the glacier. Figure 2 presents a 2005 GPS record from near the pole shown in Figure 1. Here we see that there is no general increase in summer speeds, but rather that the summer is characterized by sudden speed up events superimposed on the winter base-speed. Also shown on this figure is daily ablation a few meters from the GPS pole, as recorded by a sonic ranger. Between ice-melt beginning in mid-June and snowfalls beginning in August, there is a clear correlation between the ablation rate and the speed of the glacier. Not only does a temporal correlation exist, but the magnitude of the melt seems to affect the magnitude of the speed. The same trends are seen at other poles and also in 2003 and 2004. Our preliminary interpretation is that the cause of the speed variations are variations in melt-water supply to the bed, and further that the basal drainage system may stay small and immature throughout the year, such that any increases in water flux leads to overpressurization of the conduit system and a decrease in the shear stress that the bed can support. Understanding these dynamic responses to mass balance on McCall Glacier will be a major focus of our efforts for the IPY's Glaciodyn project.

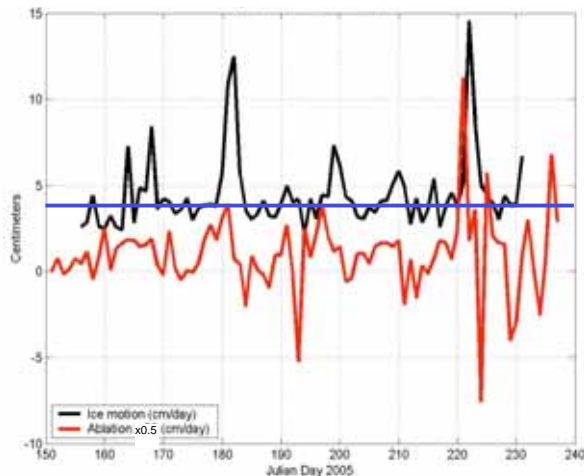


Figure 2. Daily speed and ablation in 2005 of a pole in the mid-ablation area. The blue line represents the average winter speed. As can be seen, the summer increase in speed is characterized by rapid motion events, rather than a smooth increase. Further, the rapid motion events appear to be related to the melt rate.

SHORT SCALE VARIATIONS IN MASS BALANCE AND DENSITY OF THE GREENLAND SNOWPACK AND FIRN

VICTORIA PARRY¹, PETER NIENOW¹, DOUGLAS MAIR², JEMMA WADHAM³, BRYN HUBBARD⁴ AND JULIAN SCOTT¹

¹ School of Geosciences, University of Edinburgh, UK.

² School of Geography and the Environment, University of Aberdeen, UK

³ School of Geographical Sciences, University of Bristol, UK

⁴ Centre for Glaciology, University of Aberystwyth, UK

Within the percolation zone of a given ice mass, meltwater generated at the surface refreezes at depth in the snowpack/firn thereby playing an important role in the mass balance (Pfeffer et al 1991). However, the proportion of the positive annual mass balance contributed by refreezing and the spatial variations in density structure, which result from refreezing remains poorly understood. In this study we aim to investigate spatial and temporal variations in firn/snowpack density and mass balance in the percolation zone of the Greenland ice sheet. The fieldwork site is located along the EGIG line at T5 (T5 - 69° 51'N 47° 15'W) at ~1950 m elevation in the percolation zone. Fieldwork was carried out before and after the onset and cessation of melt in spring (April-May) and autumn (September) 2004 respectively. A nested grid array was used, with sites investigating snowpack/firn density located at 1 m, 10 m, 100 m, and 1 km intervals, from T5 parallel to the EGIG line towards the dry snow zone, and perpendicular to the EGIG line.

At each site density measurements were taken from each stratigraphic layer in a snowpit dug to the previous end of summer (2003) layer. In addition, a 3 m core was retrieved from each site and density measured according to its stratigraphy. One long core (18 m depth) was retrieved and the density logged at 0.1 m resolution. Snow/firn samples were taken from stratigraphic layers in each pit, and at 0.1 m intervals down the long core and the ionic concentrations were measured.

By using depth density profiles taken from the autumn shallow cores across the nested grid, the effect of meltwater percolation and refreezing on spatial variability in the density could be investigated. Despite significant density changes throughout all the profiles, no consistency was seen across the area. Differences seen in density profiles taken from three sides of a 1 m² snowpit, demonstrate the short length scales at which density varies.

A significant change in bulk density of the snowpack was seen between spring and autumn. The average density of each pit in spring was 0.27 g cm⁻³, which had increased to 0.40 g cm⁻³ by autumn. Although the average density increase was in part due to superimposed ice that accounted for on average 10% water equivalent of each autumn pit, the firn between the individual ice layers had also increased in density.

In order to investigate whether meltwater was percolating below the current year's accumulation the change in density from spring to autumn for the 1.5 m firn columns beneath the end of summer 2003 layer were measured. The expected change in density due to compaction was predicted from the changes in density observed in the 18m long core (Fig. 1). The results suggest that only ~50% of the *observed* densification would be expected as a result of compaction therefore suggesting that a significant amount of meltwater does percolate down below the previous summer's melt-surface.

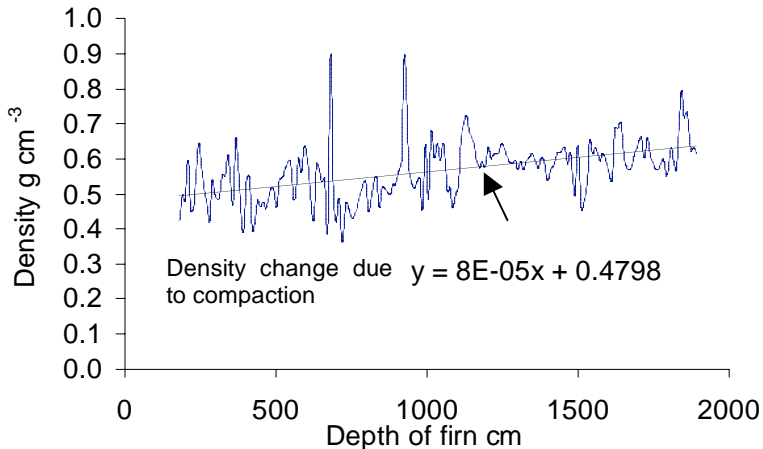


Figure 1. 10 cm resolution depth density profile from long core taken in spring 2004.

In addition to estimating likely rates of compaction, the long core was retrieved in the hope of generating a longer mass balance time series. Density measurements were taken in the lab at a 10 cm resolution in an attempt to establish annual layers (Fig. 1). However, whilst there were clear fluctuations in density, it was not possible to detect patterns indicating annual layers. The long core was therefore analysed at 10 cm resolution to determine whether variations in ionic concentrations could be used to distinguish annual layers.

Each 10cm 'bulk' sample was thus analysed for Chloride, Sulphate, Nitrate, Sodium, Potassium, Magnesium and Calcium. Of these Chloride is the most stable within the pack, so should give a better indication of any annual signal present. Unfortunately, annual layers could still not be reliably resolved (Fig. 2) and the core will now be further analysed to determine whether oxygen isotopes can resolve an annual time series.

Meltwater percolation and refreezing accounts for a 33% increase in the average 2003-2004 snowpack density. However measuring the contribution it has to the positive annual mass balance is complicated by short scale density variations of less than 1 m². Generating a longer time series using the 18m core has not been possible yet as annual layers cannot be identified through density changes or ionic chemistry signals. In addition to this, for accurate mass balance estimates, the

volume of meltwater percolating below the previous summer melt horizon must be accounted for.

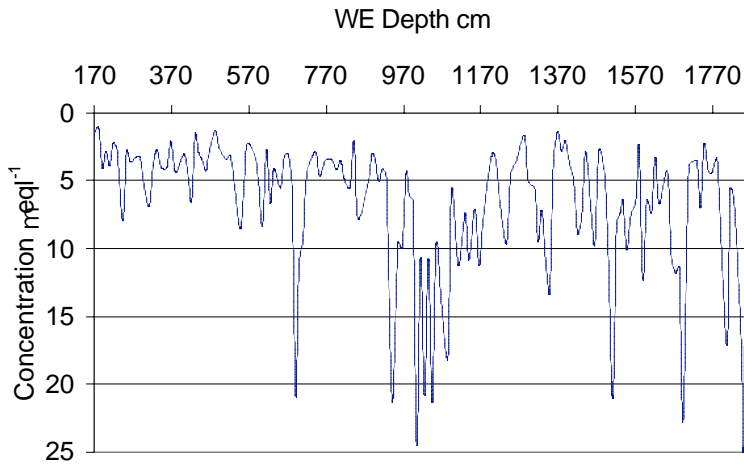


Figure 2. Chloride concentrations at 10cm resolution from the long core

References

Pfeffer, W., F. Meier, T. Illangasekare. 1991. Retention of Greenland runoff by refreezing: Implication for projected future sea level change. *J. Geophys. Res.*, **96** (C12), 22,117-22,124.

COLUMBIA GLACIER AT MID-RETREAT

W.T. PFEFFER

Institute of Arctic and Alpine Research, University of Colorado, Boulder, USA

Since the early 1980s, Columbia Glacier has retreated 15 km from its original endpoint in the Pacific Ocean in Alaska's Prince William Sound, thinned approximately 400 m at the position of the present (2006) terminus, and in the period 1994-1997 reached flow speeds as high as 27 m/day. The glacier is the largest single contributor to sea level rise among all North American glaciers, and accounts for about 10 percent of total glacial discharge from the Alaska/Yukon region each year. Flow speeds have diminished to ~10-15 m/d since their peak in 1994-1997 for reasons which are not immediately apparent. Calving rate remains high.

The retreat of Columbia Glacier is part of a cyclic pattern of slow advance and abrupt retreat typical of Alaskan tidewater glaciers. Alaskan tidewater retreats provide a model for apparently similar retreats now beginning on the outlet glaciers of southern Greenland, although in light of the current world-wide retreat of land-terminating glaciers, it is an open question as to whether re-advance will be possible following retreat, either in Alaska or Greenland.

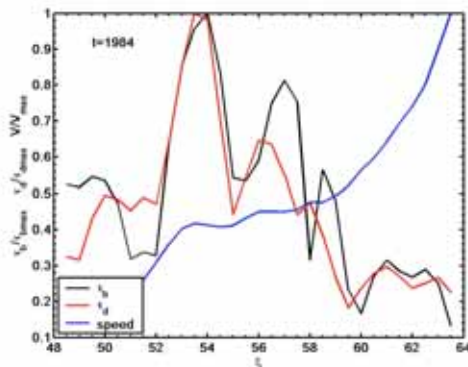


Figure 1. Relationship between force balance terms and velocity, for typical conditions during retreat, shown here for 1984. Terms are normalized; τ_b is basal drag, τ_d is driving stress. Velocity toward terminus (increasing τ) increases with diminishing τ_d . Prior to retreat, velocity diminished with diminishing τ_d .

Force balance calculations have been made (O'Neel et al, 2005) from the time series of 21 photogrammetrically-determined velocity fields (Krimmel, 2001) spanning the retreat of Columbia Glacier, from 1977 (before the onset of retreat) to 2004. The results of the force balance calculations show that both driving stress and basal drag diminish toward the terminus, consistent with thinning and reduction of surface slope. The dominant source of resistance to flow lies in the basal drag term, but is located at a position upstream from the terminus, and the

location of maximum basal drag migrates upstream as retreat and thinning progress. As a consequence of the upstream location of maximum basal drag, longitudinal stresses in the low-slope, high-velocity terminus region are extensile, which contributes to further thinning.

The glacier sliding speed is inversely correlated with local driving stress following the onset of retreat, although a more normal pattern (reduction in velocity associated with reduction in driving stress) is apparent for velocity fields from before the retreat (Figure 1).

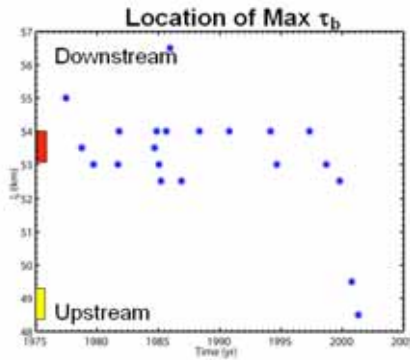


Figure 2. Location of maximum basal drag along the centreline coordinate of Columbia Glacier, shown as a function of time. The abrupt jump from ~km 53-54 (the location of a major lateral constriction) to ~km 48-48 occurred as the retreating terminus entered the constriction in 2000.

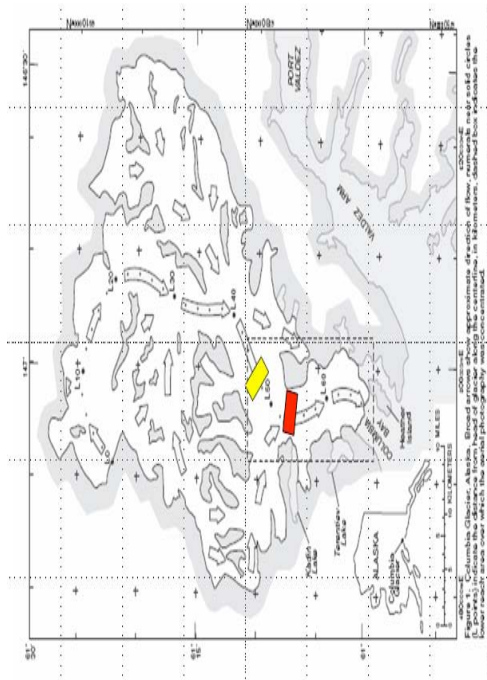


Figure 3. Location map, showing position of maximum basal drag before and after jump in 2000. Base map from Krimmel, 2001.

The position of maximum basal drag did not migrate smoothly upstream, but jumped upstream recently from a position of major lateral constriction as the terminus approached that constriction, as shown in Figures 2 and 3. This migration should place the ice between the present terminus (still near km 54) and the new position of basal drag in extension, promoting thinning. This extensile regime, combined with a broadening channel, deepening water, and reduced flow speed, should accelerate calving, and speed the retreat of the terminus toward km 48-49. Ice in the terminus region is presently grounded in water and at ~60-90% of floatation. The glacier bed does not rise above sea level for another ~15 km upstream from the terminus, and continued retreat over this distance is anticipated during the next ~20-25 years.

References

- O'Neel, Shad; Pfeffer, W. Tad; Krimmel, Robert; Meier, Mark Evolving force balance at Columbia Glacier, Alaska, during its rapid retreat. *J. Geophys. Res.*, Vol. 110, No. F3, F03012 10.1029/2005JF000292, 20 September 2005
- Krimmel, R.M., Photogrammetric data set, 1957-2000, and bathymetric measurements for Columbia Glacier, Alaska, USGS Water-Res. Inv. Rpt. 01-4089, 40 pp. 2001

CONSIDERATIONS ON SHORT-TERM AND SEASONAL FLUCTUATIONS OF HANSBREEN - A SVALBARD TIDEWATER GLACIER

DARIUSZ PUCZKO¹, JACEK A. JANIA², PIOTR GŁOWACKI¹ AND KRZYSZTOF MIGAŁA³

¹ Institute of Geophysics, Polish Academy of Sciences, Warszawa, Poland

² Faculty of Earth Sciences, University of Silesia, Sosnowiec, Poland

³ Institute of Geography, Wrocław University, Poland

Mass loss due to calving is an important component of the mass balance of tidewater glaciers. Calculation of the calving flux needs proper data on glacier speed near its terminus. Velocity of Svalbard tidewater glaciers are changing in space and in time (Pillewizer, 1939; Voigt, 1979; Jania, 1988). Glacier movement increases towards the calving front and short period fluctuations of glacier speed have been also noted (Vieli *et al.*, 2004). Available data on glacier velocity for Svalbard and for the whole Arctic are very limited and sparse.

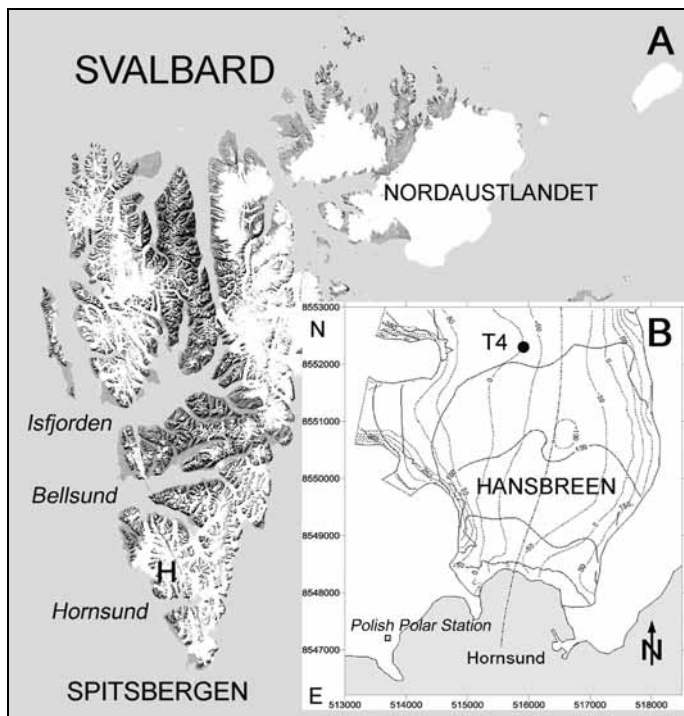


Figure 1. Location maps. A) Svalbard, Spitsbergen: H, Hansbreen (courtesy of the NPI). B) Lower part of Hansbreen: T4, location of the stake where glacier superficial velocity has been surveyed by electronic distance meter and precise GPS receiver; solid lines, elevation contour lines; dotted lines, bedrock contour lines; glacier centreline is marked.

This is the motivation for studies of flow speed of Hansbreen. To record diurnal, short time, seasonal and inter annual fluctuations of the glacier speed and detect factors driving such changes. An important aim of this project in progress is also an attempt to obtain correct mean annual flow velocity close to the glacier terminus. One element of the project is related to comparison of the InSAR data on glacier speed, usually derived from March or April images, with annual course of glacier velocity. An answer to the question of how representative are the short time-span InSAR data for mean annual velocity (c.f. Jania, 2002) is important for estimation of calving flux.

Hansbreen is a medium size polythermal grounded tidewater glacier in South Spitsbergen, Svalbard (Fig. 1). Its area is c. 56 km²; length c. 16 km and mean slope along the centreline 1° 40'. Ice thickness is reaching 400 m. Floor of the glacier valley lies well below sea level, having three overdeepened basins (Moore *et al.*, 1999). The uppermost one is located under lower part of the main accumulation area.



Figure 2. Electronic distance meter on a permanent metal tripod on the slope of Fugleberget. Location of stake T4 is marked on the Hansbreen surface (Photo by D. Puczko).

Survey of Hansbreen velocity has been conducted by an electronic distance meter from a permanent metal tripod on the slope of Fugleberget (Fig. 2) on intervals of 1-3 weeks (dependent on weather conditions). Positions of 6 stakes were determined by general accuracy +/- 4 cm (while the instrument nominal accuracy is 1 ppm). In this work velocity at the stake T4 only is considered. The stake is located c. 4 km from the terminal ice cliff (cf. Fig. 1). Longer series of the precise differential GPS time-lapse survey of the glacier velocity was conducted close to this stake in 2003, 2004 and have been recorded continuously since fall 2005. An automatic weather station with ultrasonic ranger is also located close to stake T4.

Results show that Hansbreen flow velocity fluctuates on the diurnal, short period, seasonal and interannual time scales. Glacier speed at the T4 reacts to additional water supply from the surface to its bed at the beginning of melting in late spring. It is well visible by comparison of melting rate and mean daily glacier velocity (Fig. 3).

Heavy rainfalls and positive air temperatures were noted in January 2006 as exceptional winter events. As a consequence increase of glacier speed was recorded by the precise GPS receiver (Fig. 4).

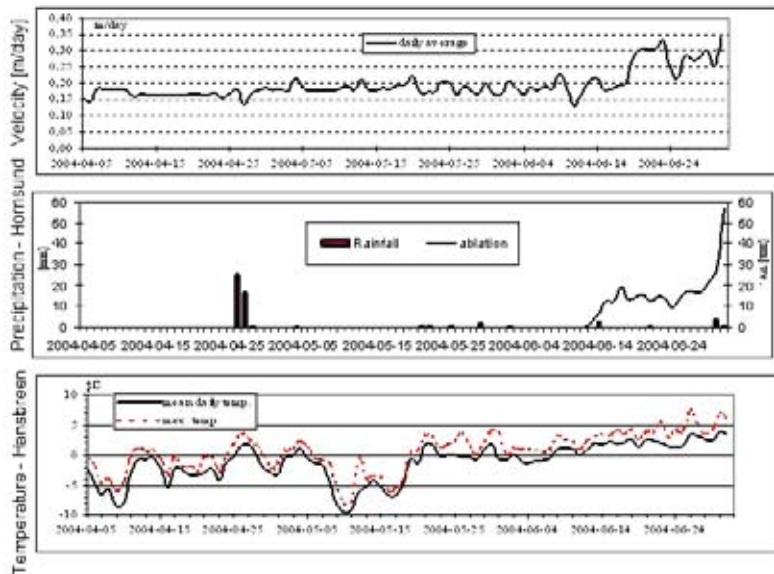


Figure 3. a) Fluctuations of glacier velocity in spring and beginning of summer 2004. b) Comparison with ablation on stake T4 (204 m a.s.l.). c) Mean and maximal daily air temperature and liquid precipitation events at the Hornsund meteorological station (9 m a.s.l.).

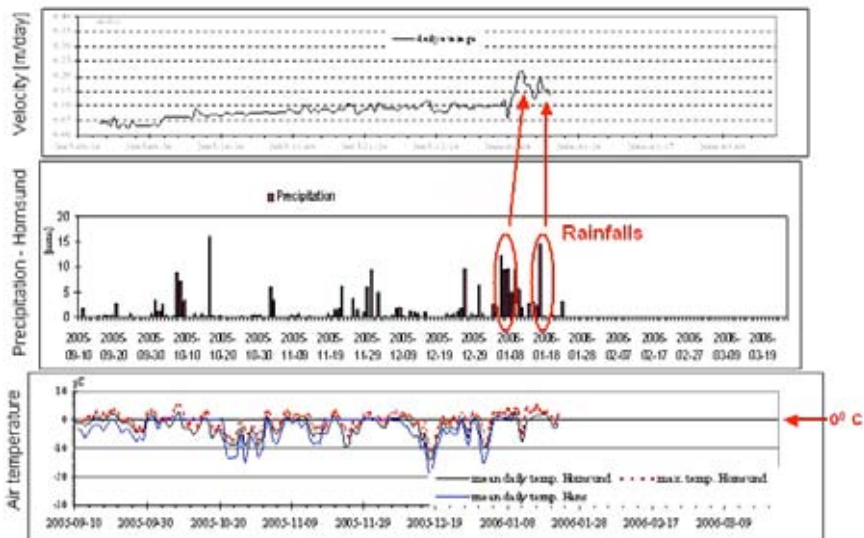


Figure 4. a) Course of glacier velocity at stake T4 (201 m a.s.l.) in the period 10 September 2005 – 20 January 2006 in comparison to b) precipitation in the Hornsund station (9 m a.s.l.). Rainfall events in January 2006 are marked in red. c) Mean daily air temperatures near stake T4 and mean and maximal daily air temperatures in Hornsund.

Presented observations are in agreement with results of similar studies on Hansbreen conducted during last 10 days of June and in July 1999 (Vieli *et al.*, 2002). In summer, the englacial drainage system is well developed and melt water could migrate to the glacier bed, increasing subglacial water pressure and in consequence basal sliding (as observed in 1999). Increases of glacier velocity after rainfalls during winter (January 2006) and when air temperature raised in early spring (April 2005) suggest high sensitivity of the glacier to additional intake of water into the system even in the cold period of the year. Hansbreen bed topography is favourable for retention of subglacial water due to a low glacier slope and overdeepenings of the subglacial valley.

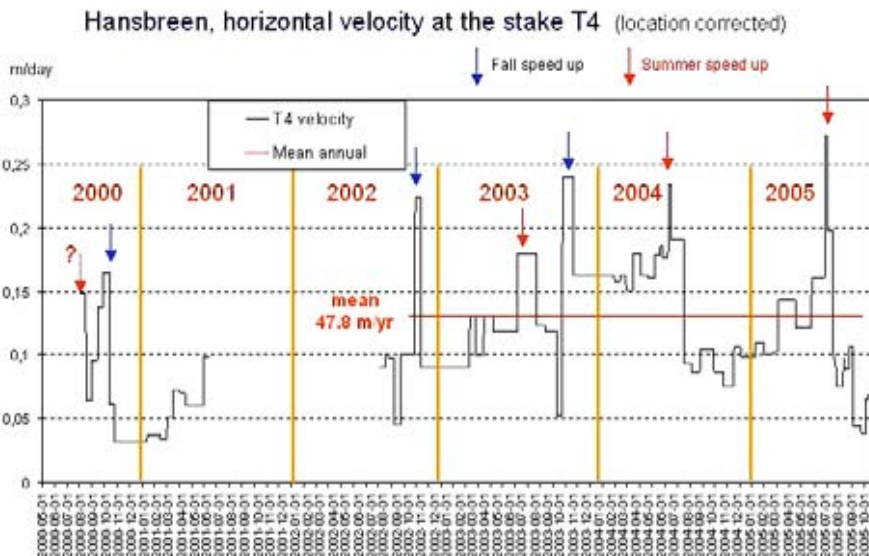


Figure 5. Seasonal fluctuations of the glacier velocity in the period 2000 – 2005. Results of the survey by the electronic distance meter. Summer and fall speed up events are marked by arrows. Mean annual flow velocity for years 2002/2003 – 2004/2005 is marked.

Seasonal fluctuations of glacier velocity have been detected and differ from the classic course (Fig. 5). Significant acceleration of movement has been noted also in fall (e.g. 2002, 2003). Presented data are the longest for Svalbard glaciers. Unfortunately, they are still insufficient to answer the question why after well pronounced summer speed up the fall one is not observed (e.g. 2004, 2005). Interannual differences in mean winter level of velocities appear from the presented record. Glacier velocities during winter 2003/2004 are higher than in other cold seasons. Reasons of it are unclear and probably affected by several factors.

One of the possible hypothesis is a longer time of retention of melt water within the accumulation area due to its slow percolation through firn and englacial drainage system down to the bed. Simple estimation basing upon a melting rate of Hansbreen during these particular summers suggests delay by c. 2 years.

In conclusions it could be stressed that:

- Short term fluctuations of the glacier speed during winter and spring might cause significant differences between the InSAR data on flow velocity (derived usually in the cold period of the year) from realistic mean annual values.
- Mass loss due to calving of Svalbard glaciers couldn't be calculated from the InSAR survey but only estimated with an accuracy +/- 20-30%. Svalbard tidewater glaciers have in majority small slopes and overdeepened subglacial valleys. They seem to behave similarly to Hansbreen in respect to fluctuations of velocity on different time scales.
- Definition of the role of particular factors driving glacier velocity changes needs further study. Proximity of the Polish Polar Station, Hornsund is giving possibilities for the continuous record of the glacier velocity and meteorological conditions responsible for melting rate on the glacier.

Acknowledgements

We wish to thank Artur Adamek, Piotr Dolnicki and other colleagues from particular wintering crews of the Polish Polar Station for support in the field and on-line reporting of results of measurements. The project is supported by the Polish Ministry of Education and Science under terms of the research grant No. PBZ-KBN-108/P04/2004 and partly by the University of Silesia (grant No. BS/KG-2/2006).

References

- Jania, J., 1988: Dynamiczne procesy glacialne na południowym Spitsbergenie [Dynamic glacial processes in South Spitsbergen – English summary]. *Prace Naukowe Uniwersytetu Śląskiego*, No. 955, Katowice, 258 pp.
- Jania, J., 2002: Calving intensity of Spitsbergen glaciers. [in:] J.B. Ørbæk, K. Holmèn, R. Neuber, H.P. Plag, B. Lefauconnier, G. de Prisco, H. Ito (Eds.) *The Changing Physical Environment. Proceedings from the Sixth Ny-Ålesund International Scientific Seminar*. Tromsø, Norway, 8-10 October 2002, Norsk polarinstitutt, Internrapport Nr. 10, 117-120.
- Moore J.C., Päli A., Ludwig F., Blatter H., Jania J., Gądek B., Głowacki P., Mochnecki D., Isaksson E., 1999. High-resolution hydrothermal structure of Hansbreen, Spitsbergen mapped by ground-penetrating radar. *Journal of Glaciology*, 45 (151), 589 – 590.
- Pillewizer, W., 1939: Die kartographischen und gletscherkundlichen Ergebnisse der deutschen Spitzbergen-Expedition 1938. *Petermanns Mitteilungen, Ergänzungsheft*, Nr. 238, Gotha, 46 pp.
- Vieli, A.; Jania, J.; Blatter, H.; Funk, M., 2004: Short-term velocity variations on Hansbreen, a tidewater glacier in Spitsbergen. *Journal of Glaciology*, 50 (170), 389-398.
- Voigt, U., 1979: Zur Blockbewegung der Gletscher. *Geod. Geoph. Veröff.*, R. 3 (44), 128 pp.

MODELLING FUTURE GLACIER MASS BALANCE AND VOLUME CHANGES OF STORGLACIÄREN, SWEDEN, USING ERA40-REANALYSIS AND CLIMATE MODELS DATA

VALENTINA RADIĆ AND REGINE HOCK

Department of Physical Geography and Quaternary Geology, Stockholm University, Stockholm, SWEDEN

Mass balance and volume evolution of Storglaciären, a small valley glacier in Sweden, is predicted until 2100 using a temperature-index mass balance model, ECMWF re-analysis (ERA-40) and input from climate models, with emphasis on the sensitivity of results to the choice of climate model and variants of adjusting ERA-40 temperatures to local conditions. ERA-40 temperature and precipitation series from 1961-2001 are validated and used as input to the mass balance model and for statistical downscaling of one regional (RCM) and six global climate models (GCMs). Future volume projections are computed using volume-area scaling [Bahr et. al., 1997] and constant glacier area.

Validation of ERA-40 in the Storglaciären's region showed that ERA-40 temperature explains more than 80% of variance for observed daily, monthly and annual temperatures at station close to the glacier and that inter-annual variability is captured well. Precipitation from ERA-40 explains, on average, 50% of variance from observed precipitation sums and inter-annual variability is captured sufficiently well for use in the mass balance modelling.

The mass balance model driven by nine variants of ERA-40 input performs similarly well regardless of temporal resolution of the input data (daily or monthly averages) and regardless of adjusting ERA-40 temperatures to observations in order to fit better to station data. However, the model explains more variance of measured mass balance (70%) when the ERA-40 temperatures are reduced prior to input to mass balance model to coincide better with locally colder air temperatures at the glacier surface. This reduction is derived from optimizing the lapse rate when tuning the model and therefore is independent of observations.

Projected future volume series derived from the mass balance model which is forced by statistically downscaled outputs of one regional and six GCMs with B2 emission scenarios result in a volume loss of 50-90% of the initial volume by 2100. The differences in these projections vary with 40% of the initial volume and are mainly due to different climate projection from the GCMs (Fig 1d). Each volume projection varies in a range of 20% due to applied volume-area scaling or constant area (Fig 1c). The choice of the method in the mass balance modelling, after excluding obvious outliers, gives the uncertainty range of 10% to each volume projection (Fig 1a), while the choice of the baseline period for the downscaling method results in 3% uncertainty range (with the outlier excluded) (Fig 1b).

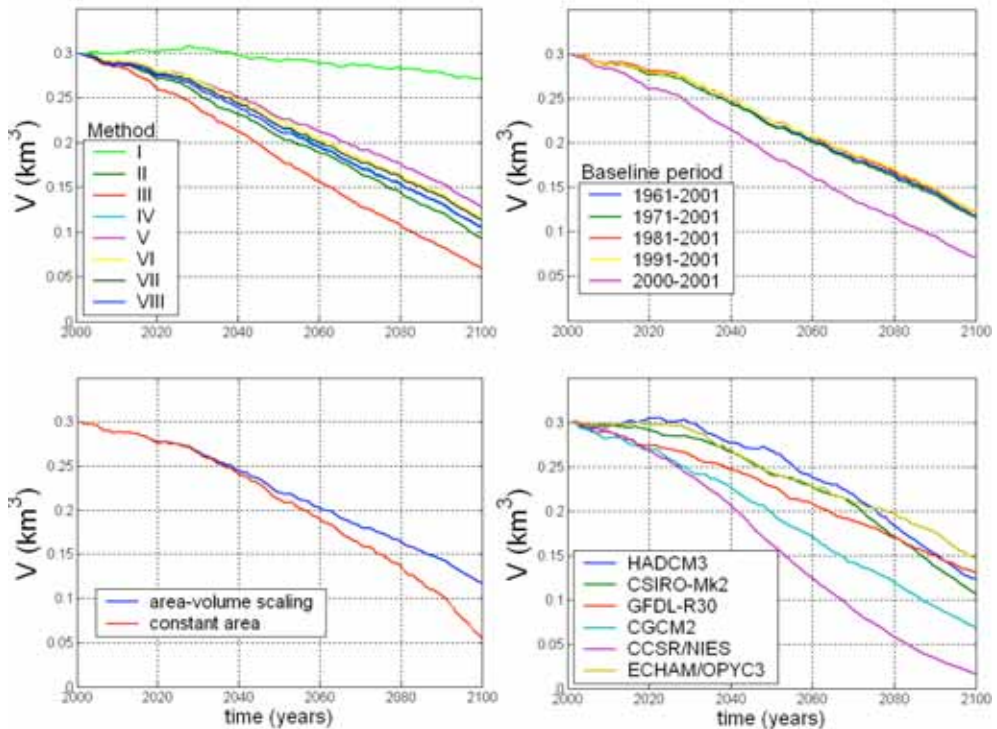


Figure 1. Volume projections for Storglaciären in the 21st century derived from: (a) eight methods (I-VIII) of the mass balance model and RCM output downscaled with ERA-40 reference climate for the baseline period 1961-2001, (b) method VII applied on the RCM output downscaled by use of five different baseline periods, (c) method VII applied on the RCM, downscaled using the 1961-2001 baseline period, and with volume-area scaling and constant area, (d) method VII applied on the six GCMs which are downscaled using 1961-2001 baseline period. In all projections, unless noted differently, the volume is derived from volume-area scaling.

Modelled projections are not only highly sensitive to the choice of GCMs but can completely offset the results if the biases in GCMs output are not corrected by the reference climate i.e. if the proper downscaling method is not applied. The static mass balance sensitivities to future temperature and precipitation change, calculated as running difference between 20-year averages of net mass balance (b_n) and averaged b_n over the reference period 2001-2020, show very small variations in time with the mean value of $db/dT = -0.48 \text{ m a}^{-1} \text{ K}^{-1}$ and $db/dP = 0.025 \text{ m a}^{-1}$ per 1% precipitation increase.

The applied mass balance model is capable to determine future volume changes that are comparable with those derived from more sophisticated models [Oerlemans et al., 1998; Schneeberger et al., 2001] and that the estimated static mass balance sensitivity corresponds well to previous estimates [Braithwaite et al., 2002; de Woul and Hock, in press]. A possible way of using our results for global assessment of glacier volume change in the 21st century is direct application of the model to other glaciated regions taking advantage of the model's simple

requirements for meteorological data, which are widely available from ERA-40 reanalysis. However this has an inevitable shortcoming in the need of measured seasonal mass balance, which are necessary for calibrating the model. Further study is needed to evaluate how far the calibrated mass balance model for one glacier is transferable to other glaciers and whether representative sets of model parameters can be found for glaciers in similar environmental settings.

References

- Bahr, D.B., M.F. Meier, and S.D. Peckham (1997), The physical basis of glacier volume-area scaling, *J. Geophys. Res.*, 102(B9), 20355-20362.
- Braithwaite, R. J., Y. Zhang, and S. C. B. Raper (2002), Temperature sensitivity of the mass balance of mountain glaciers and ice caps as a climatological characteristic, *Z. Gletscherk. Glazialgeol.*, 38(1), 35-61.
- De Woul M., and R. Hock, Static mass balance of Arctic glaciers and ice cap using a degree-day approach, *Ann. Glaciol.*, 42, in press.
- Oerlemans J., B. Anderson, A. Hubbard, Ph. Huybrechts, T. Jóhannesson, W. H. Knap, M. Schmeits, A. P. Stroeven, R. S. W. van de Wal, J. Wallinga, and Z. Zuo (1998), Modelling the response of glaciers to climate warming, *Clim. Dynam.*, 14, 267-274.
- Schneeberger, C., O. Albrecht, H. Blatter, M. Wild, and R. Hock, R. (2001), Modelling the response of glaciers to a doubling in atmospheric CO₂: a case study of Storglaciaren, northern Sweden, *Clim. Dynam.*, 17(11), 825-834.

THE MULTI-LAYER SNOW MODEL SOMARS IN A DISTRIBUTED ENERGY AND MASS BALANCE MODEL

CARLEEN REIJMER¹ AND REGINE HOCK²

¹Institute for Marine and Atmospheric Research, Utrecht University, Utrecht, the Netherlands

²Department of Physical Geography and Quaternary Geology, Stockholm University, Stockholm, Sweden.

Summary

The multi-layer snow model SOMARS was implemented in a distributed energy and mass balance model. The model was applied on Storglaciären, a small valley glacier in Northern Sweden. The results were validated using automatic weather station observations and surface mass balance observations using stakes and a sonic altimeter. The model is well capable of reproducing the temporal variations in mass balance at the weather station site. The spatial distribution of the mass balance is less well reproduced with large underestimation of melt at the lower part of the glacier. Largest change in mass balance when introducing the multi-layer snow model occurs in the accumulation area and is due to internal accumulation, which lowers the calculated average summer balance of the glacier by 10% from 1.43 m we to 1.29 m we.



Figure 1. Picture of Storglaciären (photo: Regine Hock).

Introduction

In recent years effort has been put into the development of distributed models to calculate glacier melt in order to obtain better estimates of the summer balance of glaciers in addition to obtaining a better understanding of the spatial distribution of melt on glaciers. Here, we present a distributed energy and mass balance model in which we implemented a multi-layer snow model in order to improve the calculation of the surface temperature, and mass loss. Furthermore, the multi-layer snow model will provide us with more information on the internal structure of the snow and firn layer, especially on internal accumulation and the formation of super imposed ice. We applied the model on Storglaciären, a small valley glacier in northern Sweden (Figure 1). The advantage of this glacier is the amount of data

available to force our model and to validate our results with. Here, we will focus on the summer mass balance of the glacier in 1999.

Model

We use the distributed energy and mass balance model of Hock and Holmgren (2005). The model solves the surface energy balance as described by the following equation at each grid point of a grided area:

$$S_{in}(1 - \alpha) + L_{in} - L_{out} + H + LE + Q_R + Q_G = Q_m, \quad (1)$$

where S_{in} is the short wave incoming (or global) radiation, α is the surface albedo, L_{in} and L_{out} are the incoming and outgoing long wave radiation, H and LE are the turbulent fluxes of sensible and latent heat, respectively, Q_R is the energy supplied by rain, Q_G is the sub-surface energy flux and Q_m is the energy used for melt. Fluxes towards the surface are defined positive. The method to determine each component of the energy balance at each grid point is described extensively by Hock and Holmgren (2005). Here we focus on the calculation of Q_G , Q_m and the surface temperature T_0 , the latter is needed for the calculation of L_{out} , H and LE .

In the original model T_0 is determined by way of an iterative method. First, the assumption is made that Q_G is small and set to either 0 Wm^{-2} or a small constant value. Next, T_0 is set to 0°C and the different terms in Eq. 1 are calculated. In case Q_m is positive or 0 Wm^{-2} no further steps are taken and Q_m is used to calculate melt, which is equal to runoff. In case Q_m is negative T_0 is lowered by 0.25°C and the calculation is repeated. This procedure is repeated until Q_m is 0 Wm^{-2} . This method produces reasonable results as long as Q_G is indeed small, as is the case on temperate glaciers.

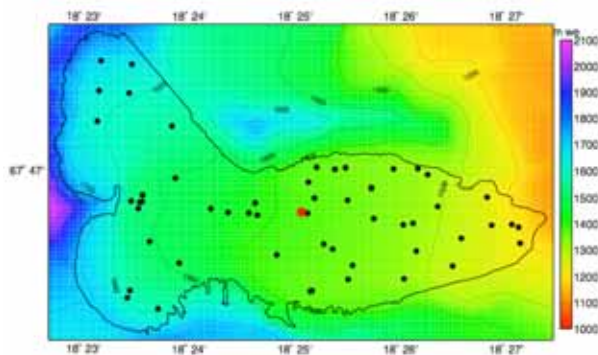


Figure 2. Digital elevation model Storglaciären. A black contour line outlines the glacier. The black dots indicate the stake locations and the red dot indicates the location of the weather station.

A more sophisticated way of determining T_0 , Q_G and Q_m is by using a multi-layer snow model. The model implemented here is the SOMARS model (Simulation Of glacier surface Mass balance And Related Sub-surface processes) developed by

Greuell and Konzelmann (1994) and tested extensively by Bougamont et al. (2005). The model solves the thermodynamic energy equation on a vertical grid extending from the surface to ± 30 m depth. Model output consists of vertical profiles of snow temperature, density and water content. The model takes into account percolation and refreezing of melt water, slush formation and densification of snow.

The model is applied on Storglaciären, a small valley glacier in northern Sweden (Figure 1). The area of the glacier is 3 km^2 and the elevation ranges from ~ 1120 m to ~ 1730 m asl). The model is forced with automatic weather station observations for the period 9 May - 2 September 1999. The AWS was located on the glacier at 1370 m asl, close to the equilibrium line. For validation, T_0 derived from L_{out} observations, data from a sonic altimeter located close to the weather station, and mass balance data from 53 stakes on the glacier were used (Figure 2).

Results

Figures 3 and 4 present the results of the validation. The mass balance produced by the model is very sensitive to the albedo parameterization, the description of the turbulent fluxes, especially the surface roughness lengths, and the description of snow fall. As a result, after tuning, the model represents the temporal variations in surface mass balance at the weather station site very well (Figure 3a). However, the spatial distribution of the summer balance is more difficult to reproduce correctly. The model underestimates the amount of melt in the lower regions of the glacier. A reason for this could be spatial variations in surface albedo of ice that are not included in the model. The iterative method has the same problem.

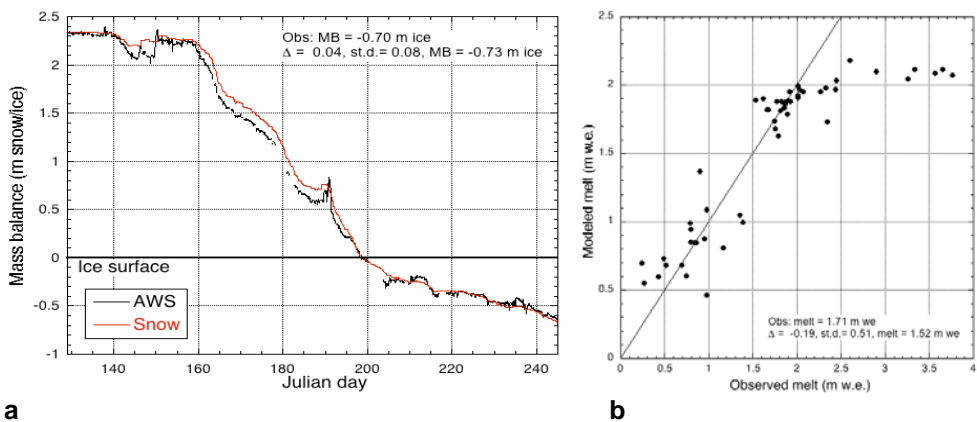


Figure 3. a) Time series of mass balance at the AWS site. b) Modelled summer melt as a function of observed at 53 stakes on the glacier. Stake locations are plotted in Figure 2.

The spatially distributed summer balance is plotted in Figure 4a. Over the complete glacier melt occurs in summer. Values range from 5 mm we on the southern highest parts to a maximum of 2.27 m we on the lowest northern parts of the glacier, clearly showing the effects of sun exposure on melt. The snowline on 2 September was at about 1480m asl. The modelled average summer balance for

the glacier is -1.29 m we. From observations the summer balance for 1999 was estimated to be -1.51 m we. The too low value from the model can be attributed to the fact that the observations include the month of September.

One of the advantages of the multi-layer snow model over the iterative method is the possibility of melt water to percolate into the firn where it can refreeze. In the iterative method all melt immediately results in mass loss. As a result the average mass balance produced by the iterative method is larger than in the multi-layer snow model. Figure 5 gives an impression of the spatial distribution of the internal accumulation. To obtain this figure first the snow cover on 2 September was subtracted from the snow cover on 9 May. The snow cover on 9 May is the winter balance and the difference is therefore the amount of last winter snow that melted during the summer. From this difference the modelled summer balance at each grid point was subtracted. Resulting negative values indicate that all last winter snow has melted, plus an additional amount of firn or ice. A value of 0 indicates that only last winter snow has melted but nothing more, while a positive value indicates that the amount of last winter snow melted is more than the mass loss indicated by the summer balance at that grid point. This means that the part of the melted snow has percolated into the firn and has not yet resulted in mass loss. The figure therefore gives an impression of the horizontal distribution of internal accumulation in the firn area.

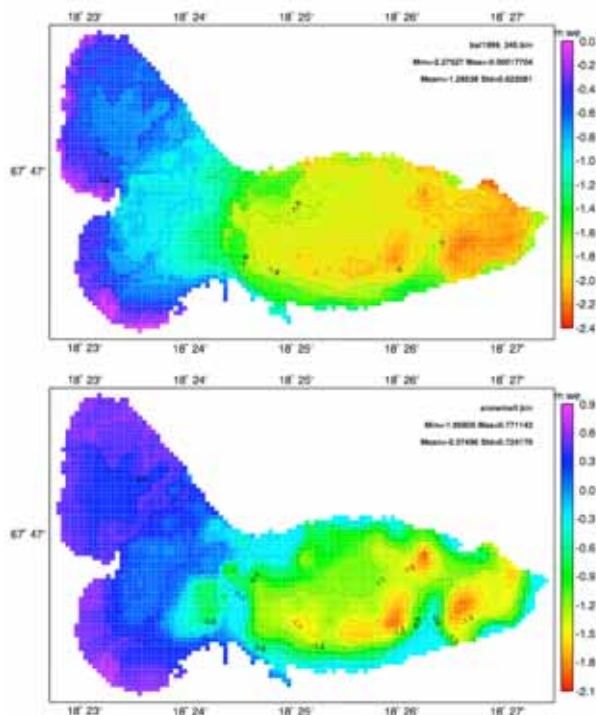


Figure 5. a) Summer balance of Storglaciären calculated over the period 9 May - 2 September 1999. b) Amount of last winter snow melted away on 2 September minus the summer balance. See text for further explanation.

To give an impression of the effect of taking into account internal accumulation on the average mass balance of the glacier, the mass balance was also calculated assuming that all melt resulted in immediate mass loss, as is the case in the iterative method and is assumed when using stake readings to estimate the summer balance. Including this extra mass loss the average modelled summer balance would have been -1.43 m we, which is 10% more than including internal accumulation (-1.29 m we).

Conclusions

The multi-layer snow model is well capable of calculating the mass balance of the glacier. It is more suitable to be used on polythermal glaciers where Q_G cannot be neglected. The model additionally provides information on the sub-surface. Internal accumulation is computed and (not presented here) the formation of superimposed ice.

References

- Bougamont, M., J. L. Bamber, and W. Greuell. Development and test of a surface mass balance model for the Greenland ice sheet, *J. Geophys. Res.*, 110, F04018, doi:10.1029/2005JF000348, 2005.
- Greuell, W., and T. Konzelmann. Numerical modelling of the energy balance and the englacial temperature of the Greenland ice sheet. Calculations for the ETH-camp location (West Greenland, 1155 m a.s.l.), *Global and Planetary Change*, 9, 91-114, 1994.
- Hock, R., and B. Holmgren, A distributed surface energy balance model for complex topography and its application to Storglaciären, Sweden, *J. Glaciol.*, 51(172), 25-36, 2005.

A SURFACE MASS BALANCE MODEL FOR AUSTFONNA, SVALBARD

THOMAS V. SCHULER¹, TROND EIKEN¹, JON OVE HAGEN¹, EVEN LOE¹, KJETIL MELVOLD^{1,3}, ANDREA TAURISANO²

¹Institutt for geofag, Universitetet i Oslo

²Norsk Polarinstittutt, Tromsø

³now at: Norsk Vassdrags- og Energidirektoratet (NVE), Oslo

Continuous meteorological data series of the 2004/05 period were retrieved from two automatic weather stations (AWS) which were operated on the Austfonna ice cap, Svalbard. In addition, mass balance measurements were conducted using a network of stakes distributed across the ice cap. The distribution of snow accumulation was determined along several profile lines using radar sounding. These data form the basis for a model of the surface mass balance. The spatial accumulation pattern was derived from the snow depth profiles using regression techniques and ablation was calculated using a temperature-index approach.

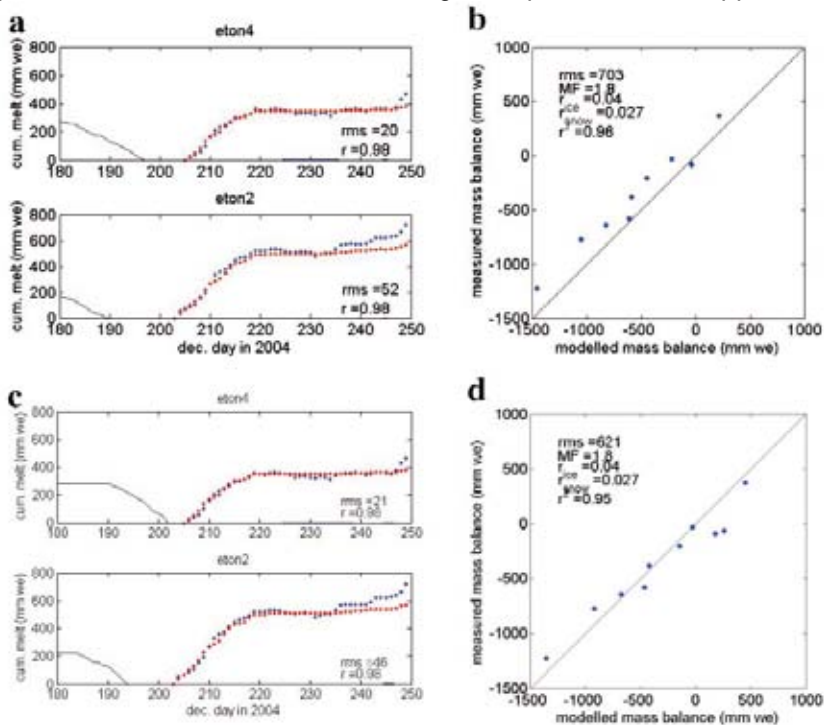


Figure 1. Comparison of the model performance for two different variants of model formulation. Lefthand column shows modelled (red) and measured (blue) ice ablation at the two AWS Eton 2 and Eton 4 (a and c). The scatter plots on the righthandside compare modelled (x-axis) and measured (y-axis) net mass balance at the individual stakes. Results a and b were produced without taking refreezing into account, whereas the computation of c and d included a formulation of superimposed ice formation.

The model parameters were calibrated using the available field data. Parameter calibration was complicated by the fact that several different parameter combinations yielded equally acceptable matches to the stake data. However, the resulting glacier net mass balance differed a lot between the different combinations. Validating model results against multiple criteria is an effective method to face equifinality. In doing so, a range of different data and observations was compared to several different aspects of the model results. Some of these criteria are semi-quantitative, thereby inhibiting to be included in an automatic method to estimate parameter values. However, we prefer to use all available criteria instead of applying an automatic procedure and hence, the manual calibration of the model requires extensive interaction by the operator. Nevertheless, this procedure makes it easier to directly identify the potential source for misfits and therefore, contributes to improve the model conceptually. As such, the systematic underestimation of net balance while at the same time ice ablation was reproduced correctly, suggests that refreezing processes play an important role. To represent the formation of superimposed ice, a simple p-max approach was included in the model formulation. Adopting p-max values in line with those used in previous studies, a satisfying model performance was achieved (Fig. 1). Used as a diagnostic tool, the model suggests that the surface mass balance for the period May 2004 – May 2005 was negative (~ -0.3 m w.e.; compare Fig. 2).

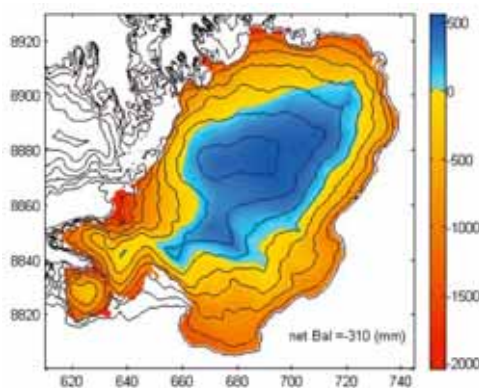


Figure 2. Map showing the distribution of modelled net mass balance of Austfonna over the period May 2004 – May 2005. Values are given in mm w.e. and the coordinates are in km Northing (y-axis) and Easting (x-axis) UTM33.

In the future, work will be undertaken to define appropriate criteria enabling automatic parameter estimation and more advanced methods to describe the formation of superimposed ice will be implemented. Then, the model offers the possibility to predict or reconstruct the mass balance evolution when applying projected or reanalyzed meteorological data. At that stage, it can be coupled to an ice-dynamic model to assess the response of Austfonna to climate change.

Acknowledgements

Contributions of the European Space Agency (ESA) and the Norwegian Space Centre enabled the field work. The data analysis was conducted and supported within the EU-project “Space borne measurements of Arctic Glaciers and Implications for Sea Level – SPICE” (EC-5FP EVK2-2001-00262).

EXEGESIS OF INTERFEROMETRIC AND ALTIMETRIC OBSERVATIONS IN SOUTH SPITSBERGEN

ALEKSEY I. SHAROV

Institute of Digital Image Processing, Joanneum Research, Graz, Austria

The present paper is based on the main outcomes of the INTEGRAL (EC FP6) and SIGMA (ESA AO No.2611) research projects devoted to enhanced modelling of glacier mechanics and studying the regime and changes of large European tidewater glaciers from satellite interferometry and altimetry. Synthetic aperture radar interferometry (INSAR) is regarded as a highly informative remote sensing method for glacier studies. Still, the exegesis [from Greek *exegeisthai* - to explain, interpret] or critical interpretation of the spaceborne interferograms taken over labile glacial environments is by no means straightforward and necessitates additional constraints and precise topographic reference models. Precipitous glacier faces, rapid changes and the lack of adequate reference models pose essential difficulties in geocoding of glacier interferograms and distinguishing between the impacts of ice surface topography and surface displacement on the interferometric phase.

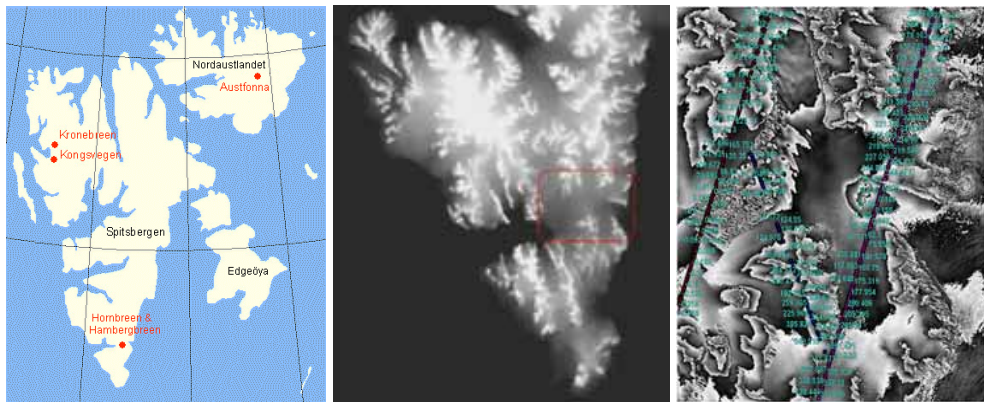


Figure 1. H-H test site in a small-scale map of Svalbard (a), in raster DEM of South Spitsbergen (1936, b), and in INSARAL composite (1996-2003, c).

The underlying concept of the research is to facilitate the geometric processing of interferometric data and to compensate for the lack of reliable reference models in extensive glacial areas with precise altimetric and photogrammetric data, yet without or independently of the use of surveyed control points. The study area comprises the Sör-Spitsbergen National Park in south Svalbard, Norwegian Arctic with a total land area of approx. 4,500 km². The basic test site of smaller size covers the system of Hornbreen and Hambergbreen tidewater glaciers (H-H) situated in the southernmost part of the Svalbard archipelago (Fig. 1a) and characterized with high rate of spatial changes. The character and causes of these

changes are not fully understood at present. Up-to-date topographic maps and digital elevation models of the test site are either nonexistent or of limited quality and coverage. The geometric constraints needed for the precise interferometric modelling of the study glaciers were thus derived from spaceborne ICESat-GLAS altimetric transects and ASTER-VNIR imagery.

The Hornbreen-Hambergbreen system is composed of two relatively thin and flat grounded tidewater glaciers flowing in opposite directions, terminating and calving in deep waters of Hornsund in the west and Hambergbukta in the east, and forming a relatively narrow ice isthmus, which connects Sörkapp Land with the main island of Spitsbergen. According to available topographic maps the width of the “ice bridge” exceeded 35 km in 1900 and was still about 25 km in 1936. Ice surface elevation does not exceed 220 m a.s.l. over the most part of the elongate glacier-covered valley between Hornsund and Hambergbukta. The vague ice divide separating Hornbreen from Hambergbreen is dissected by two nearly parallel melt-water channels flowing eastwards 2 km apart from each other. There are no nunataks at the H-H ice divide and there is strong evidence that the glacier bed lies below sea level in this area. The ground penetrating radar surveys performed by Finnish colleagues in the year 2000 after the airborne radio-echo soundings done by Russian and British explorers in 1980-s could neither verify nor negate the hypothesis about the presence of a sub-glacial strait between Torell and Sörkapp lands, which was first expressed 30 years ago by V.Koryakin.

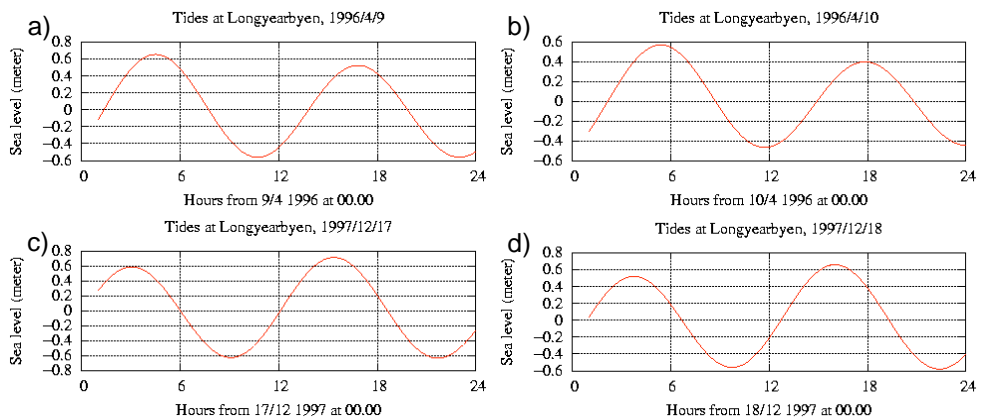


Figure 2. Predicted tides for the instants of INSAR surveys: 09/10.04.96 (a / b) and 17/18.12.97 (c / d).

Surprising is that tides in south Svalbard, which can reach 1.5 m (Fig. 2) and might essentially influence ice-loss processes in marginal parts of tidewater glaciers, had not been taken into account in previous studies. We therefore tried to apply tide-coordinated INSAR data to determining the modes of ice motion, deformation and destruction in the ice-bridge area, which becomes thinner and narrower with time. 7 spaceborne repeat-pass ERS-1/2-SAR interferometric tandem pairs taken in 1995 - 1997 at 1-day intervals under steady cold weather conditions were selected so as to provide short spatial baselines within the range of 0 – 100 m (Tab 1). The INSAR

data was processed in a standard way using the RSG 4.6 in-house software package. The amplitude of astronomical tides at Longyearbyen was determined for the times of INSAR data acquisition using the tidal prediction service provided by the University of Oslo (Fig. 2). The INSAR image data obtained in March and April 1996 shows an extensive area of fast sea ice attached to tidewater glacier faces and along glacier-free coasts. This feature was used for the regional estimation of tidal effects and indirect interpretation of tide-induced glacier ice motion.

Table 1. List of ERS-1/2 INSAR pairs for south Svalbard.

Satellite	Date Acquired	Orbit	Frame	Normal baseline, m	Tide / Atm. pressure, mb
E1/ E2	30.05.95 / 31.05.95	20251 / 0578, D	2025	- 3	● 20 cm diff / H
E1/ E2	23.10.95 / 24.10.95	22346 / 02673, D	2043	+ 33	● 5 cm diff / H
E1/ E2	07.12.95 / 08.12.95	22985 / 03312, D	2025	+ 29	○ 10 cm diff / H
E1/ E2	10.12.95 / 11.12.95	23028 / 03355, D	2025	+ 17	⊕ 15 cm diff / 1005 > 1000
E1/ E2	05.03.96 / 06.03.96	24259 / 04586, D	2025	+ 169	○ 10 cm diff / H
E1/ E2	09.04.96 / 10.04.96	24760 / 05087, D	2025	- 39	⊕ 1 cm diff / H > 1000
E1/ E2	17.12.97 / 18.12.97	33597 / 13924, A	1557	-108	⊕ 25 cm diff / H

Fig. 3 represents typical fragments from multitemporal ERS-1/2-SAR interferograms showing the H-H ice bridge at small (≤ 5 cm, a), medium (≤ 15 cm, b) and large (> 15 cm, c) differences in water level. The comparative analysis of multitemporal interferometric products revealed very interesting motion features that increase in length and number with water level difference. In the case of high water level and large level differences, these features join together to form a lambda-shaped stripe that spans the Hornsund Fjord and Hambergbukta (Fig. 3b and c). The general origin of these features is believed to be related primarily to the vertical displacement of the ice surface forced by tidal motions.

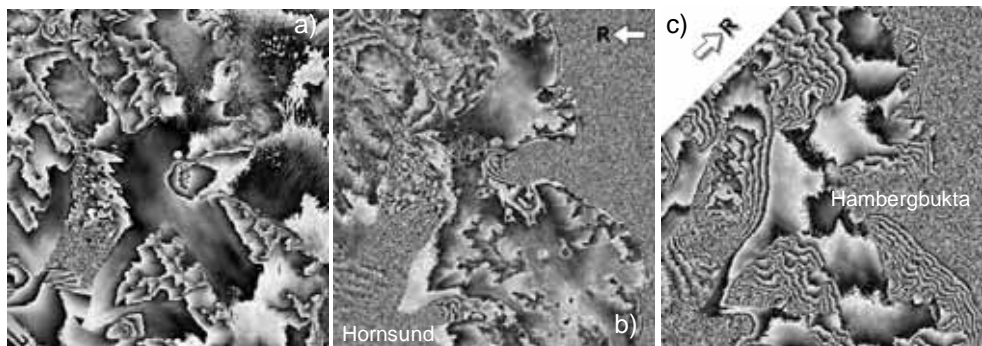


Figure 3. H-H ice bridge in the multitemporal interferograms taken under small (09/10.04.96, a), medium (07/08.12.95, b) and large (17/18.12.97, c) differences in water level.

Preliminary measurements in geocoded INSAR amplitude images showed that the width of the ice isthmus decreased from 14.4 km in 1990 to 10.2 km in 1996. The present width of the more or less steady (unstressed) part of the ice bridge at the narrowest point was estimated at approx. 2.1 km. INSAR amplitude and phase-gradient images of 1996 showed an increase in surface roughness and ice deformation in marginal parts of the ice bridge (Fig. 4). Hence, we expected to see their continued destruction in the nearest future. The hypothesis about faster changes of stressed areas at glacier margins has recently been proved. The ASTER-VNIR optical image taken on August 7, 2004 showed that large frontal parts of both Hornbreen and Hambergbreen glaciers had disintegrated, and the ice bridge width had decreased from 10.2 to 8.8 km. Only broken sea ice and icebergs can be seen offshore Ostrogradskifjella, which turned into Cape Ostrogradski. Sikorabreen, formerly a tributary of Hambergbreen, had become a separate tidewater glacier. It was confirmed that the high glacier strain rates manifested in our phase-gradient images reliably indicated both glacier retreat and advance, the latter was detected at the front of Mendeleevbreen, which had advanced about 400 m from its position of 1990.

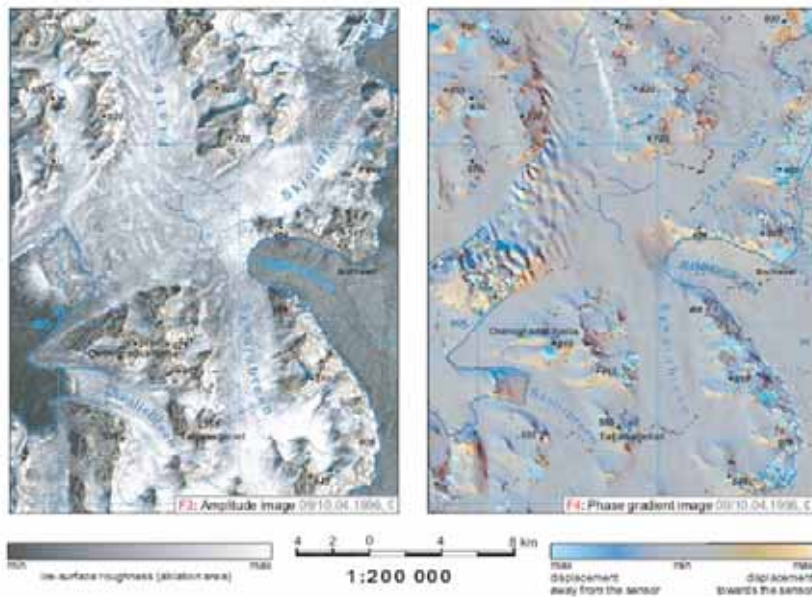


Figure 4. H-H ice bridge deformation in SAR interferometric products: amplitude (left) and phase gradient image (right).

Our glacier interferometric and elevation models were further upgraded with laser altimetry data obtained by the ICESat satellite in March, October and November 2003. 7 ICESat altimetric tracks were co-registered to corresponding maps, elevation models and SAR interferograms using a straightforward transformation, precise orbits and ERS-SAR sensor imaging model. The co-registration error was

characterized by an r.m.s. value of ± 1.2 pixel and the r.m.s. difference between cartographic and altimetric heights of steady targets was given as ± 0.7 m. The results of co-registration were represented in the form of INSARAL composite products so that every height spot within each altimetric transect is given corresponding interferometric phase and coherence values (Fig. 1c). Such a combination allows the actual glacier heights at specific target points between altimetric transects to be determined and controlled. This provided the basis for determining the present height of tidewater glacier fronts above sea level, upgrading available DEMs of the study area and measuring glacier elevation changes.

The comparison of ICESat altimetric transects with the hypsometric profiles derived from existing topographic maps corroborated the significant (up to 100 m) lowering of the glacier surface in the study area. The H-H ice-bridge elevation decreased by even 130 meters and the surface roughness of the ice isthmus increased drastically over the past years (Fig. 5). The sides of Hornbreen and Sykorabreen have steepened. The H-H ice-bridge withdrawal was animated using all available multitemporal models. The calculations revealed an almost linear decrease of the ice-bridge width over time, and it was concluded that, under current environmental conditions, the H-H ice isthmus will disappear by 2020.

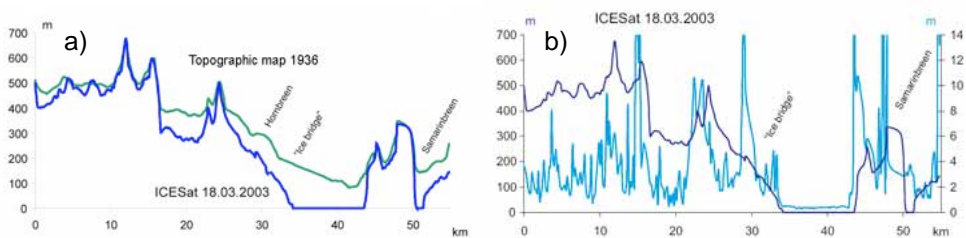


Figure 5. Glacier changes in the H-H test site: a) hypsometric profiles from topographic maps (green) and ICESat altimetry data (blue); b) ICESat roughness (cyan) and ICESat elevation (blue).

Table 2. Quantitative estimations of glacier changes in south Spitsbergen

Parameter	Period	Change	Note
Ice coast length	1936 - 2004	+ 24.1 \pm 0.5 km (+ 23 %)	Due to irregular outlines of calving glacier faces
Glacier area	1900 – 1936	- 210 \pm 1 km ² (- 5.6 %)	-
Glacier area	1936 – 2004	- 351.5 \pm 0.5 km ² (- 9.7 %)	-
Average ice thickness	1900 - 1976	- 41.6 m	-
Average ice thickness	1936 – 2004	- 65 m	-
Ice volume	1900 – 1936	- 79.2 km ³ (- 10.9 %)	Total ice loss
Ice volume	1936 – 2004	ca. – 100 km ³ (- 15.5 %)	Total ice loss
Ice volume	1936 – 2004	- 28.12 km ³	Ice loss due to marginal disintegration
Ice wastage	1936 – 2004	0.0025 km ³ /(a km)	Extrapolated from local estimates

Both horizontal and vertical glacier changes were legibly represented in the form of satellite image maps covering the whole Sør-Spitsbergen National Park at 1:300

000 scale. The resultant maps and the animation can be accessed at <http://dib.joanneum.at/integral/> (cd results). Quantitative integral estimations of glacier changes in the study area are given in Table 2. Our practical work confirmed that it was much more convenient and, therefore, expedient to perform integral planimetric measurements of glacier changes in linear and areal terms over the whole study region from precise cartographic products than from separate raw images. The approximate thickness of the submerged part of glacier faces needed for the estimation of glacier changes in volumetric terms was determined from available hydrographic charts and previous publications. The resultant values of glacier changes correlate well with previous estimations made by other explorers and show that, in the past decades, the rate of land-ice-loss processes in south Spitsbergen have not changed significantly.

References

- Dowdeswell J., et al., 1984: Airborne radio echo sounding of sub-polar glaciers in Spitsbergen. NPI, Skr. 182.
- Hagen J.O., et al., 1993: Glacier Atlas of Svalbard and Jan Mayen., Meddelelser, Nr. 129, 141 pp.
- Kotljakov V.M. (Red), 1985: Glaciology of Spitsbergen, Nauka, Moscow, 200 pp (in Russian).
- Pälli A., et al., 2003: Glacier changes in southern Spitsbergen, Svalbard, 1901-2000. *Annals of Glac.*, 37, 219-225.
- Sharov A.I. and Etzold S., 2005: Simple rheological models of European tidewater glaciers from satellite interferometry and altimetry. Proc. of the ENVISAT Symposium, 06-10.09.04, Salzburg, ESA SP-572.
- Sharov A.I. and Osokin S., 2006: Controlled interferometric models of glacier changes in south Svalbard. Proc. of the FRINGE'05 Conference, 28.11 – 02.12.2005, Frascati, ESRIN, ESA (in print).
- Troitskiy L.S., et al., 1975: Glaciation of the Spitsbergen (Svalbard), Nauka, Mosow, 276 pp (in Russian).

PARAMETERIZING SCALAR TRANSFER OVER A ROUGH ICE SURFACE

C.J.P.P. SMEETS AND M.R. VAN DEN BROEKE

Institute for Marine and Atmospheric Research, Utrecht University, Utrecht, the Netherlands

Background

Scalar transfer over ice surfaces in meso-scale and large-scale atmospheric models, and from Automatic Weather Station (AWS) data is typically calculated using the single level bulk-aerodynamic method. For this method the momentum (z_0) and scalar roughness (z_s) lengths are the key parameters. Usually z_0 in the ablation area during summer melt is taken to be constant while z_s is calculated with a well known surface renewal model (Andreas, 1987). We test this method with data obtained in the ablation area of the Greenland ice sheet along the so-called K-transect (Figure 1).

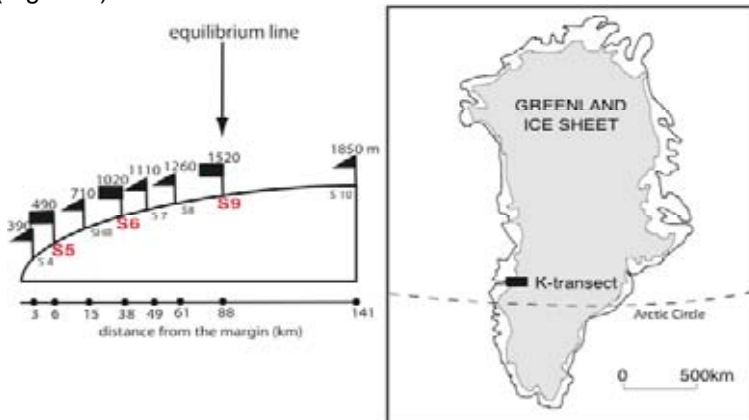


Figure 1. The K-transect and site locations in the ablation area of the Greenland ice sheet. AWS sites are S5, S6, and S9 (red).

Since August 2003 three Automatic Weather Stations (AWS) located at sites S5, S6 and S9 are operational (Figure 2). In addition, year-round Eddy-Correlation (EC) measurements were performed at S6 from August 2003 to August 2004 in order to study the surface processes.

Bulk-aerodynamic method

The bulk-aerodynamic method relates, e.g. for sensible heat flux, the temperature difference between the surface and some height and a transfer coefficient with the turbulence flux:

$$H = \rho c_p C_{H_z} U(z) [T_0 - T(z)] \quad \text{and} \quad C_{H_z} = \frac{k^2}{[\ln(z/z_0) - \alpha_z/L][\ln(z/z_T) - \alpha_z/L]}$$

with ρ the air density, C_p the specific heat of air, C_{Hz} the transfer coefficient, $U(z)$ the wind speed at height z , $T(z)$ temperature, T_0 the surface temperature, k the von Karman constant (0.41), and $\alpha.z/L$ the static stability correction (relatively well known if the static stability is not large). The most uncertain parameters in this equation are z_0 and z_T (subject of this abstract).



Figure 2. AWS (background) and eddy-correlation measurements (foreground) at S6.

Momentum roughness lengths

The AWS are equipped with two measurement levels so that we can derive year-round z_0 estimates for S5, S6 and S9. However, good care has to be taken in the data analysis since z_0 derived from two level wind profile data is very sensitive to all kinds of errors. Thorough validation of AWS against EC data for location S6 resulted in strict selection criteria that guaranteed a selection of good quality z_0 results from our two level AWS data (see also Smeets and Van den Broeke, 2006). In Figure 3 we show the year-round results of z_0 for S5, S6, and S9 on the left, and a photograph from AWS5, the location with the roughest surface, at the end of the melt season in August 2003 on the right.

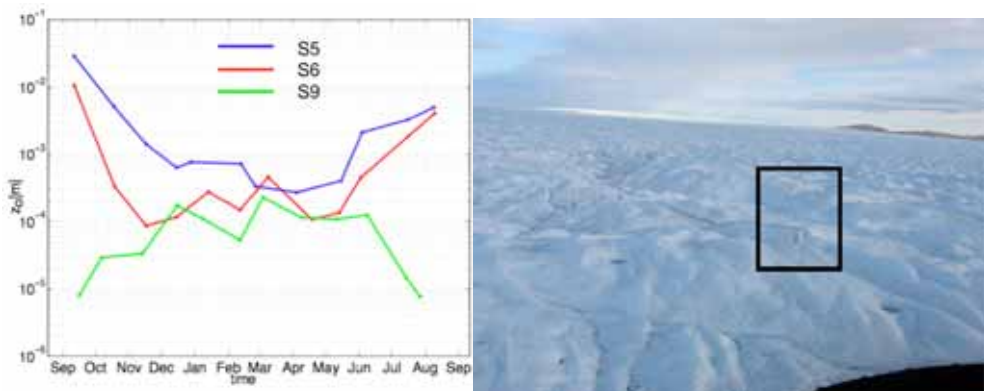


Figure 3. Left: year-round momentum roughness lengths (z_0) for location S5, S6, and S9. Right: a photograph of S5 taken from a helicopter at the end of the melt season in August 2003. The rectangle marks the AWS.

Throughout winter (November to May) the surface is in general snow covered and z_0 is fairly constant throughout the ablation area. However, when the melt season starts in May, spatial variations in z_0 rapidly increase to a factor 1000 between the lower ablation area (S5) and the equilibrium line (S9). These demonstrate the importance of large temporal and spatial variations of z_0 throughout a large part of the ablation area during the melt season. This result strongly contrasts with the general assumption in turbulence flux calculations in models or from AWS data of constant z_0 in the ablation area.

Scalar roughness lengths

Scalar roughness lengths are usually calculated with the renewal model presented by Andreas (1987). Up to now the results of the model are validated over relatively smooth snow/ice surfaces. The data we are presenting here enables us to test the model results for a range of much larger z_0 values. First we straightforwardly compare the EC- and bulk-flux results. Bulk-fluxes are calculated with inclusion of a linear time dependence of z_0 as derived from our data. The surface temperatures are derived from longwave outgoing radiation measurements. We select cases with neutral to moderate stability. In Figure 4 we plotted the ratio of EC and bulk flux as a function of binned z_0 classes. We plotted sensible and latent heat flux results from S6 in Greenland. In addition, we plotted sensible heat fluxes from 2 locations obtained during an experiment on a broad outlet glacier at the Vatnajökull ice cap in Iceland in the summer of 1996 (e.g. Smeets et al., 1999).

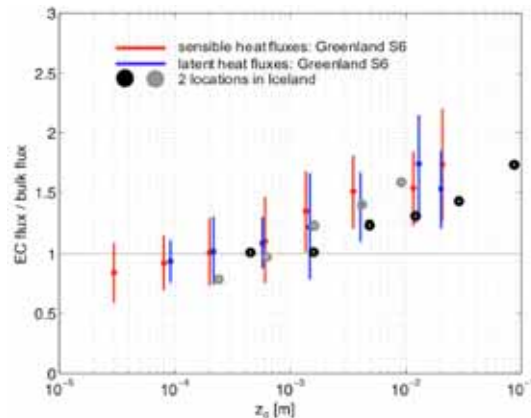


Figure 4. The ratio of EC and bulk-flux as a function of binned z_0 values. Year-round results from S6 on the K-transect in Greenland and from two locations on a broad outlet glacier from the Vatnajökull ice cap (Iceland, summer 1996).

In agreement with results from others, the fluxes agree well when the ice surface is flat and smooth with z_0 up to threshold values of 0.1 to 1 mm. However, when during the melt season the surface becomes hummocky, and z_0 grows substantially larger than the threshold, the ratio of EC- and bulk-flux increases well above 1 in a consistent fashion for all data (between 1.5 and 2 for $z_0 > 10$ mm).

We recognize that, in case of a flat ice surface, z_0 is dominated by surface stress originating from the substrate ice crystal cover. When the surface becomes hummocky, however, form drag rapidly starts to dominate z_0 . Furthermore, our results indicate that a hummocky ice surface promotes substantially higher heat transfer than predicted by the model, meaning much too small z_s values.

We hypothesize that the substrate ice crystal cover, that essentially controls the heat transfer close to the surface, is better 'ventilated' in case of a hummocky ice surface. Notice that this concept agrees with observations over rough vegetated surfaces that can have scalar transfer efficiencies comparable to momentum (e.g. Garratt, 1992). In other words, z_0 and z_s can be equal in contrast to the usual findings in a rough flow regime that $z_0 \gg z_s$.

As a convenient alternative to Andreas model for smooth ice/snow surfaces we fitted our hummocky ice data to the same model type yielding different coefficients: $\ln(z_T / z_0) = 3.5 - 0.7 \ln(R_*) - 0.1 \ln(R_*)^2$. In Figure 5 we plotted the results as is usually done in this business, that is $\log(z_s/z_0)$ versus $\log(R_*)$, with $R_* = u_* z_0 / \nu$ the Reynolds roughness number. Both model curves are plotted together with our smooth and rough ice data. In addition, we plotted some results from vegetated surfaces (Garratt, 1992) to present our results in a broader perspective.

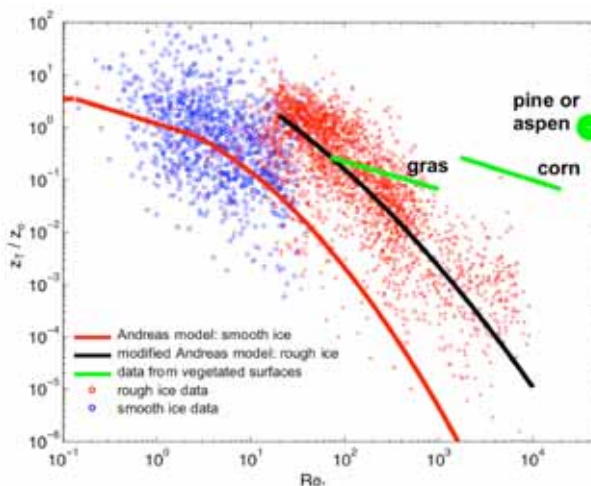


Figure 5. Ratio of scalar and momentum roughness lengths as a function of the Reynolds roughness number.

Conclusions

Data from ablation areas in Greenland and Iceland show that the use of the bulk-aerodynamic method in models or for AWS data can be subject to large errors. The momentum (z_0) and scalar roughness (z_s) lengths are the key parameters and the former is usually taken constant while the latter is calculated with the model of Andreas (1987). The data illustrate that during the melt season, in strong contrast with assumptions, the momentum roughness lengths throughout the ablation area

show very large spatial and temporal variations (between 0.1 and 10 cm). Furthermore, when the surface becomes hummocky during the melt season, the model of Andreas seriously underestimates heat transfer (up to 100%), i.e. the calculated scalar roughness lengths are too small. We suggest, in case of hummocky ice, the use of an alternative model fit derived from fitting our rough ice data.

References

- Andreas, 1987. A theory for the scalar roughness and the scalar coefficients over snow and ice. *Bound.-Layer Meteorol.*, **38**, 159-184.
- Garratt, J.R., 1992. *The Atmospheric Boundary Layer*, Cambridge University Press, Cambridge, pp 316.
- Smeets, C.J.P.P., Duynkerke, P.G., and H.F. Vugts, 1999. Observed wind profiles and turbulence fluxes over an ice surface with changing surface roughness. *Bound.-Layer Meteorol.*, **92**, 101-123.
- Smeets, C.J.P.P. and M.R. Van den Broeke, 2006. Temporal and spatial variation of momentum roughness length in the ablation zone of the Greenland ice sheet. *Bound.-Layer Meteorol.*, In prep.

ASSESSING UNASPIRATED TEMPERATURE MEASUREMENTS USING A THERMOCOUPLE AND A PHYSICALLY BASED MODEL

C.J.P.P. Smeets

Institute for Marine and Atmospheric Research, Utrecht University, Utrecht, the Netherlands

Introduction

Since 1991, IMAU has deployed several AWS on different glaciers in different climate regimes: Greenland, Morteratsch glacier Switzerland, Breidamerkurjökull (Vatnajökull) Iceland, Hardangerjökulen and Storbreen Norway, and also Antarctica. In Figure 1A the location of the k-transect in the ablation area of the West-Greenland ice sheet is shown with currently three AWS locations (S5, S6, S9). S6 is depicted in Figure 1B. All AWS are equipped with the same unaspirated and shielded temperature/humidity sensor, Vaisala HMP45C (see Figure 1C). Unaspirated sensors are well known to give excess temperatures in relation to incoming/reflected shortwave radiation and wind speed. In August 2003 year-round turbulence measurements, including a fine wire thermocouple (Campbell FW3, \varnothing 7.6e-5 m, Figure 1D), were placed next to the AWS at location S6 on the Greenland ice sheet (Figure 1B). This enabled a good comparison of the two instruments.

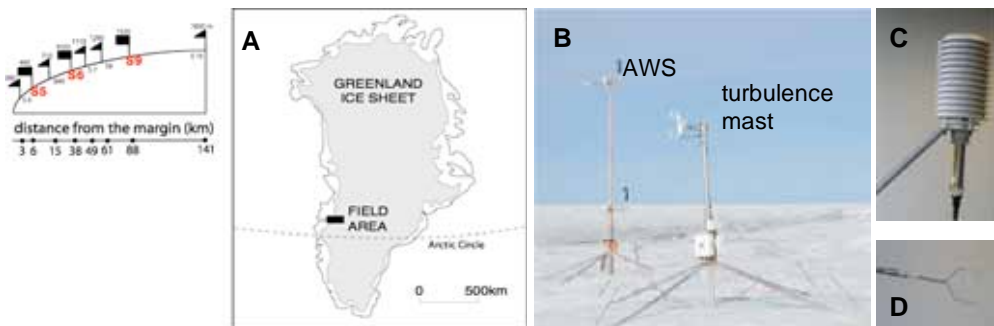


Figure 1. A) Cross section of the K-transect with three AWS locations (S5, S6, S9), Kangerlussuaq area in West- Greenland, B) AWS and turbulence mast at location S6, C) shielded Vaisala sensor, D) thermocouple.

A model to describe the temperature excess

In order to model the Vaisala temperature excess we first derive a model for the excess temperature of the thermocouple wire. Following Jacobs and McNaughton (1994) and Fritchen and Gay (1979) we assume a balance between the radiation absorption and forced convection. The excess temperature of the sensor is written as follows:

$$\Delta T = \frac{Cak}{h} \quad \text{with } h \text{ derived from } Nu = hd\lambda^{-1}, \quad Nu = 0.32 + 0.51Re^{0.51}$$

and $Re_* = udv^{-1}$ [1]

- C - geometry constant, the ratio of diameter and perimeter of the wire (= $1/\pi$)
- a - absorption coefficient of the wire for short wave radiation (= 0.25)
- k - the sum of incoming- and outgoing short-wave radiation
- h - convective heat transport coefficient
- d - thickness of the wire
- Nu and Re - Nusselt and Reynolds numbers for a circular wire
- λ - molecular thermal conductivity of still air (= 0.025 W/mK)
- ν - kinematic viscosity (= $1.5 \cdot 10^{-5}$ m²/s)

When above expressions are combined we arrive at $\Delta T = k / (1319 + 4913u^{0.52})$ (**Note:** in the poster this function included erroneous coefficients!). The same model concept is applied to the Vaisala sensor excess. We compare the data to the uncorrected thermocouple results and derive the coefficients by fitting the data by eye. For $U \geq 2$ m/s:

$$\Delta T = \frac{k}{(A + Bu^C)} = \frac{k}{(9.6 \cdot 10^{-3}k + 6.3)(12U)^{1.25}} \quad [2]$$

and for $U < 2$ m/s, a linear relation is calculated between $\Delta T(U=2\text{m/s})$ and $\Delta T(U=0\text{m/s}) = 4.14e-3 \cdot k - 0.15$. Since the above excess temperature correction is derived relative to the uncorrected thermocouple temperature the thermocouple excess temperatures from [1] have to be subtracted from the results of [2]. In Figure 2 I give an example of various excess temperatures for cases with $k > 1000$ W/m². The excess temperature of the Vaisala increases rapidly above 0.5°C when U is below 4 m/s.

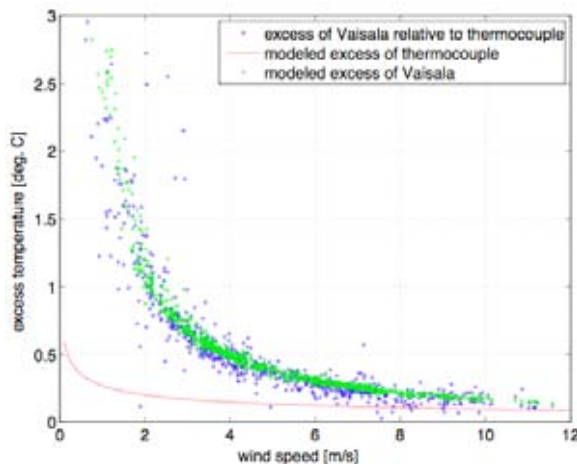


Figure 2. The variation of various excess temperatures with wind speed for cases with $k > 1000$ W/m².

Table 1 presents examples of the consequences for the year-round data from the three AWS at the k-transect. The Table presents percentages of cases with an excess temperature above 0.5°C and 1°C, and uncorrected (H_u) and corrected (H_c) average sensible heat fluxes all for cases with $k > 200$ W/m².

Table 1. Examples of the influence of the temperature excess corrections for year-round data (August 2003-August 2004) from our AWS at the k-transect. The data used are cases with a substantial amount of radiation present, that is, $k > 200 \text{ W/m}^2$. I give percentages of cases with an excess temperature above 0.5°C and 1°C , and uncorrected (H_u) and corrected (H_c) average sensible heat fluxes.

AWS	$\Delta T > 0.5^\circ\text{C}$ [%]	$\Delta T > 1^\circ\text{C}$ [%]	H_u (W/m^2)	H_c (W/m^2)	ratio H_u/H_c
S5	25	9	-32.6	-36.6	0.89
S6	16	5	-15.4	-18.1	0.85
S9	9	2	-3.9	-5.9	0.66

Conclusions

The excess temperature of an un aspirated and shielded Vaisala temperature sensor is corrected using a physical model and thermocouple measurements as a reference. A well defined relation is derived for the excess temperature related to the wind speed and the sum of incoming- and outgoing short-wave radiation. For cases with substantial radiation ($k > 200 \text{ W/m}^2$) the bulk sensible heat fluxes from the three AWS in the West-Greenland ablation area appear to be at least 10% reduced after the excess temperature correction.

References

- Jacobs, A.F.G. and McNaughton, K.G., 1994. The excess temperature of a rigid fast-response thermometer and its effects on measured heat flux. *J. Atmos. Oceanic Technol.*, 11(3), 680—686.
- Fritschen, L.J. and Gay, L.W., 1979. *Environmental instrumentation*. Springer-Verlag, New York, 216 pp.

DYNAMICS OF LARGE TIDEWATER GLACIERS IN EAST GREENLAND: RECENT RESULTS FROM SATELLITE REMOTE SENSING AND FIELDWORK

LEIGH STEARNS AND GORDON HAMILTON

Climate Change Institute, University of Maine, Orono, USA

Histories of ice velocity and calving front position of five outlet glaciers in East Greenland (Figure 1) are reconstructed from field measurements, aerial photography, and satellite imagery, and show a north-south gradient in glacier response to external forcings. The northern three glaciers, located in Scoresby Sund (Daugaard-Jensen, Vestfjord, and Graah glaciers), have not undergone any substantial change in flow speed or terminus position over the last few decades (Olesen and Reeh, 1969; Stearns et al., 2006). Kangerdlugssuaq and Helheim glaciers, located approximately 400-500 km south of Scoresby Sund, appear to have undergone a series of substantial changes in the last ~2 years, including a 40-300% acceleration in flow speeds, widespread glacier thinning, and rapid retreat of the calving fronts.

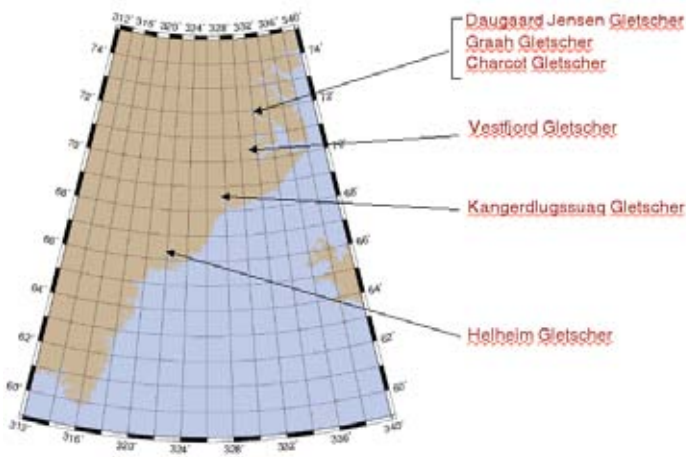


Figure 1. Map of East Greenland showing location of studied glaciers.

Terminus positions

The earliest observations of calving front position date from 1933 for Kangerdlugssuaq and Helheim glaciers, and 1950 for the Scoresby Sund glaciers. Observations since the 1970s were made using Landsat and ASTER imagery, with most images acquired in the summer months of June–August.

The calving front positions of the Scoresby Sund glaciers have remained remarkably constant since 1950 (Stearns et al., 2005). Field mapping of the calving fronts in June 2005 places them in similar locations as they were in 2001. Kangerdlugssuaq and Helheim glaciers no longer maintain the quasi-stable calving

front positions they had occupied for ~30 years prior to 2003. Kangerdlugssuaq Glacier, which occupied a stable terminus position from 1972 to 2004, retreated ~5 km between June 2004 and July 2005 according to an analysis of sequential ASTER imagery. Helheim Glacier retreated ~3 km between June 2003 and July 2005 after maintaining a near-steady front since 1972, based on a similar analysis.

Glacier velocities

The flow patterns of Daugaard-Jensen, Graah, and Vestfjord glaciers were first measured in the late 1960s by Olesen and Reeh (1969) using terrestrial surveying techniques. Velocities were obtained by repeated theodolite intersections from bedrock stations to natural targets on the glacier surface. We remapped flow patterns for 2001 for all five glaciers by applying a feature tracking technique (Scambos et al., 1992) to sequential high-resolution visible imagery (either ASTER or Landsat ETM+). The displacement of surface features (crevasses, seracs) was derived by matching patterns of brightness in a reference chip from the first image to identical patterns in a search box from the second image using an automatic cross-correlation technique. This method yields a dense array of velocity vectors for each glacier.

Modern velocities were determined from repeat high-precision differential GPS surveys conducted in June/July 2005. Each glacier was surveyed several times at five to twelve locations along its trunk, over a two-five day time span. The ice velocity records for the Scoresby Sund glaciers are remarkably different from those of Kangerdlugssuaq and Helheim glaciers. All three northern glaciers were moving at similar speeds in June 2005 as they were in July 2001. Daugaard-Jensen and Vestfjord glaciers, which have ice velocity records extending to 1968, have been flowing at the same speed for the past 37 years (Stearns et al., 2006).

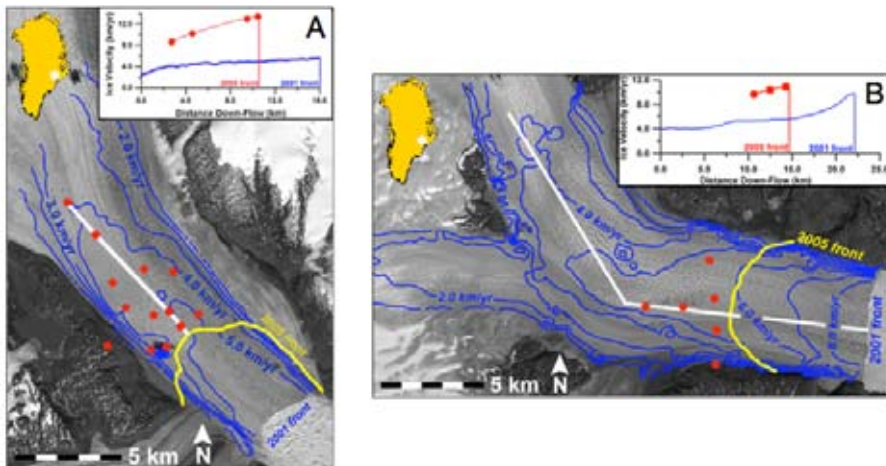


Figure 2. (A) Velocity map for Kangerdlugssuaq Glacier from sequential Landsat ETM+ satellite images acquired July 3 and July 12, 2001. (B) Velocity map for Helheim Glacier from sequential Landsat ETM+ satellite images acquired July 8 and August 2, 2001. In both images, dots denote the locations of field GPS surveys in July 2005. Insets show the profiles of velocity along the thick white lines, based on 2001 data, and corresponding velocities calculated from 2005 GPS data.

Kangerdlugssuaq and Helheim glaciers have undergone rapid changes in flow speed (Figure 2). In 2001 both glaciers sustained maximum velocities of ~6 km/yr. GPS surveys from July 2005 indicate that Kangerdlugssuaq Glacier accelerated to ~14 km/yr within 1 km of the terminus. Helheim Glacier is now flowing faster than 11 km/yr near the terminus and approximately 10 km/yr at a site ~5 km upglacier.

Surface lowering

Both Kangerdlugssuaq and Helheim glaciers exhibited 100-200 m of surface lowering of the main trunks accompanying their rapid retreat and acceleration. Surface lowering was both observed in the field (the thinning glaciers left trim lines of stranded ice on the adjacent ridges) and modelled using ASTER imagery. The ASTER instrument acquires stereo imagery using a nadir (3N) and backward (3B) viewing telescope in the VNIR band 3 (Yamaguchi et al., 1998). Together, these stereo bands can be used to generate a ~15 m horizontal-resolution digital elevation model (DEM) of a 60 km x 60 km scene. We applied this technique to Helheim Glacier using ASTER imagery acquired in July 2004 and August 2005. Between the times of the two image acquisitions, the glacier surface lowered by 100 m or more. The thinning occurred throughout the lower 10 km section of the glacier.

Discussion

The mechanism driving the observed changes of Kangerdlugssuaq and Helheim glacier cannot be resolved with the available data, although it is likely that the dynamics of both glaciers have responded to recent changes in climate (either surface warming, or warming of ocean waters). These glaciers are not the only glaciers in Greenland known to be undergoing rapid and recent changes. Jakobshavn Isbræ, a tide-water glacier at a comparable latitude (69°N) in west Greenland, accelerated 30% between 2000 and 2003 and retreated more than 3 km over the same period (Thomas et al., 2004). The combined observation from all three glaciers indicates that large changes in ice dynamics can occur on short timescales, and the near-coincident timing of the changes suggests that a common trigger mechanism might be responsible. If this mechanism affects other Greenland outlet glaciers, the mass balance of the ice sheet will become increasingly negative unless balanced by an equal increase in snow accumulation, and rates of sea level rise will increase much faster than current models predict.

References

- Olesen, O.B. and N. Reeh. 1969. Preliminary report of glacier observations in Nordvestfjord, East Greenland. *Grønlands Geologiske Undersøgelse Rapport*, Nr. 21.
- Scambos, T.A., M.J. Dutkiewicz, J.C. Wilson and R.A. Bindschadler. 1992. Application of image cross-correlation to the measurement of glacier velocity using satellite image data. *Rem. Sens. Env.*, 42, 177-186.
- Stearns, L.A., G.S. Hamilton, N. Reeh. 2006. Multi-decadal record of ice dynamics on Daugaard Jensen Gletscher, East Greenland, from satellite imagery and terrestrial measurements, *Annals of Glaciology*, 42, in press.
- Thomas, R.H. 2004. Force-perturbation analysis of recent thinning and acceleration of Jakobshavn Isbræ, Greenland, *Journal of Glaciology*, 50, 57-66.
- Yamaguchi, Y., A.B. Kahle, H. Tsu, T. Kawakami, and M. Pniel. 1998. Overview of Advanced Spaceborne Thermal Emission and Reflection Radiometer (ASTER). *IEEE Transactions on Geoscience and Remote Sensing*, 36 (4), 1062-1071.

NEW RESULTS FROM GEODETIC MASS BUDGET STUDIES AT SWISS CAMP (GREENLAND) AND EXTENSION OF RESEARCH AREA TO LOWER ALTITUDES

MANFRED STOBER

Stuttgart University of Applied Sciences

Introduction

Geodetic ground measurements had been performed in Greenland especially during the EGIG campaigns (Expédition Glaciologique Internationale au Groenland) in a West-East-profile across Greenland in latitude of about 70°. Major aims were the determination of ice flow vector components (velocity, flow direction) and elevation change of the inland ice. Main campaigns had been performed in 1959, 1968 and 1987-93 (Möller et al. 1996). No results were available near the western ablation area, because repeated measurements at same place were not possible here. Since 1991 the author decided to fill this gap with a test field, located at the SWISS-Camp, managed originally by ETH Zurich/Switzerland, and later by University of Colorado at Boulder/USA (CU). In 1994 a new test area, called ST2, was established in lower altitude, in order to study mass budget parameters in different altitudes.

The geodetic terrestrial measuring technique, in particular if using GPS, offers the advantage that heights and height changes in different years can be determined directly on the ground. Also position and position changes (movement, deformation) of stakes can be precisely determined. Elevation changes are important indicators for climate change. Flow velocity and strain rates are used in ice sheet modelling (Huybrechts et al. 1991, Abe-Ouchi 1993). Another application is validation and calibration of airborne or satellite remote sensing methods.

The geodetic measuring program 1991 – 2005

The test field at Swiss-Camp (ETH/CU-Camp), established in 1991, is situated 80 km East from the West Greenlandic coastal village of Ilulissat, latitude = 69° 34' N, longitude = 49° 20' W, elevation 1170 m a.s.l near the equilibrium line altitude (Reeh 1989).

The test field consists of 4 stakes, forming a triangle with a point in its centre. The side length of the network is about 1,5 km. The 3D-positions of the stakes are measured by GPS in relation to a fix point on solid rock at the coast. In order to determine temporal elevation changes of the ice surface, in all subsequent campaigns the previous positions of stakes are reconstructed and actual heights are re-measured. The topography of the whole surface is measured by gridding 200 m and by kinematic GPS profiling. Digital elevation models are derived in every epoch, so elevation changes and volume changes between different epochs can be calculated. The distortion of the network and strain rates are derived from

plane coordinates. It is a long term research project with campaigns performed in the years 1991, 94, 95, 96, 99, 2002 and 2004.

In 2004, the research area was extended by a new deformation network (ST2), situated in lower altitude (1000 m a.s.l) in order to compare elevation change depending on altitude and distance from ice margin. ST2 is located in latitude = 69° 30' 28" N; longitude = 49° 39' 09" W, ellipsoidal height = 1000 m, so 170 m deeper than Swiss-Camp. That location is in the same cross section like the automatic weather stations JAR1-JAR3 and smart stakes SMS1-SMS4 from the GC-Net project (Steffen et al. 2002).

Results

Area "Swiss Camp"

The topography at Swiss-Camp is rather smooth with uniform slope (about 1-2%) and only little undulations.

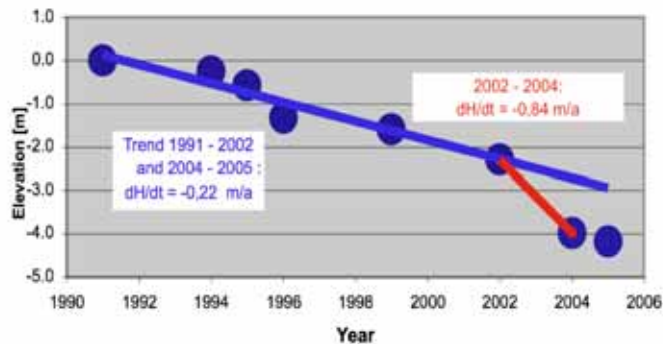


Figure 1. Swiss-Camp, elevation change of ice horizon 1991 - 2005.

The elevation change of the ice surface is shown in figure 1. The adjusted straight line over the period 1991-2002 represents an elevation decrease of $-0,22$ m/a (Stober et al. 2003), agreeing with results from airborne laser altimetry for the period 1993-1999 (Krabill et al. 2000). Obviously, the extraordinary warm summers 2003 and 2004 had effected an extremely big elevation decrease of $-1,7$ m, or $-0,85$ m/a. In 2004-2005 we obtain again the long-term decrease of $-0,22$ m/a.

According to calculations of Reeh 1989, the Swiss-Camp formerly had been situated at the equilibrium line, but now it seems to belong to the ablation area. The equilibrium line now obviously was shifted to higher regions. This results in growing of the ablation area with high melting rates at the ice margin, which was also stated at several other research areas, especially in South Greenland, reported for example by Taurisano & Boeggild 2004 or Krabill et al. 2004.

The ice flow vector was determined by comparison of stake positions in different years. The resulting ice flow velocity in average is $0,317$ m/d, with slightly increasing values over the years (figure 2). So we expect little growing ice mass outflow. The flow direction (azimuth) in average is $260,54$ gon, with little significant

turn to North-West, which may be caused by bedrock topography. The azimuth indicates the draining ice masses towards the “North glacier” nearby the Jakobshavn glacier.

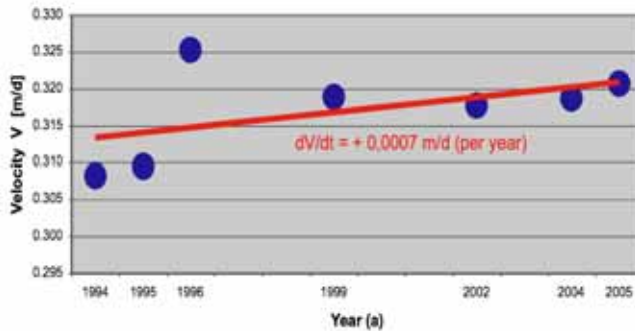


Figure 2. Swiss-Camp, flow velocity 1991 - 2005

Summarizing it is shown that elevation change and melting since 1991 are continuously increasing with even extremely high rates in last years.

This corresponds to global warming with particularly high temperature increasing in the research area, figure 3 (Steffen, personal communication 2005). We see a clear correlation between elevation change and summer air temperature, which was increasing +0,15 K per year. The warmest summers 1995 and 2003 (positive temperature) coincide with the highest ablation rates and elevation decreasing, respectively.

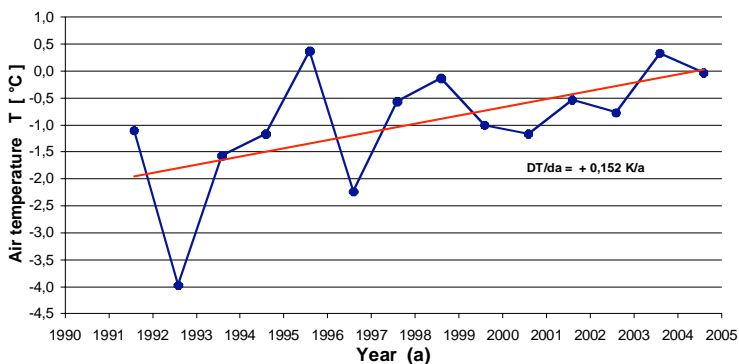


Figure 3. Summer air temperature at Swiss-Camp, average of the 3 warmest months (June, July, August) 1991 – 2005 (Steffen 2005).

Area "ST2"

As mentioned above, a new deformation network was established in 2004 and re-measured first time in 2005. Design of the network and measuring methods are the same like at “Swiss Camp”. The stakes and the topography were measured by

static and real-time kinematic GPS. Compared to Swiss-Camp, the digital elevation model at ST2 demonstrates more topographical structures and steeper, less regular terrain inclination.

The comparison of ice horizons in both years results in an elevation change of $-0,38$ m/a with standard deviation $\pm 0,06$ m/a, which is indicating a greater variability over all the area. The flow vector has a velocity of $0,205$ m/d with an azimuth of $265,9$ gon.

Comparison of "Swiss-Camp" and "ST2"

The most important results and parameters of the two research areas are shown in Table 1.

Table 1. Comparison of mass budget parameters at Swiss-Camp and ST2

Test area	Swiss-Camp	ST2
Altitude ellipse. WGS84 [m]	1150	1000
Altitude a.s.l. [m]	1120	970
Distance from ice margin in flow direction [km]	48	33
Elevation change [m/a]		
	1991 - 2002	-0,22
	2002 - 2004	-0,85
	2004 - 2005	-0,22
Flow velocity [m/d]		-0,38
	1991 - 1994	0,308
	1994 - 2004	0,315
	2004 - 2005	0,321
Flow azimuth [gon]	260,54	0,21
		266,02

The flow azimuth in ST2 is greater than in Swiss-Camp. So the flow lines show an outflow of the ice masses towards the North Glacier, which runs into the Jakobshavn Icefjord. This area is representing 6,5 % of all greenlandic ice masses (WEIDICK 1995), and therefore is most important for the mass budget of all Greenland. The flow velocity at Swiss-Camp is substantially faster than at ST2. This result is unexpected, because usually velocities become faster towards the ice margin and glacier mouth. The flow velocity at the mouth of North glacier is not determined, but from the Jakobshavn Isbrae it is well known, that it is flowing now with about 40 m/d. The causes for unexpected slower velocity at ST2, for example due to bedrock topography and ice thickness, will be investigated in future.

The elevation decreasing at ST2 is almost double of that at Swiss-Camp. These results confirm experiences from other parts in Greenland with increased thinning in the ablation areas near the ice margin, caused by climate change, especially in North polar regions.

References

Abe-Ouchi, A., 1993. Ice Sheet Response to Climate Change, Zürcher Geographische Schriften, Nr. 54, ETH Zürich, Geographisches Institut.

- Huybrechts, P., A. Letreguilly, N. Reeh, 1991. The Greenland ice sheet and greenhouse warming. *Paleogeography, Paleoclimatology, Paleoecology* (Global Planetary Change Section) 89pp. 399-412. Elsevier Science Publishers B. V., Amsterdam.
- Krabill, W.B., W. Abdalati, E. Frederick, S. Manizade, C. Martin, J. Sonntag, R. Swift, R. Thomas, W. Wright, J. Yungel. 2000. Greenland Ice Sheet: High-Elevation Balance and Peripheral Thinning, *Science*, Vol. 289, 428-430.
- Krabill, W.B., R.H. Thomas, C.F. Martin, R.N. Swift, 2004. Recent observations of increased thinning of the Greenland Ice Sheet measured by aircraft GPS and Laser Altimetry, *International Symposium on Arctic Glaciology, Geilo/Norway, 23.-27.8.2004*.
- Möller, D., Ch. Homann, H. Salbach, R. Stengele, 1996. Die Weiterführung der geodätischen Arbeiten der Internationalen Glaziologischen Grönland-Expedition (EGIG) durch das Institut für Vermessungskunde der TU Braunschweig 1987-1993, *Deutsche Geodätische Kommission, Reihe B, Nr. 303*.
- Reeh, N., 1989. Parametrization of melt rate and surface temperature on the Greenland Ice Sheet, *Polarforschung* 59(3), 113-128.
- Steffen, K., J. Box, N. Cullen, T. Albert, 2002. Variability and forcing of climate parameters on the Greenland Ice Sheet : Greenland climate Network (GC-NET), CIRES Boulder, NAG5-10857, Annual Report to NASA, January 2002.
- Stober, M., M. Scheufele, U. Buck, 2003. Terrestrial geodetic investigations at the ETH-CU-Camp 2002. In: Steffen, K. et al: Variability and forcing of climate parameters on the Greenland Ice Sheet, Greenland climate Network (GC-NET), CIRES Boulder, NAG5-10857, Annual Report to NASA, March 2003.
- Taurisano, A., C.E. Boeggild, 2004. Interpretation of over a half century of glacier elevation changes in West Greenland, *International Symposium on Arctic Glaciology, Geilo/Norway, 23.-27.8.2004*.
- Weideck, A, 1995. Satellite Image Atlas, *Glaciers of the World: Greenland*. US Geological Survey, Professional Paper 1386-C and GGU Denmark, Washington 1995.

A STATISTICAL APPROACH TO ESTIMATING THE CONTRIBUTION OF GLACIERS TO FUTURE SEA-LEVEL RISE

ANDY WRIGHT, ROS DEATH, TONY PAYNE AND JEMMA WADHAM

Bristol Glaciology Centre, School of Geographical Sciences, UK

Valley glaciers and small ice caps are expected to supply the bulk of the cryosphere's contribution to anthropogenic sea-level rise over the coming century (~ 0.23 m (IPCC, 2001)). The estimation of this contribution is hampered by the lack of quantitative data for the vast majority of glaciers worldwide (only 100 glaciers out of over 160,000 present have mass-balance records for longer than 5 years). The issues surrounding the parameterization of subgrid scale processes, uncertainties in parameter values and the propagation of errors in model prediction of sea-level rise are similar to those experienced in the prediction of discharge from ungauged river basins. Given the similarities between valley glacier systems and their hydrological counterparts, it may be appropriate to use the techniques developed for hydrological modelling. Therefore, to calculate sea-level rise with an associated error we propose the following four-stage procedure. First, a generic valley-glacier system model that allows for variations in width, depth, accumulation and ablation along the glacier is developed. Second, the model is calibrated against the small number of glaciers on which we have sufficient data. Third, a response surface of sea-level contribution as a function of glacier climatology and topography is constructed. Entailed in this stage is a rigorous assessment of the uncertainty propagated through the model due to uncertainties inherent in the input parameters. The final fourth stage is then to sample the response function, in accordance with estimates of the global distribution of glaciers in the climate-topography phase space, in order to estimate sea-level rise with a meaningful estimation of error. The use of methods traditionally employed by the hydrological community to a different study area highlights issues that contribute to an understanding of the limitations in defining variability within a system and quantifying uncertainty.

GLACIODYN

GLACIODYN PLANNING MEETING

GLACIODYN has a logo! Thanks to Jack Kohler who, after some trials, came up with the following design:



Please use it whenever you like; it can be downloaded from the website.

What is GLACIODYN?

The following is the (slightly modified) text from the IPY proposal as submitted to the IPY Joint Committee. GLACIODYN has been fully endorsed by the Joint Committee.

Global warming will have a large impact on glaciers in the Arctic region. Changes in the extent of glaciers will affect sea level, and may lead to substantial changes in sediment and fresh water supplies to embayments and fjords.

In ACIA, a simple approach was taken to estimate the runoff of all glaciers in the Arctic for a set of climate-change scenarios. Changes in the surface mass balance were calculated without dealing with the fact that glacier geometries will change. It was also assumed that the rate of iceberg production at calving fronts would not change.

To arrive at more accurate predictions, we propose an internationally-coordinated effort to study the dynamics of Arctic glaciers and develop new tools to deal with this dynamic response. The key elements of this effort are (i) to *make better use of observational techniques* to assess the detailed dynamics of a key set of glaciers, and (ii) to *develop models* that can be used to aggregate data and that are sufficiently robust to have predictive power. A set of target glaciers have been identified for intensive observations (in situ and from space) for the period 2007-2010. This set covers a wide range of climatic/geographical settings and takes maximum advantage of prior long-term studies.

The target glaciers are:

- Academy of Sciences Ice Cap (Severnaya Zemlya)
- Glacier No. 1 (Hall Island, Franz Josef Land)
- Austfonna (Svalbard)
- West Svalbard tidewater glaciers: Hansbreen, Kronebreen, Kongsvegen, Nordenskiöldbreen
- North Scandinavia transect (Langfjordjøkelen, Storglaciären, Marmaglaciären)
- Ice caps of Iceland (Vatnajökull, Hofsjökull, Langjökull)
- Kangerlussuaq basin (West Greenland)
- Hellheim Glacier (East Greenland)

- Devon Ice Cap (Canada)
- McCall Glacier (Alaska)
- Hubbard Glacier and Columbia Glacier (Alaska)

Among the target glaciers are glaciers for which information is available on length/area in historical times [reports, drawings, photographs, old maps, etc.]. This information will be combined with the newly derived maps to reconstruct glacier evolution from the Little Ice Age into the present. This will provide a better perspective for projecting changes in the coming century.

Special attention will be given to tidewater glaciers. We want to look carefully at the interaction between surface processes and dynamics (e.g. the influence of meltwater supply on ice velocities and consequently calving rates; interactions between terminal moraines, sediment flux, and ice velocities). In a warming world some glaciers will transform from cold to polythermal, or from polythermal to temperate. We want to study the effect of such transitions on glacier dynamics and related rates of retreat. Another important aspect of study is the surface albedo. Poor drainage of meltwater may lead to more extensive zones of soaked snow and supraglacial lakes (as seen in large parts of the Greenland Ice Sheet), thus enlarging the sensitivity of ablation rates to warming.

Model development will be conducted in parallel with the observational programmes. The modelling work will deal with processes acting on the smaller scale (e.g. parameterization of the calving process) and on the larger scale (e.g. global dynamics of tidewater glaciers, response to climate change, interaction with sediment dynamics).

The major deliverables of GLACIODYN have been identified as:

- #1 Extensive datasets for target glaciers around the Arctic.
- #2 A better understanding of the factors that control the dynamic response of Arctic glaciers to climate change.
- #3 Improved techniques to retrieve glacier parameters from satellite data.
- #4 Models that can be used to predict glacier behaviour for imposed climate change scenarios.
- #5 Improved estimates of the contribution of Arctic glaciers to future sea-level rise

Organizational structure of GLACIODYN

GLACIODYN has a simple and open organizational structure. It has a coordinator (J. Oerlemans, Utrecht University) and co-coordinator (J.-O. Hagen, University of Oslo). The IASC Working Group on Arctic Glaciology, in which there is a Committee of National Representatives, is used as forum for discussion and planning. When the need arises a smaller steering committee will be established.

Discussion and outreach

A web-based email forum has been established. Here anyone can register to become part of the forum and read old emails and attachments. To send an email

to the entire group, use the address glaciodyn@yahoo.com. The general purpose of the forum is to facilitate discussion of GLACIODYN issues in an open, easily accessible manner.

As part of our initial outreach efforts, soon we will develop applications for Google Earth and other 3D GIS engines that will highlight the locations of our target research glaciers, provide links to further information them, and incorporate the latest digital elevation models, imagery, and locations of field instrumentation. GLACIODYN members or anyone in the public will be able to interactively fly through these virtual globe applications, as well as download movies flying from space to each of the glaciers, for use in presentations or other outreach endeavours.

Plans of individual research groups

In the first GLACIODYN planning meeting the emphasis was placed on the plans of individual research groups. There were sixteen short presentations (listed below) enabling the GLACIODYN participants to get an overview and make plans for future collaboration. Such plans will now be developed on the basis of small groups that will establish themselves, sharing logistics and expertise as much as possible. Much depends on the funds that will become available, of course. There are large differences among the participating countries. In most countries special funds have been allocated to IPY activities, but the available budgets vary widely. In a few countries no additional funds seem to become available. In most cases the process of submitting and judging applications is still running, and it is expected that in the beginning of 2007 a full picture will emerge about GLACIODYN activities that receive significant support.

Next planning meeting and workshops

The next GLACIODYN planning meeting will be held in early 2007 in Norway. It will be combined with the general workshop of the Working Group on Arctic Glaciology. GLACIODYN will also facilitate the organization of additional workshops on topics of interest to the GLACIODYN participants. Such topics may range from very practical (e.g. equipment for in situ measurements on glaciers) to theoretical (e.g. modelling of calving glaciers).

A point of particular concern is the way data will be handled and stored. When possible existing structures will be used (e.g. World Data Centers for Glaciology), but it was agreed to establish a metadata base connected to the website of the Working Group.

CONTRIBUTIONS

1. M. Kuhn (Austria)
Holtedahlfonna, Kronebreen, Kongsvegen (Svalbard), Frans Jozef Land
2. J. Kohler (Norway) and F. Obleitner (Austria)
Holtedahlfonna, Kronebreen, Kongsvegen (Svalbard)
3. J. Jania (Poland)
Hansbreen, Amundsenisen, Renardbreen (Svalbard)
4. A. Glazovsky (Russia)
Fridtjovbreen, Austfonna (Svalbard), Hall Island glacier No.1 (Franz Josef Land)
5. F. Navarro (Spain)
Radar observations in cooperation with Russian and Polish colleagues
6. J.O. Hagen (Norway)
Austfonna (Svalbard)
7. C.H. Tijm-Reijmer (Netherlands)
Kangerlussuaq basin (Greenland), Nordeskiöldbreen (Svalbard), ...
GPS and melt observations on several Arctic glaciers
8. A. Sharov (Austria)
Radar interferometry Svalbard glaciers
9. L. Copland (Canada)
Devon Ice Cap, Queen Elizabeth Islands (Canada)
The Dynamic Response of Arctic Glaciers to Global Warming
10. M. Nolan (USA)
McCall glacier (Alaska)
11. T. Pfeffer (USA)
Hubbard glacier, Columbia glacier (Alaska)
Tidewater/Outlet Glacier Dynamics & Glacier/Ice Sheet Response to Warming
12. H. Björnsson (Iceland)
Vatnajökull ice cap, Iceland
13. T. Jóhannesson (Iceland)
Mass balance Icelandic glaciers
14. L.M. Andreassen (Norway)
Langfjordjøkelen, northern Norway
15. M. Jackson (Norway)
Engabreen, northern Norway
16. P. Holmlund (Sweden)
Mårmaglaciären, Storglaciären, northern Sweden